Society For Biomaterials

Review Article

Are synthetic scaffolds suitable for the development of clinical tissue-engineered tubular organs?

Costantino Del Gaudio,[1]* Silvia Baiguera,[2]* Fatemeh Ajalloueian,[2] Alessandra Bianco,[1] Paolo Macchiarini[2]

[1]University of Rome "Tor Vergata", Department of Industrial Engineering, Intrauniversitary Consortium for Material Science and Technology (INSTM), Research Unit Tor Vergata, Rome, Italy
[2]Advanced Center for Translational Regenerative Medicine (ACTREM), Karolinska Institutet, Stockholm, Sweden

Received 18 March 2013; revised 11 July 2013; accepted 17 July 2013
Published online 2 August 2013 in Wiley Online Library (wileyonlinelibrary.com). DOI: 10.1002/jbm.a.34883

Abstract: Transplantation of tissues and organs is currently the only available treatment for patients with end-stage diseases. However, its feasibility is limited by the chronic shortage of suitable donors, the need for life-long immunosuppression, and by socioeconomical and religious concerns. Recently, tissue engineering has garnered interest as a means to generate cell-seeded three-dimensional scaffolds that could replace diseased organs without requiring immunosuppression. Using a regenerative approach, scaffolds made by synthetic, nonimmunogenic, and biocompatible materials have been developed and successfully clinically implanted. This strategy, based on a viable and ready-to-use bioengineered scaffold, able to promote novel tissue formation, favoring cell adhesion and proliferation, could become a reliable alternative to allotransplatation in the next future. In this article, tissue-engineered synthetic substitutes for tubular organs (such as trachea, esophagus, bile ducts, and bowel) are reviewed, including a discussion on their morphological and functional properties. © 2013 Wiley Periodicals, Inc. J Biomed Mater Res Part A: 102A: 2427–2447, 2014.

Key Words: tissue engineering, organs and tissues, synthetic biomaterials, *in vitro* and *in vivo* evaluation

How to cite this article: Del Gaudio C, Baiguera S, Ajalloueian F, Bianco A, Macchiarini P. 2014. Are synthetic scaffolds suitable for the development of clinical tissue-engineered tubular organs?. J Biomed Mater Res Part A 2014:102A:2427–2447.

INTRODUCTION

Tissue engineering is currently regarded as a promising approach to treat the end-stage condition of a variety of tissues and organs. However, only a few *in vivo* preclinical and clinical studies have shown effective preliminary results and this may be related to the fact that even "simple" organs, devoted only to transport functions (e.g., air, food, and liquids), represent a challenge. The careful selection of materials and processing techniques should reproduce the native histological organ structure and function. Moreover, when organs of respiratory or digestive systems are considered, the specificity of the microenvironment further increases the complexity of the bioengineering process, due to the presence of both muscular and nervous tissues. This aspect reflects the shift from a *passive* state, associated for example with the trachea (i.e., air passage avoiding organ collapse), to an *active* one, typical of gastrointestinal (GI) organs (i.e., peristalsis). Specifically, none of the so far generated scaffolds is able to exactly reproduce the esophageal architecture and functions[1] or provide specific binding sites and biochemical cues to elicit and support a positive cell response.

This review focuses on the currently developed synthetic tissue-engineered substitutes for tubular organs, examining *in vitro* feasibility, preclinical *in vivo* analyses, and follow-up studies with clinical *in vivo* results. As a final remark, here the term "synthetic" is referred to all those materials not directly derived from a biological tissue as a result of a decellularization procedure. Therefore, biologically derived polymers, like gelatin or collagen, are to be intended as isolated polymers directly available to research laboratories.

Tissue-engineered tubular substitutes; the concept

Tubular organs are characterized by complex structural, mechanical and motility patterns responsible for specific functions. The trachea's main function is to conduct air from the nose or mouth to the lungs and for this aim is composed by (i) a cartilaginous structure that prevents

*These authors contributed equally to this work.
Correspondence to: P. Macchiarini; e-mail: paolo.macchiarini@ki.se

TABLE I. Main Tracheal Pathologies

Tracheal Pathologies	Incidence	Mortality	Treatment
Benign			
Tracheomalacia			
Congenital	1:2100 newborns	Extremely rare. Can cause cyanosis due to episodic severe airway obstruction	Allowing time to pass noninvasive ventilation, pharmacological treatment Surgical therapy: stenting, endotracheal or tracheostomy tube Pharmacological and/or conservative treatments Non invasive, positive-pressure ventilation
Acquired	No definitive rates are available		Surgical therapy: stenting, tracheostomy, aortopexy
Stenosis			
Congenital	<1:2,00,000 people	28% after surgical intervention 53% in patients with intracardiac anomalies 73% in patients younger than 1 month	Tracheal dilation using rigid bronchoscope Laser surgery
Acquired	10–22% (1–2% of the patients are symptomatic or have severe stenosis) Severe stenosis: 4.9 cases/million/year	2–5% after surgical intervention	Tracheal resection and primary anastomosis (stenosis length <50% in adults and 30% in children)
Tracheoesophageal fistula			
Congenital	1:2000/4000 live births	Usually fatal: in case of tracheal atresia 5–20% for infants with comorbidities 0% for healthy infants undergoing surgical repair	Surgical treatment (usually using tracheal prosthesis)
Acquired nonmalignant	0.5% of patients undergoing tracheostomy	10.3%	For critically ill patients: conservative treatment Surgical repair
Acquired malignant	4.5% for primary esophageal tumor	33–61%	Palliative (esophageal exclusion, bypass, resection, endoprosthesis) or supportive (nasogastric drainage, tracheostomy, gastrostomy) treatment
	0.3% for primary lung tumor		Radiation therapy
Malign			
Tracheal tumor	0.1 person /100.00 (89–90% are malignant)	Median survival: 6 months (squamous cell carcinoma: median survival 44months, 5-year survival 34% adenoid cystic: median survival 115months, 5-year survival 78%; carcinoid: 5-year survival 95%)	Laser resection, stenting as palliative Radio–chemo therapy Surgery therapy: resection

collapse during respiration, provides flexibility and assures patency of the lumen; (ii) muscular tissue that reduces lumen size during the cough reflex and facilitates airway clearance; and (iii) mucosal membrane that allows air conditioning and prevents the epithelium dehydration.

The GI organs and the bile ducts are characterized by sophisticated motility patterns to perform a variety of functions to support ingestion, digestion, absorption of nutritive elements, and excretion of waste. Motility is the result of chemical (mediated by the release of neurotransmitters, hormones, or paracrine signals) and electrical (mediated by gap junctions and/or Ca^{2+} channels) interactions among smooth muscle, intramural innervations, interstitial cells, and mucosal epithelial layers.

TABLE II. Main Gastrointestinal Pathologies

Pathologies	Incidence	Mortality	Treatment
Esophagus			
Stenosis (stricture)			
Congenital (atresia)	1 in 3000–4500 live births (85% of affected babies will have a tracheaoesophageal fistula (see Table I))	75% (if detected prenatally) 21% (if not detected prenatally)	Surgical treatment (gastrostomy)
Acquired	1.1 per 10,000 person-years 7–23% of untreated patients with reflux disease	0.5%	Pharmacological treatment Endoscopic dilation using mercury-filled bougies, guided wire, or balloon dilators. Surgical treatment
Gastroesophageal reflux	10–20% of the population	4–6/million/year	Pharmacological treatment for recurrent non progressive form (80%): Surgical treatment for progressive form (20%)
Esophageal motility disorders			
Achalasia	1–3 cases/100,000 population/year	Can lead to malnutrition, weight loss, dehydration, and esophageal cancers	Pharmacologic therapy
Spastic motility disorders	Lack of population-based studies	Very rare	Endoscopic dilation Surgical treatment (myotomy)
Secondary motility disorders (such as scleroderma esophagus)		Systemic complications are the major cause of mortality	
Esophageal cancer	30–800 cases/100,000/year (95% are squamous cell carcinoma)	87% 5-year survival rate: 20–25%	Stenting as palliative Radio–chemo therapy Surgery therapy: resection (esophagectomy)
Small intestine			
Short bowel syndrome	2 cases/million population/year	Patients with parenteral nutrition: 4-year survival rate 70% Patients subject to organ transplant: 1-year survival rate 90%; 4-year survival rate 60%	Drug therapy Parenteral nutrition Surgery, including intestinal lengthening, tapering and intestinal or combined liver–intestinal transplantation
Malignant neoplasm	2.0 cases/100,000/year (40% are adenocarcinomas)	0.4 per 100,000/year 5-year overall survival rate: 30–35% for adenocarcinoma; 25% for sarcomas 40–60% for who undergo resection	Radio–chemo therapy Surgery therapy: bypass procedure or limited tumor removal (as palliative) resection
Large intestine			
Hirschsprung disease (congenital aganglionosis)	1 case per 1500–7000 newborns	80% for untreated patient; 30% for treated cases	Medical care (to treat complications, as temporary measures, to manage bowel function after reconstructive surgery). Surgical management: full-thickness rectal biopsy, primary pull-through procedure, diverting colostomy

TABLE II. *Continued*

Pathologies	Incidence	Mortality	Treatment
Inflammatory bowel disease			
Ulcerative colitis	0.5–24.5 cases/100,000/ year	7% (overall mortality seems not increased among patients with ulcerative colitis)	Medical approach: symptomatic care (i.e., relief of symptoms) and mucosal healing Surgical treatment (25–30% of patients): proctocolectomy with ileostomy and total proctocolectomy with ileoanal anastomosis.
Crohn disease	0.1–16 cases /100,000/ year (30% involve the small bowel, 30% involve only the colon, and 40% involve both the small bowel and colon)	15-year survival rate: 93.7%	Medical approach: symptomatic care (i.e., relief of symptoms) and mucosal healing Surgery (conservative, not curative) approach (70–75% of patients): stricturoplasty; segmental resection

A wide spectrum of pathologies may affect tubular human structures, ranging from benign to malignant conditions, and some are potentially life threatening, implying significant morbidity and mortality. Most *tracheal* disorders cause airway narrowing and ultimately obstruction with subsequent respiratory insufficiency; others, such as fistulas, may be equally deleterious (Table I). A partial or complete loss of any part of the GI tract causes debilitating and potentially life-threatening complications and significantly worsen the quality of life (Tables II and III). Current medical and surgical treatments are often suboptimal for tubular tissue diseases and long-segment reconstruction, for advanced structural disorders, is still a challenging surgical issue. Tissue-engineered substitutes, with anatomical, physiological, and biomechanical properties similar to the native tissue, might represent a solution for the functional reconstruction of tubular tissues. Although specific differences are necessary requirements, an ideal tissue-engineered tubular graft should be characterized by some common properties, as it expected to (i) resemble the tissue extracellular matrix (ECM; e.g., selecting the most appropriate fabrication technique), (ii) provide adequate structural support to maintain luminal patency, (iii) integrate within the recipient tissue (in particular muscular, neuronal, and mucosal layers), (iv) be biocompatible, free from the need for immunosuppression and inducing a little inflammatory response, (v) promote epithelialization and vascularization, and (vi) be readily available and easily implantable.

In the last few years, there has been considerable progress in the clinical translation of tissue-engineered organs, obtained using natural or synthetic scaffolds repopulated with terminally differentiated cells or stem cells.[2,3] Recently, an ECM-derived tracheal prosthetic substitute was successfully developed, providing encouraging early clinical results as the implanted scaffold was vascularized and lined with complete respiratory neomucosa (Fig. 1).[4,5] However, this approach is mainly limited by the shortage of cadaveric donor organs, which might significantly delay the availability of biological scaffolds and increase the waiting time for the patients. Moreover, the chosen decellularization process might induce severe structural and surface modifications thus affecting the long-term performance (or biomechanical integrity) of the biologically derived graft.[6] To overcome these drawbacks, various synthetic substitutes have been recently proposed. Main advantages of this approach are the time reduction of the preprocessing procedures and the chance to overcome donor shortage, a critical issue especially for pediatric patients (Table IV). In addition, scaffold size and shape can be tailored to fit the anatomy of the recipient.[7] Biocompatible, nonimmunogenic and

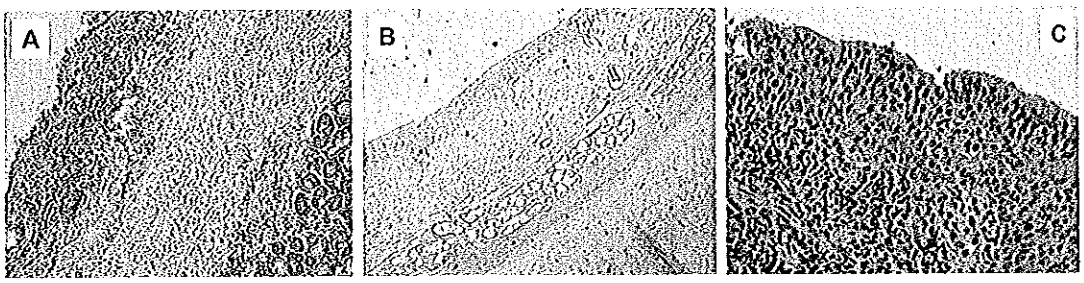

FIGURE 1. Hematoxylin and eosin staining of native trachea (A), decellularized trachea (B), and implanted trachea after 1-year follow-up (C) showing epithelial regeneration. [Color figure can be viewed in the online issue, which is available at wileyonlinelibrary.com.]

TABLE III. Main Bile Duct Pathologies

Bile ducts			
Atresia	1 per 10,000–15,000 live births	Survival rate (after surgery): 47–60% at 5 years and 25–35% at 10 years	Surgery approach Liver transplant (in case of complete atresia)
Stricture	0.2–0.3% after open cholecystectomy; 0.4–0.6% after a laparoscopic cholecystectomy	4–13% (surgical mortality)	Medical treatment (eradicate the infection) Endoscopic or percutaneous balloon dilatation Endoscopic biliary stenting Surgical management (biliary-enteric anastomosis, pancreaticoduodenectomy for long-standing stricture)
Primary sclerosing cholangitis	6.3 cases/100,000/year	Survival rates (after liver transplantation): 93.7% at 1 year, 92.2% at 2 years, 86.4% at 5 years, and 69.8% at 10 years	Pharmaceutical approach as palliative treatment
Primary biliary cirrhosis	2.7 cases/100,000/year	92% at 1 year and 85% at 5 years Median survival duration: 7.5 years for symptomatic patients; 16 years for asymptomatic patients	Liver transplantation
Cholangiocarcinoma	2–6 cases/100,000/year (90% are adenocarcinoma)	5-Year survival rate: for nonresectable cases (90%), less than 5% (overall median survival: less than 6 months); for surgical cases, 20–50%	Stenting and photodynamic therapy as palliative Radio–chemo therapy Surgery resection (only for early-stage disease, 10%)

noncarcinogenic synthetic material(s) must be chosen, being able also to support cellular (i.e., epithelial and muscular) resurfacing, avoiding stenosis and late buckling and resisting to bacterial colonization.[8] For instance, to recapitulate most of the desired characteristics that a synthetic scaffold should provide, a tissue-engineered esophagus, produced by electrospinning and currently under development, could represent an effective way to combine a fibrous microarchitecture, properly tailored to favor cell adhesion and proliferation, with suitable mechanical characteristics to allow the appropriate function as hollow organ (Fig. 2).

TRACHEA

In vitro assessment

Several research groups have begun to evaluate potential scaffolds for airway replacement using bioresorbable polymers. As an example, poly(lactic-*co*-glycolic acid) (PLGA) was considered to assemble a tubular construct with mesenchymal stem cell (MSC) sheets.[9] The fabrication process started by culturing MSC macroaggregates to obtain cell sheets (composed of 5–8 cell layers with an approximately matrix thickness of 150–200 μm) to be wrapped around a fibrous PLGA scaffold (about 13 μm average fiber diameter). This hybrid structure was wound up against a glass rod, to maintain the tubular shape (2.5–3 cm length), and then cultured in dynamic conditions. After 4 weeks of *in vitro* incubation, the PLGA scaffold was completely degraded and a tracheal cartilage graft was obtained, showing fusion among macroaggregates, a pearly opalescence, and an aggregate modulus of 128.95 ± 8.06 kPa. Cell sheet-based tissue engineering could represent an interesting approach for the fabrication of scaffold-free grafts, but this method might not be suitable for the reproduction of tissues with considerable amounts of ECM. To address this issue, a scaffold-free cylindrical cartilage, obtained by *in vitro* dynamic cultures of auricular chondrocyte cell sheets and self-produced ECM, was realized and evaluated.[10] Cell sheets were looped around a sterile silicone tube (7 mm diameter) and after 6 weeks type II collagen was expressed in the central region, whereas type I collagen was expressed in the surface region. Mechanical properties of dynamic and static cultivation groups were not significantly different. These studies could be regarded as promising methods for bioengineering a tracheal graft; however, a scale-up of the construct should be considered for an effective implantable substitute. To move toward a more anatomical scaffold, fibrous tissue-engineered tracheal tubes were proposed.[11] Two different cylindrical hollow scaffolds (i.e., cylindrical and toroidal) and one anatomic-shaped trachea segment were fabricated by means of rapid prototyping technique, the material was a block copolymer of polyethylene oxide terephthalate and polybutylene terephthalate. The anatomic replica was produced from a computed tomography (CT) image dataset, prototyping an entire tracheobronchial tree, although only the tracheal portion was considered for the subsequent study (about 4 cm length). The scaffolds were geometrically

TABLE IV. Comparison of Material Properties for Tubular Substitutes

Properties	Tubular Substitute	
	Natural Derived (Decellularized)	Synthetic
Material	Extracellular matrix structure and proteins	Natural and/or synthetic polymers
Three-dimensional aspect and measurements	Dependent on cadaveric tissues/organs	Based on patient CT
Mechanical properties		
In vitro	Suitable decellularization approach does not affect tissue mechanical properties	Choosing the proper polymeric material and fabrication technique, it is possible to obtain a scaffold with suitable mechanical and viscoelastic properties
In vivo	Decellularization process, affecting the scaffold properties and surface topography, could have an effect on the long-term graft properties	Nondegradable materials maintain mechanical characteristics
Cell adhesion	ECM proteins seem not to be affected by decellularization process, maintaining the native environment for cells	Depending on the technique used. Using electrospinning it is possible to recreate the submicro/nano-ECM-like architecture. Possibility to condition scaffold surface with bioactive molecules
Pros	Conservation of the natural ECM composition	Scaffold dimensions and shape can be tailored to fit the anatomy of the recipient
	Production of nontoxic biodegradable products	Material properties (strength, degradation time, porosity, and microstructure) can be easily controlled
	Capability not to induce inflammation During degradation release of growth factors and peptides that could stimulate tissue remodeling	No depending on donor availability
Cons	Depending on donor availability Can be immunogenic (if not properly decellularized) Possibility of contamination during harvesting and *in vitro* manipulation	Can induce inflammation processes (due to degradation products or to no biocompatible material)

characterized by a lumen diameter of about 5.5 mm and a wall thickness of 2.5 mm (about 80% porosity, 170 ± 15 μm fiber diameter), the *in vitro* evaluation was performed using rat chondrocytes. After 21 days, cell viability revealed the lowest value for the anatomical scaffold, while glycosaminoglycan formation (ECM production) was the highest one. This was correlated to the creation of "native-like" local niches, where enhanced cell–cell contacts triggered the production of higher amount of ECM. This approach showed the capability to realize a structure based on the anatomic specifications of a patient, helping to regain the original shape and supporting larger tissue formation, and thus functioning as a potential matrix for tissue regeneration. However, the complex tracheal structure could be difficult

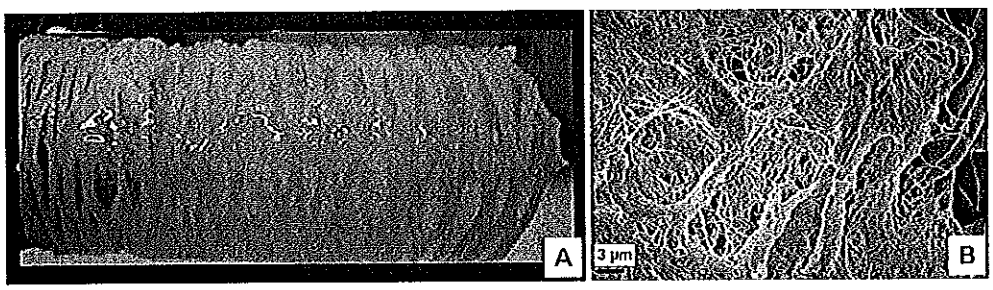

FIGURE 2. Scaffold fabrication for esophageal tissue engineering. A composite three-dimensional prosthesis is realized covering electrospun PET-PU nano-/microfibers with collagen nanofibers (A) and scanning electron micrograph of the final microstructure (B). [Color figure can be viewed in the online issue, which is available at wileyonlinelibrary.com.]

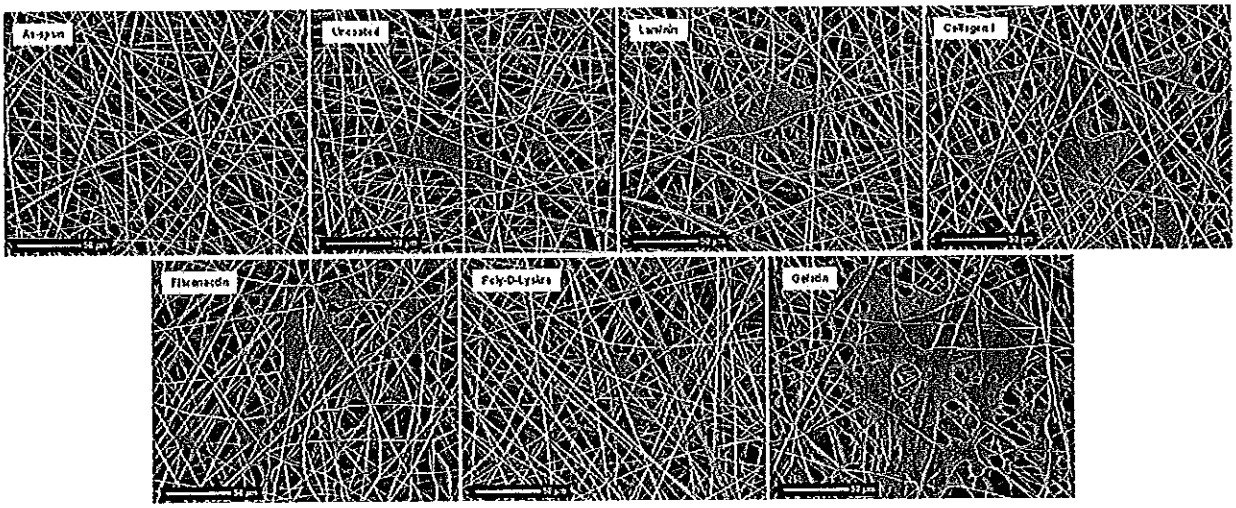

FIGURE 3. Scanning electron micrographs of electrospun PET and the *in vitro* response of rat mesenchymal stromal cells to different adhesion proteins.

to reproduce, because cartilaginous rings and *pars membranacea* have not been considered, realizing an homogeneous scaffold that could affect the physiologic function of the entire organ. For instance, the authors themselves referred to compliance as a key parameter that allows tissue deformation during movement and contributes to prevent stenosis. A similar technical approach was considered for the fabrication of cylindrical tracheal scaffolds, made of poly(ϵ-caprolactone) (PCL) or poly(lactic acid) (PLA), by means of fused deposition modeling.[12] The biocompatibility of the produced models (30 mm internal diameter, 1.5–4 mm wall thickness, and 0.5–1.5 mm pore size) was confirmed culturing human gingival cells for 14 days. However, results were evaluated only by means of optical and scanning electron microscopy, without any specific biological assays that could further support the reliability of the proposed scaffolds.

A suitable scaffold that resembles the microstructure of the physiologic tissue (an ECM-like substrate) is considered a key-starting point for the development of a viable device able to replace the impaired or lost function of an organ. Obviously, the replication of the complex three-dimensional (3D) architecture is a partial approach to the problem, because the ECM is a complex mixture of structural and functional proteins, arranged in a dynamic and unique tissue-specific microenvironment that provides mechanical support, binding sites, and a cascade of signaling factors. Synthetic polymers cannot supply all these cues and a surface modification can be requested to promote an effective cell response. Gustafsson et al.[7] investigated the biological response of rat mesenchymal stromal cells cultured on electrospun polyethylene terephthalate (PET) and polyurethane (PU) fibers, coated with different adhesion proteins. Coated and uncoated mats showed similar results in terms of cell adhesion and proliferation (Fig. 3). In addition, cells retained their phenotype, suggesting that the multilineage potential was maintained. This is of particular relevance when reseeding of the scaffold is necessary before implantation. The authors concluded that ECM-derived adhesion proteins did not result in any significant improvement in cell adhesion, proliferation or phenotype, suggesting that neat PET and PU electrospun scaffolds provide a favorable substrate for cell response. Based on these results, an

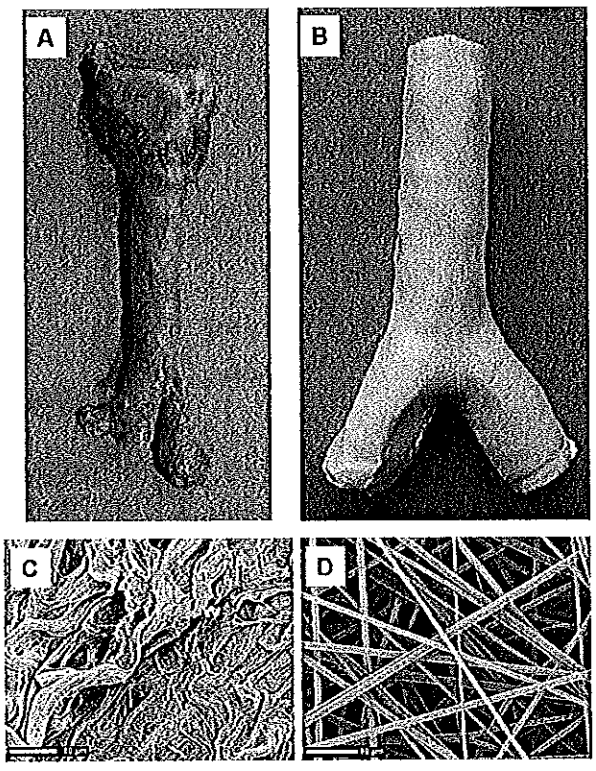

FIGURE 4. Synthetic trachea as a tissue-engineered scaffold for surgical replacement. Native trachea (A), electrospun trachea (B), scanning electron micrographs of the native (C), and synthetic trachea (D). [Color figure can be viewed in the online issue, which is available at wileyonlinelibrary.com.]

electrospun scaffold reproducing the entire trachea has been obtained and the assessment of its performance is currently ongoing (Fig. 4).

A novel and alternative selection of materials for the fabrication of an ECM-like platform was presented by Hinderer et al.,[13] electrospinning a hybrid substrate made of PCL, gelatin, and decorin. The microstructure of the collected mat was characterized by nanofibers with an average diameter of 0.42 ± 0.20 μm and average pore size of 14.4 ± 6.4 μm^2. Immunofluorescence analysis showed that decorin patterns were randomly distributed throughout the entire scaffold. Human primary airway epithelial cells were cultured onto the electrospun mat. The presence of physiologically spread cells was detected, in great contrast to the control case PCL/gelatin mat, on which only rounded and spherical cells were observed. Electrospinning a protein concurrently with a polymer can be an effective approach when a biologically active substrate is requested to improve the cell response. However, several issues might be highlighted, being related to the mechanical performances of an electrospun matrix used for trachea tissue-engineering applications. To address this issue, a composite scaffold made of several materials that combine specific characteristics and exhibit tailored mechanical properties and biological cues, at the same time, can be a suitable approach. This fabrication concept was considered by Shi et al.,[14] who presented an N-carboxyethylchitosan/nanohydroxyapatite (NCECS/nHA) scaffold as a potential biomaterial for a tissue-engineered trachea. A colloid solution, obtained combining NCECS solution with nHA, was freeze-dried to obtain a porous thin film (pore size range: 300–600 μm). The resulting scaffolds were mechanically tested in dry and wet conditions and their cytocompatibility was assessed *in vitro* using rabbit tracheal chondrocytes. However, at this early stage the reported results seem to be very preliminary for a possible application for tracheal tissue engineering. The authors stated that the mechanical properties were in the range of normal cartilage as resulted from literature data, while a direct comparison with tracheal cartilage would have been more representative.

In vivo scaffold assessment

Several scaffolds, made up of one or more synthetic polymers [e.g., polyglycolic acid (PGA), PLA, PLGA, polyester urethane, poly(ethylene oxide)-terephthalate/poly(butylene terephthalate), polyethylene oxide/polypropylene oxide copolymer (Pluronic F-127), gelatin sponge] have been investigated *in vivo* for tracheal repair.[15] In this regard, preseeding with cell lineages or treating with peripheral blood, coating with peptides, and dealing with multilayered scaffolds appeared to be three most promising approaches to obtain tracheal regeneration.

Several cell types have been utilized for tracheal tissue engineering, from chondrocytes to MSCs, obtained from different donor tissues. The presence of preseeded chondrocytes, either mixed with biodegradable hydrogel (Pluronic F127) and seeded on a cylindrical shaped high density polypropylene (20 mm length and 8 mm diameter)[16] or seeded on PLA/PGA fibers wrapped around a silicone tube (15 mm length and 6 mm diameter),[17] alleviated the postimplantation inflammatory reaction and improved the formation of cartilaginous-like tissue with native-like biomechanical properties. To create a biomimetic construct, multicell-type approaches have been evaluated: PGA meshes, wound around a helical template (50 mm length and 20 mm diameter) and seeded with nasal septal chondrocytes and fibroblasts, were anastomosed into a 5-cm defect within a sheep trachea. Even if tissue morphology and composition were similar to native tracheal tissue, the implanted constructs collapsed and tracheomalacia was observed in animals after anastomosis.[18] In a subsequent report, PGA matrix (30 mm × 40 mm × 2 mm) seeded with chondrocytes (derived from nasal septum), and wrapped around a silicon tube (30 mm length and 7 mm diameter), has been implanted subcutaneously into mice. After 6 weeks, nasal epithelial cells suspended in a hydrogel were injected into the embedded cartilaginous cylinder. The silicon tube was then removed and the construct was implanted. After 4 weeks, the morphology of the implants resembled that of native trachea, suggesting the possibility to regenerate both the cartilage and epithelial portion of the trachea.[19] Subcutaneous implantation into athymic mice was also considered to *in vivo* evaluate the biological and mechanical response of PGA mesh sheets (Neoveil®) seeded with rabbit auricular chondrocytes.[20] After 2 and 3 weeks of implantation, Young's modulus of engineered cartilage was significantly lower than that of native tracheal cartilage, whereas after 6 and 8 weeks could not be measured.

A polypropylene mesh tube (260 μm pore size), reinforced with a polypropylene spiral, coated on both sides with a solution composed of type I (70%) and type III (30%) collagens and infiltrated with peripheral arterial blood, has been evaluated as a tracheal patch. The results confirmed a favorable epithelialization, with proper reconstruction of original contours.[21] Using a similar prosthesis soaked with peripheral blood, bone marrow aspirate or bone marrow MSCs, Nakamura et al.[22] showed that bone marrow and MSCs seemed to facilitate healing and functional recovery, in particular the ciliar movement of the reconstructed tracheal segment. However, these promising approaches have been used only to repair tracheal defects and further long-term observation is required. An interesting alternative, based on the reciprocal interaction of gingival fibroblasts (GFBs) and adipose-derived stem cells (ASCs), seeded onto an artificial multilayered graft collagen sponge/polypropylene mesh, was presented by Kobayashi et al.[23] The scaffold was implanted in rats with tracheal defects (approximately 3 mm wide by 6 mm long), and a tight adhesion of multilayered epithelium to a subepithelial layer was reported at 1 week after transplantation. After 2 weeks, highly ciliated pseudostratified epithelium associated with goblet cells and basement membrane was observed. This study demonstrated that the presence of cells, in particular GFBs and ASCs, induces epithelial regeneration, secreting specific growth factors with distinct effects on epithelial proliferation and differentiation. Surface

modifications represent an alternative approach to enhance cell adhesion and proliferation. Treating synthetic prosthesis with different peptides, proteins and/or tissue growth factors has been investigated by several authors. For example, PGA meshes (18 mm × 6.5 mm, 1.5 mm average thickness), embedded with alginate encapsulated chondrocytes and conditioned with RGD, were implanted either subcutaneously or as tracheal patches (15 mm × 3.5 mm). Both implants allowed the formation of mature cartilage, even if the presence of RGD did not have any remarkable effect on the regenerative process.[24] PGA meshes (100 mm × 10 mm × 2 mm), seeded with MSCs and placed in the grooves of a silicone helical template (50 mm length and 20 mm diameter), have been conditioned with transforming growth factor β2-loaded gelatin microspheres. After subcutaneous implantation, the constructs resulted very similar to native tracheal cartilage, thus effectively promoting cartilage regeneration *in vivo*.[25] PU sponges conditioned with collagen, RGD, fibronectin or apatite and implanted as tracheal patches (8 mm × 8 mm), showed that the latter two agents favored epithelialization, tissue ingrowth and lower inflammatory response.[26] Regeneration of tracheal epithelium was assessed *in vivo* using a collagen *vitrigel* scaffold characterized by a smooth surface to facilitate epithelial cell migration after implantation.[27] The proposed scaffold, obtained by stacking collagen sponge, polypropylene mesh, collagen sponge, and *vitrigel*, was implanted into rats to repair a tracheal defect (approximately 2 mm wide by 4 mm long), with the *vitrigel* layer facing the lumen. The average thickness of the regenerated epithelium was greater in the *vitrigel* model group compared to the control group, the latter being an analogous scaffold without the *vitrigel* layer (follow-up 28 days). This result was attributed to the smoothness of the collagen sponge surface due to the presence of the *vitrigel* layer, contributing to the migration of epithelial cells from outside of the defect. The same research group, more recently, followed a modified route in which the collagen *vitrigel*-sponge scaffold was loaded with basic fibroblast growth factor (b-FGF).[28] Loaded (10 or 100 ng of b-FGF) and control scaffolds were implanted as described previously. Infiltration of inflammatory cells within the scaffold loaded with 10 ng of b-FGF was observed at 7 days. Fibroblasts were observed only in scaffolds loaded with 100 ng of b-FGF, this occurrence being associated to the formation of a thick subepithelial layer, promoted by growth factor release. This has to be considered a positive result because it might contribute to offer resistance to external environmental insults, for example, coughing. Moreover, the incorporation of b-FGF into a scaffold contributed to overcome the problems associated to its short half-life (2.5 days), sustaining proliferation of ciliated cells and angiogenesis. However, only limited success has been reported using b-FGF as an active concurring factor to heal tracheal defects.[29] To further investigate this issue, a hybrid mesh of PLGA and collagen was implanted into rabbits for 6 months to repair an anterior defect created in the tracheal rings (5 mm wide and 10 mm long). The implanted trachea was externally reinforced with a bioresorbable stent of PCL-PLA copolymer (25:75), partially cut in a longitudinal slit, wrapped with a gelatin hydrogel sheet, and loaded with 100 μg of b-FGF. The outcome was marginally positive as the presence of the hybrid scaffold resulted in a weak inflammatory reaction in the early phase, but subsequently inflammatory cells moved to the submucosal layers in the native trachea. Moreover, even if b-FGF-loaded scaffolds were characterized by a significantly higher elastic modulus, compared to the control cases (gelatin hydrogel with saline and control), it remained significantly lower with respect to native trachea. This study also demonstrated that the chosen strategy did not allow the complete replacement of the tracheal defect.

The effectiveness of collagen scaffolds in therapeutic strategies, aimed at speeding up the regeneration process, relays of the fact that this protein is the major component of ECM and plays an active role in cell migration and proliferation. However, the mechanical characteristics of collagen-based scaffolds may be inadequate to retain the ring structure of the trachea after implantation, thus requiring a structural support. A ring-shaped type II collagen sponge, reinforced by a PCL scaffold, was proposed by Lin et al.[30] A PCL stent was firstly molded into a grooved hollow cylinder to partially reproduce the stacked cartilaginous rings of the trachea. The polymer solution was frozen and freeze dried in vacuum to obtain a porous structure. Subsequently, the scaffolds were soaked in a collagen solution, frozen and freeze dried again in vacuum. Finally, the dried collagen sponge was cross-linked by 1% 1-(3-dimethylaminopropyl)−3-ethyl-carbodiimide hydrochloride. The shape of the resulting prosthetic device did not resemble the anatomical one, lacking both of the typical C-structure and the *pars membranacea*. Cell seeding was carried out using articular chondrocytes, and the construct was cultured for 7 days before implantation in standard incubator conditions. The graft was then implanted subcutaneously, for 4 or 8 weeks, in nude mice. At the end of the experimental period, all tissue-engineered tracheal implants retained their initial shape, and the modulus was about 60% higher compared to neat PCL scaffolds, as measured by dynamic mechanical analysis in the three-point bending mode.

To develop scaffolds of improved biocompatibility and appropriate mechanical properties to support the formation of cartilage *in vivo*, multilayered approaches have been evaluated by combining collagen with different bioresorbable materials. A biodegradable scaffold, consisting of a collagen sheet, a PGA mesh, and a copolymer (L-lactide/ϵ-caprolactone) coarse mesh, seeded with auricular chondrocytes, was implanted into a defect in the cervical trachea of rabbits.[31] Before implantation seeded constructs were incubated for 1 day in standard conditions. The response elicited by this scaffold was compared to that of similar scaffolds treated with b-FGF-loaded gelatin microspheres. Tracheal lumens, for all the retrieved specimens at autopsy, were affected by a slight deformation. The result was ascribed to the mechanical properties of the scaffolds and to the degradation profile. At 1 month after implantation, epithelial migration from the native tissue was detected, but cartilage was

not observed in the constructs. Only after 3 months a small amount of cartilage appeared in the constructs, more evident in those scaffolds treated with b-FGF. However, the efficacy of the multilayered approach was not assessed.[31] Although evaluated only in one dog, another multilayered construct (silicon stent, collagen sponge, and gelatine sponge) was implanted to repair a circumferential defect and resulted in a patent trachea even after silicon stent removal.[32] Following this fabrication procedure, it is possible that the collagen layer could be detached either during the surgical procedure or after implantation. This was the rationale that led Sato et al.[33] to an *in vivo* assessment of the performance of a prosthesis consisting of two collagen layers separated by a polypropylene framework with the luminal surface coated by a biodegradable layer of poly(L-lactide-*co*-caprolactone) (PLLC). The tubular scaffold (30 mm long, 15 mm internal diameter, and reinforced with 5 rings of polypropylene monofilament) was implanted in adult dogs in the left main bronchus position after resection of a 10-mm segment. Bronchoscopic evaluation confirmed that the polymer protected the collagen layer for 7–14 days after implantation. The luminal surface was completely covered with epithelium, containing ciliated columnar and squamous epithelium, in four of five dogs, suggesting that the protection of the collagen layer is crucial for the promotion of an effective epithelialization.

To assess the potential of an ECM-like scaffold, a synthetic trachea was fabricated by electrospinning *DegraPol®*, a degradable block polyesterurethane consisting of crystallizable blocks of poly((R)-3-hydroxybutyric acid)-diol and blocks of poly(ε-caprolactone-*co*-glycolide)-diol linked by a diisocyanate.[34] The toothed profile was obtained by firstly collecting the polymeric fibers onto a rotating mandrel at ~300 rpm (5 mm diameter) to obtain a 2-mm thick scaffold made up of fibers whose diameters ranged between 6 and 25 μm. Then, a 1-mm thick blade for metal cutting was used to run for 2 mm along the longitudinal section of the scaffold and leaving a 0.5-mm layer of fibers on the mandrel. The *in vivo* study was not carried out considering the prosthesis for its intended use, because the construct was implanted into rabbits in an isolated vascular flap, using the common carotid artery and the external jugular vein as blood carriers, and a Teflon cylinder was also introduced inside the lumen to prevent tissue overgrowth. After implantation, the novel *in vivo* synthesized collagen was organized in bundles of tightly packed fibrils with regular and parallel arrangement, CD31 positive cells (progenitor endothelial cells) crowded the external surface of the scaffold. After short time from cell invasion, the expression of CD31 was localized to the endothelial cells forming the blood vessel walls. Cell population increased over time, and the differentiation into muscle fibers occurred as validated by expression of α-smooth muscle actin.

Assessment of the first *in situ* human tissue-engineered trachea, as defined by the authors themselves, was reported by Omori et al.[35] A *Marlex* mesh coupled with collagen sponge, derived from porcine dermal collagen, was implanted into a 78-year-old woman affected by thyroid cancer. The right half of three rings of the trachea was resected and the scaffold properly trimmed to repair the defect. After 2 months, the synthetic material was covered by the epithelium, and a complete coverage was observed after 20 months without complications.

Tissue engineering the entire trachea

Tubular or trachea-like scaffolds were tested in orthotopic *in vivo* studies to evaluate tissue regeneration and healing after long segment resection. Several approaches were proposed using both straight and bifurcated devices fabricated with different materials and techniques.

In 1994, Vacanti et al.[36] fabricated a tubular scaffold starting from sheets of fibrous polyglycolic acid (15 μm fiber diameter), seeded with chondrocytes. After an incubation period, cell–polymer constructs were wrapped around 8F *Silastic* tubes (3 cm length) and implanted subcutaneously into nude mice. Cylindrical specimens were explanted at 4 weeks, evaluated grossly and used to replace large (four to six rings) circumferential segments of resected trachea into rats. However, the four implanted animals died in a very short period after the surgical procedure, the last of them surviving just 1 week, and the cause of death was not mentioned.

The importance of a functional epithelium lining the lumen of a prosthetic trachea was stressed by Kanzaki et al.,[37] who proposed a straight vascular *Dacron* prosthesis reinforced with a spiral-shaped polypropylene monofilaments. The scaffold was first implanted subcutaneously into rabbits to allow blood vessels and connective tissue to migrate and infiltrate within the synthetic material. After 4 weeks, the graft was vertically opened and two cultured tracheal epithelial cell sheets (cells cultured onto temperature-responsive culture dishes by grafting poly(N-isopropylacrylamide)) were transplanted to the inner surface of the prosthesis. The resulting bioartificial trachea was implanted, after resection of cervical trachea (3 cm length), into rabbits. A mature columnar epithelium was found at the interior portions of the graft where the cell sheets were transplanted at 1 month.

A tracheal prosthesis of PCL was developed and *in vivo* tested in rabbits. The main advantages of using this polymer are the slow degradation profile and mechanical characteristics potentially suitable to maintain the long-term patency.[38] PCL was dissolved in 1,4-dioxane, the solution was poured into a copper cylindrical mold and frozen at −20°C for 8 h. Solvent crystals were then removed by freeze-drying for 48 h in vacuum to obtain a highly porous hollow cylinder (10–40 μm pore size). The lumen surface of some of the tubes was modified with genipin cross-linked gelatin. However, the resulting prosthesis did not resembled the natural trachea anatomy, lacking of the typical grooved morphology and *pars membranacea*. The scaffolds were implanted in six adult rabbits, the survival being higher for animals receiving surface-modified PCL tubes (43 ± 8 vs. 30 ± 10 days for control tubes). PCL tubes without gelatin coating were completely covered with epithelial cells layered on the granulation tissue, and the recipient animals died due to the

stenosis located at the center of the tube. PCL tubes coated with gelatin prevented granulation tissue overgrowth, but the lack of an epithelial lining caused ingrowth of granulation tissue from the anastomotic sites into the lumen which eventually led to occlusion. A copolymer of L-lactide and PCL was used to produce a sponge-like tubular structure reinforced by a woven fabric of PGA and coated with gelatin to prevent air leakage (80% porosity; 20–100 μm pore size).[39] The graft (6 cm length) was implanted into sheep, as cervical tracheal replacement, by performing end-to-end telescopic fashion anastomosis, with a silicone stent (7 cm length) inserted temporarily to prevent graft collapse. An axial approximation of the trachea was observed, which was considered a result of the natural healing of a tracheal defect supported by a bioresorbable scaffold. However, a complete and spontaneous reconnection of the native trachea was not observed in sheep that reached the 9-month follow-up, in addition the survival was not assured without stenting. It was stated that, given the close proximity of the native tracheal ends, an end-to-end anastomosis could be performed at that time. From this study the regenerative/healing process of the native tissue, using an engineered scaffold, was confirmed, but the approach implies a second surgical stage to completely repair the original defects. This event can expose the patient to several complications, because morbidity and mortality rate of tracheal surgery is significantly higher when repeated procedures are needed.

A different approach for the development of an artificial trachea was followed by Naito et al.[40] A scaffold was produced using fibroblast and collagen hydrogels, mechanically supported by osteogenically induced MSCs in ring-shaped 3D-hydrogel cultures, and implanted into rats to bridge a 5-mm defect beneath the larynx. Six of nine animals died during the implantation, whereas three animals survived for 24 h and died the following day. The macroscopic evaluation of the excised samples revealed the presence of strictures in the anastomotic regions. The main limitation of this approach, as stated by the authors themselves, can be traced back to the lack of epithelium on the lumen of the scaffold.

The majority of tracheal tissue-engineered approaches has been focused on the development of scaffolds for large circumferential defect repair; less common are the Y-shaped substitutes for bifurcation repair. A Y-shaped scaffold made of *Marlex* mesh (polypropylene, 260 μm pore size), reinforced with polypropylene spiral and coated with porcine skin collagen types I and III, was implanted into dogs.[41] A Y-shaped silicon stent was inserted into, but non fixed to, the prosthesis, and 8 weeks after surgery it was removed endoscopically. Of the 20 dogs, 14 died after experimentation due to obstruction of the main bronchus, omental necrosis, and air leakage. The same construct (60 mm long and 18 mm outer diameter), used for the replacement of the trachea-bronchial bifurcation, was evaluated after a long-term follow-up. After 5 years, the prosthesis was infiltrated by the surrounding connective tissue, completely incorporated by the host trachea and bronchus, and neither stenosis nor dehiscence was observed. Moreover, the frequency of the epithelial cilia was maintained within the normal range, indicating functional recovery of the regenerating airway.[42]

Referring to human patients, an *in situ* tissue-engineering approach was considered by Omori et al.[43] for the reconstruction of the larynx and trachea in the presence of subglottic stenosis or thyroid cancer invasion. For this aim, a *Marlex* mesh tube, covered with collagen sponge, was used as scaffold. The device, made of a polypropylene mesh (260 μm pore size) reinforced with a supporting polypropylene ring, was approximately 50 mm long with a diameter of 18, 20, or 24 mm. The inner and the outer sides of the tube were coated with collagen (porcine dermal atelocollagen, types I and III) and the resulting scaffold was heated at 140°C in vacuum to induce cross-linking reactions. The device, injected with autologous venous blood, was implanted into four patients affected by airway stenosis or cancer invasion. It was reported that a good epithelialization on the luminal surface occurred in all the patients, as verified during the postoperative observation period (8–34 months). Air leakage was observed in only one case.

A relevant and significant application of tissue-engineering concepts was clinically carried out by implanting a synthetic tracheal substitute into a 36-year old male patient affected by a recurrence of a primary tracheal mucoepidermoid carcinoma involving the distal trachea and both main bronchi.[44] The tracheobronchial graft was fabricated using a nanocomposite polymer (polyhedral oligomeric silsesquioxane - poly(carbonate-urea)urethane; POSS-PCU) and two different routes: a cast form for the cartilaginous "U"-shaped rings and a coagulated form for the "connective" tracheal portion. To obtain the tracheobronchial scaffold, the "U"-shaped POSS-PCU rings were placed around a glass mandrel of the dimension of the patient airway, at 3 mm intervals. The entire mold was placed in a POSS-PCU solution (previously prepared with 50% $NaHCO_3$) and then in deionized water for 3 days to obtain the coagulated porous scaffold. Before implantation, the bioartificial scaffold was seeded in a bioreactor with autologous bone-marrow mononuclear cells for 36 h. After dynamic culture, the cells formed dense clusters and an ECM-like structure was observed. At 1 week, postoperative bronchoscopy assessments verified a normal and patent airway, whereas biopsy samples showed the presence of necrotic connective tissue associated with fungi contamination and neovessels. After 2 months from transplantation, biopsy revealed large granulation areas associated with smooth epithelialization and some organized vessels formation while neither bacterial nor fungi contamination was observed. After 12 months, an almost normal airway and improved lung function were assessed.

ESOPHAGUS

In vitro scaffold assessment

In vitro studies, aimed to evaluate tissue-engineered scaffolds for esophagus regeneration, are mainly related to the assessment of cell response to several bioresorbable polymers and the role of their morphological characteristics

(such as porosity and pore size) as a function of the fabrication techniques. A porous collagen scaffold (*OptiMaix-3D*™ 13 mm diameter, 1.5 mm thickness, and 25–100 μm pore size) was used to seed rat esophageal epithelial cells to be statically cultured up to 8 weeks.[45] Cells expressed CK-14, demonstrating phenotypic preservation, but cell migration was not observed through the thickness of the scaffold. Interestingly, before seeding, scaffolds were sewn into tubes to mimic the esophageal structure. However, the actual influence of this shape on cell response was not investigated, also lacking the results on the respective planar scaffolds as a control case. The same scaffolds were subsequently tested for culturing ovine esophageal epithelial cells, specifically *OptiMaix*™-2D and -3D collagen scaffolds (2D, ~<0.5 mm; 3D, ~1.5 mm thick).[46] 2D scaffolds supported cell viability up to 6 weeks, leading to the formation of a single layer epithelium after 3 weeks, that not occurred in the case of cells seeded onto 3D scaffolds.

When not-naturally derived polymers are used, the lack of specific cues to promote effective cell cultures is a common concern and *ad hoc* experimental protocols are thus proposed to overcome this drawback. For this aim, porous scaffolds made of poly(L-lactic acid) (PLLA), PLGA 75/25, PLGA50/50, and PCL/PLLA and fabricated by salt leaching/gas foaming were tested by seeding rat esophageal epithelial cells and evaluating the influence of calcium concentration at two different values (1.5 m*M* Ca^{2+} and 0.03 m*M* Ca^{2+}) for 4 days.[47] Afterward, all the construct were cultured in 1.5 m*M* Ca^{2+} until the end of the experimental period (18 days). Two different pore sizes were considered, that is, 150–250 and 38–75 μm. Results showed that the smaller pore size induced less stratification and keratinization, whereas larger pores led to pockets of stratified epithelium, rather than one continuous layer. Moreover, the initial low calcium concentration contributed to a slightly better morphology and proliferation than those under high concentration. However, a natural scaffold tested for comparison, that is, *AlloDerm*, was characterized by superior cell morphology, leading to a stratification and differentiation similar to native esophagus. Using a different approach, solvent cast PLGA membranes were aminolyzed with 1,8-diaminooctane, followed by collagen immobilization with glutaraldehyde (GA) as a coupling agent.[48] The obtained scaffolds were then seeded with porcine esophageal smooth muscle cells. Results showed that collagen substantially promoted cell attachment, growth, and proliferation with respect to the control case. This kind of surface modification was further assessed considering different polymers, reagents, and other scaffold fabrication techniques. Zhu et al.[49] prepared a membrane of PLLC to be aminolyzed with 1,6-hexanediamine to introduce free amino groups as active sites for fibronectin or collagen, separately bonded with GA as a coupling agent. The membranes were tested using the three types of porcine esophageal cells, that is, smooth muscle cells, fibroblast and epithelial cells. Both the treatments well supported the cell growth, fibronectin proving to be more effective in stimulating mitochondrial activity. Subsequently, the aminolysis method was also used to graft collagen IV on PCL membranes to test the response of porcine esophageal epithelial cells.[50] This chemical treatment was also considered to modify ECM-like scaffolds, because PLLC was processed by electrospinning (to collect a fibrous mat), aminolyzed again (to introduce free amino groups as active sites for fibronectin), and seeded with porcine esophageal epithelial cells (to evaluate cell response).[51] Aminolysis confirmed its potential to accelerate the epithelium regeneration, also showing higher collagen IV synthesis compared to the control scaffold. It is well established that the replication of the natural ECM is one of the key points that drives the development of suitable tissue-engineered scaffolds, and electrospinning is considered a straightforward technique for this task. Therefore, this approach has been extensively adopted, introducing specific processing conditions to improve the resulting cell response. For this purpose, Leong et al.[52] evaluated electrospun poly(D,L-lactide) scaffolds with nanoporous surface induced by rapid phase separation of the polymer/solvent mixture during the process. The rationale was to enhance the levels of adsorbed proteins, improve the biological response of porcine esophageal epithelial cells and then compare solvent cast films and electrospun scaffolds with no pores on the fiber surface. According to the authors, the peculiar morphology of the electrospun fibers enhanced protein adsorption and cell attachment. However, biological assays were carried out only for 24 h; therefore, results for prolonged culture period should be considered to validate this approach. With the aim to mimic the mucosa of a normal esophagus, PLLC scaffolds were produced by means of thermally induced phase separation to obtain pores of different size, that is, 1–10 μm diameter on one side and ≥50–100 μm diameter on the other side and in the bulk.[53] Primary porcine esophageal epithelial cells were seeded on the microporous side and primary fibroblasts on the opposite one. The scaffold supported the coculture for 14 days, highlighting some problems related to the direct signal transferring between these two types of cells due to the reciprocal distance.

In vivo scaffold assessment

Studies considering *in vivo* scaffold implantation in esophageal position can offer a significant and more adherent model, and several reports could be cited to give an overview of different materials, approaches, and animal experimentation. However, a critical analysis to compare and identify a potential route to actually address the issue of producing a suitable tissue-engineered scaffold should be required. A typical surgical approach to obtain an esopagheal scaffold consists of wrapping a selected material around a tube to impart and retain the tubular shape after implantation, the tube is then removed and the resulting tubular scaffold should act as a functional device. This strategy was followed to evaluate a long artificial esophagus obtained by coating a silicone tube with 5 mm thick freeze-dried collagen sponge.[54] The resulting structure was implanted into dogs to recover a 10-cm defect, the tube was explanted after 6 weeks. Survived dogs at explantation (five

of seven) were allowed to live for more than 6 months. The regenerated esopaghus presented the luminal surface completely covered with epithelium, normal esophagus glands and immature muscle tissue. Similarly, a bioresorbable scaffold supported by a nasopharyngeal airway tube was used to repair a defect in the esophagus in a pig model.[55] In this study, a fiber patch composed of PLA and PCL (50:50), reinforced with PGA fibers, was implanted into a 4 cm × 2 cm oval-shaped defect. The tube, acting as a stent, was then sutured with *Vicryl Rapide* suture. The rationale of this approach was to temporarily support a deformable structure until its replacement by connective tissue at 1–2 weeks. For this aim, the suture was characterized by a short-term strength of 7–10 days, allowing the tube to fall off into the intestine. The reported results confirmed the healing process, as the squamous epithelium was regenerated at 4 weeks and the muscular layer at 8 weeks was greater than that at the previous time point, and further increased at 12 weeks, becoming similar to the native tissue. However, as stated by the authors themselves, concerns can be raised due to the presence of the dislodged stent that might cause bowel obstruction. This latter issue could be overcome using a biodegradable device. According to this approach, the possibility for the scaffold to effectively support tissue regeneration is governed by the host natural healing mechanism and this could limit its feasibility because many variables may affect the expected results. It seems therefore attractive to plan alternative strategies that can speed up the recovery process, especially when very long defects need to be treated. On this basis, even if not directly evaluating the healing process induced by a scaffold substitute for esophageal restoration, Saxena et al.[56] investigated the potential role of omentum as an *in situ* bioreactor by wrapping four types of collagen scaffolds around an endotracheal tube to impart the tubular structure and then implanting the resulting constructs into adult sheep omentum for 8 weeks. For this aim, acellular bovine pericardial collagen (*Tutoplast*™), acellular cross-linked (HDMI hexamethylene diisocyanate) porcine dermal collagen (*Permacol*™), porcine porous collagen (*OptiMaix-3D*™) and laboratory fabricated bovine tendon dual-layered (type I) collagen were investigated. The first two types, being dense scaffolds, gave contrasting results suggesting limited applications, the third one demonstrated omental integration and marked differences in cellular infiltration thus resulting the most suitable candidate. Based on the same approach, Saxena et al.[57] then investigated the role of omentum as an active means to promote vascularization of a seeded scaffold, a mandatory requirement for the reproduction of functional 3D structure. For this aim, GA cross-linked collagen sponges (about 100 μm pore size), preseeded with fibroblasts, were assessed as a substrate for ovine esophageal epithelial cells. After 48 h of culture, the constructs were wound up around a sterile endotracheal tube (8.8 mm outer diameter) to reproduce a tubular shape. The resulting structures were then implanted into the lower abdomen of lambs (10 constructs in four lambs) and wrapped with omentum, to test the induced vascularization and cell viability. At retrieval (8 or 12 weeks postimplantation), the constructs showed a tubular structure with a thickness of 4 mm. Histological evaluation revealed cellular growth within the structure and absence of inflammation. Vascular ingrowth in the peripheral regions of the collagen scaffold was confirmed after 12 weeks. A similar strategy was considered by Nakase et al.,[58] being based on the use of PGA nonwoven felt as a substrate for human amniotic membrane seeded with oral keratinocytes and fibroblasts. The scaffolds were rolled around a polypropylene tube (3 cm length and 2 cm diameter), implanted in dog abdomen and wrapped with omentum. After 3 weeks the implant was retrieved and used to replace a 3 cm resection of the esophagus. Only two cases of six developed strictures compared to the unseeded scaffold (control case), in the latter one all implants were characterized by strictures that progressed to almost complete esophageal obstruction within 2–3 weeks. However, although tissue-engineered constructs showed squamous epithelium, muscularis mucosa and smooth muscle tissue similar to that of the adjacent native esophagus and good distensibility, the presence of esophageal glands and peristalsis were absent, that is not a necessary requirement for esophageal reconstruction as claimed by the authors. This appears debatable without further evidence to support this point, especially as the final goal of tissue engineering is the regeneration of a functional tissue as close as possible to the native one. Therefore, even if the approach based on the use of bioresorbable polymers seems to offer a possible route to be eventually improved in terms of material selection and preimplantation treatment, it can be affected by negative outcomes as reported by Lynen Jansen et al.[59] Their work showed that the absorbable *Polyglactin 910* (Vicryl®) mesh led to worse results compared to those obtained using nonabsorbable polyvinylidene fluoride (PVDF) mesh to repair semicircular esophageal defects (0.5 cm × 1 cm), created 2 cm proximal to the cardia in 10 rabbits. Only two animals in the *Polyglactin 910* group survived for the entire observation period (12 weeks) and the mucosa was regenerated. However, an ulceration with abscess formation and diffuse inflammation was found in one animal, as a consequence of early degradation, probably caused by gastroesophageal acid reflux.

Cell–scaffold seeding before implantation should occur, in accordance with the tissue-engineering paradigm, thus improving the probability of success. In this regard, PGA/PLA scaffolds were seeded with rat smooth muscle-like cells.[60] The constructs were then implanted and covered with omentum to repair a defect (3 mm width and 5 mm length) created in the abdominal esophagus, 5 mm proximal to the cardia. At 10-week postimplantation, a complete re-epithelialization of the esophageal lumen, with increasing organization of the muscularis layers, was observed. At 16 weeks, a modest increase in muscularis layer regeneration, compared to the 10-week time-point, was also detected. A more sophisticated approach considered esophagus organoid units (mesenchymal cores surrounded by epithelial cells), isolated from neonatal or adult rats, and heterotopically transplanted on 2-mm-thick nonwoven PGA (15 μm

fiber diameter) shaped into 1-cm tubes (0.5 cm outer diameter and 0.2 cm inner diameter) and sealed with PLLA, which were implanted in syngeneic hosts.[1] The implanted constructs recapitulated the architecture of the implantation site with keratinized squamous epithelium and actin-positive muscularis propria, showing no signs of deterioration for 42 days in continuity with the GI tract.

INTESTINE

In vitro scaffold assessment

Most of the studies investigating intestinal tissue engineering have used *in vivo* implantation of cell–polymer constructs. The potential application of hyaluronic acid-based biomaterials, either as 3D nonwoven scaffold or flat sheet macroporous membrane, have been evaluated for intestinal tissue growth. I*n vitro* studies were performed with human epithelial colorectal adenocarcinoma cells (Caco-2 cells).[61] Long-term cell cultures demonstrated that hyaluronic acid esters, mold in flat sheet membranes, are good substrates for intestinal tissue growth and differentiation, performing better than microporous polycarbonate and thus being a potential material for tissue-engineering intestinal applications. The same cell line was used to test the influence of scaffold topographical cues and a porcine intestinal basement membrane was replicated using plasma enhanced chemical vapor deposition of poly(2-hydroxyethyl methacrylate) on native tissue.[62] Cells were characterized by a high viability (>85% over 12 days of culture), not dissimilar from that assessed onto widely used tissue culture substrates. However, the preservation of the biological topography upon poly(2-hydroxyethyl methacrylate) removal from the underlaying substrate needs to be evaluated.

To deal with 3D constructs, a chitosan/collagen (1:1 ratio) tubular scaffold was fabricated using the freezing and lyophilizing method.[63] The obtained porous scaffold (170 μm average pore size) was seeded with rat smooth muscle cells in a thrombin polymerized fibrinogen hydrogel. After 14 days, the constructs were characterized by contraction and relaxation, mediated by acetylcholine and vasoactive intestinal peptide, showing also a physiologic response to KCl similar to the control case (cell grown on tissue culture dishes).

Rat intestinal fibroblasts and epithelial cells, cocultured on different collagen-based supports, were used to produce 3D constructs with intestinal-like epithelial-type characteristics, suggesting the possibility to obtain tissue-engineered multicellular intestinal constructs.[64] Porous nanocomposite scaffolds, made of POSS and poly(caprolactoneurea) urethane, were developed using a solvent casting/particulate leaching technique, to fabricate grafts with different pore sizes (150–250 and <100 μm) and porosities (80 and 40%). All the evaluated samples had suitable physical and chemical properties, allowing adhesion and proliferation of rat intestinal epithelial cells and suggesting that the nanocomposite may represent a valuable alternative for intestinal tissue engineering.[65] Sung et al.[66] fabricated a collagen scaffold able to mimic the microscale 3D geometry of the GI tract. The idea was to combine laser ablation and sacrificial molding techniques, using an alginate hydrogel as the sacrificial template. Seeded with Caco-2 cells, it was possible to obtain finger-like structures resembling human jejunal villi covered with epithelial cells. This approach could allow to obtain, in a simple, easy and cheap way, 3D physiologically representative *in vitro* models to advance tissue-engineering research in this field. To better resemble the small intestine lumen and to simulate the cell differentiation, Caco-2 cells have been dynamically cultured on hollow fibers. Unlike cellulose acetate, polysulfone, and polyacrylonitrile, polyethersulfone (PES) hollow fibers (inner diameter of 900 μm; thickness of 330 μm; inner surface covered with microwells with 5–10 μm diameter) allowed cells to symmetrically form confluent monolayer on the inner lumen surface and to accelerate the cellular differentiation within a short time period (6 days of culture instead of 13 days of standard culture). Moreover, hollow 3D fiber cultures enhanced the activities of intestinal transports, like P-glycoprotein, suggesting that, when cultured on curvy surface similar to the topography of the small intestine, Caco-2 cells might become rapidly differentiated and polarized, sustaining the enterocyte-like structures morphologically and functionally.[67]

In vivo scaffold assessment

An ideal intestinal replacement should not only contain the different cellular components in each layer (such as circular and longitudinal smooth muscle components with intramuscular interstitial cells) but also integrate with the existing muscular and neuronal layers to receive cues from the central nervous system to facilitate peristalsis, gut motility, digestion, and excretion. Collagen [type I (70–80%) and type III (20–30%) atelocollagen] sponge grafts, freeze-dried and cross-linked, seeded with autologous MSCs, just before implantation, were used to reconstruct a 5-cm segment of dog small intestine. After 4 weeks, regeneration of the intestine was observed at the reconstructed site. However, a proper muscle layer, essential for functional peristalsis, was not obtained.[68] The failure of muscle layer regeneration might be due, as suggested by the authors, both to the low number of seeded cells and/or to the lack of adequate stimulus toward muscle differentiation before or after implantation. To accomplish regeneration of a smooth muscle layer, Nakase et al.[69] implanted collagen scaffolds (3 mm thick, 70–110 μm pore size, and 80–95% porosity), seeded with smooth muscle cells isolated from the stomach wall, as a patch graft (1 cm × 1 cm) in a canine model. At 12 weeks after implantation, cells demonstrated polarity of arrangement, appearing as a circular muscle layer, allowed neovascularization and epithelialization of the implanted construct and accelerated mucosal healing. However, no evidence of longitudinal muscle layer formation was reported and shrinkage of the graft area was observed, most probably related to the low mechanical strength of the collagen sponge.

Vacanti et al.[70] first reported the *in vivo* evaluation of synthetic tissue-engineered intestinal constructs. Filaments or small wafer discs, obtained by solvent casting or compression molding method of different synthetic absorbable

polymers, were seeded with rat enterocytes, cultured *in vitro* for 4 days and finally implanted in rat omentum or bowel mesentery. Successful cell engraftment has been demonstrated. However, an inflammatory response was induced by some polymers and functional studies have not been reported. The same group evaluated the transplantation of constructs obtained by seeding intestinal progenitor crypt cells onto sheets of nonwoven PGA wrapped around a *Silastic* stent. The constructs allowed regeneration of a stratified epithelium, even if a low construct engraftment has been reported.[71,72] One of the major limitations has been the difficulty in maintaining primary cultures of normal gut epithelium. To address this difficulty, studies have investigated the significance of epithelial–mesenchymal cell–cell interaction and the importance of isolating epithelial cells in conjunction with their underlying mesenchyme as organoid units (i.e., multicellular units derived from neonatal rat intestine containing a mesenchymal core surrounded by a polarized intestinal epithelium and all the cellular elements of a full-thickness intestinal section). Isolated organoid units, seeded on nonwoven sheets of PGA fibers (5 μm diameter, 2 mm mesh thickness, 60 mg/cm^3 bulk density, porosity 95%, and 250 μm mean pore size), have been implanted into the rat omentum either as sheets (1 cm × 1 cm) or as tubes (wrapped around a *Silastic* stent, internal diameter 5 mm). The formation of multiple cysts, composed of degrading polymer, ECM, fibroblasts, and smooth muscle-like cells and lined with neomucosa and surrounded by vascularized tissue, demonstrated the ability of these transplanted epithelial organoid units to survive, reorganize, proliferate, and regenerate intestine-like structures.[73] To enhance cell engraftment, the same PGA tubular scaffolds have been sprayed with 5% PLA, eventually coated with collagen type I, seeded with organoid units and implanted in rats. Results demonstrated that collagen-coated organoid unit polymer constructs allowed the regeneration of a neointestine (2–6 weeks) characterized by histological (columnar polarized epithelium with goblet and paneth cells, smooth muscle cells, villi, crypts, and basement membrane), and functional (transepithelial resistance and epithelial barrier function) features of the native small intestine.[74] Further studies demonstrated that the tissue-engineered intestine was successfully anastomosed to native small bowel, either in a side-to-side or an end-to-end fashion,[75–77] and that small bowel resection and portacaval shunt provided significant regenerative stimuli for cyst development and neomucosal differentiation.[78–80] Moreover, anastomosis to the native intestine was found to be an essential step for neomucosal morphological development, allowing the regeneration of key features of normal jejunal mucosa, including crypt-villus architecture, correct distribution of epithelial cellular proliferation and apoptosis, presence of nervous and muscular cells, correct spatial localization of gene expression, and presence of intestinal epithelium differentiation markers.[81,82] These results demonstrated that bioengineered neointestine is highly responsive to circulating trophic stimuli. Subsequent studies, using the same approach, demonstrated: (i) the development of a mucosal immune system, characterized by an immunocyte population similar to that of the native intestine,[83] (ii) the ability of the neointestinal epithelium to respond to specific endogenous regulatory intestinal peptides, with consequent increase in villus height, crypt depth, and crypt cell proliferation,[84] and (iii) the development, in the submucosa and lamina propria of the tissue-engineered small intestine, of functional lymphangiogenesis, an essential requirement for normal intestinal activities.[85] Regarding angiogenesis, the network of capillaries of the neo tissue-engineered intestine resulted to be different from that of the native tissue. Vascular endothelial growth factor (VEGF) and b-FGF levels were lower than that of juvenile intestine, suggesting a different mechanism driving angiogenesis in engineered intestine and in normal bowel.[86] Recently, it has been demonstrated that inducing VEGF overexpression led to larger constructs with increased villus, crypt height, and capillary density.[87]

Translating the technique to a mouse model, Sala et al.[88] have demonstrated that engineered tissue regenerates only from the implanted undifferentiated progenitor/stem cells, suggesting that the organoid multicellular approach provides the necessary cell population to regenerate large amounts of intestinal tissue morphologically comparable to native intestine. Considering the overall positive results, the tissue-engineered intestine has been evaluated in an autologous, preclinical large animal model (pigs), emulating conditions necessary for human therapy.[89] Organoid units have been obtained from a short segment of jejunum of 6-week-old swine, loaded onto biodegradable scaffold tube and implanted in the omentum of autologous host. The results demonstrated that a tissue-engineered small intestine, composed of all the anatomic layers of the native tissue, including a mucosa with epithelial cell types adjacent to an innervated muscle, and features of an intact stem cell niche can form in a larger animal model and can be successfully derived from autologous tissue.

Using organoid units, derived from full thickness sigmoid rat colon, Grikscheit et al.[90] demonstrated that the same synthetic graft can be also used to produce an effective *in vivo* large intestine substitute with morphological (intact epithelial, muscular, vascular, and nerve components) and physiological (vectorial ion transport, barrier function, and viability) features similar to the native tissue. The protocol for creating tissue-engineered intestine in a mouse model with a multicellular organoid units-on-scaffold approach has been recently described and documented.[91]

The main limit of all these studies was the short-period follow-up. Kaihara et al.[92] performed long-term study to evaluate the possible effects of the anastomosis on the development of the neointestine: after 9 months, the tissue-engineered intestine increased in size, maintaining histological structures resembling the native one. However, the overall patency rate of the anastomosis was 79%, suggesting that the anastomosis was still at risk of obstruction over longer period examination. Dense fibrous tissue, small bare areas that lacked neomucosa and a mild inflammatory reaction were also verified. As reported by the authors, the dysmotility of the tissue-engineered intestine could be not sufficient to drain the luminal contents completely. These

retained contents may cause a continuous inflammatory reaction of neomucosa followed by an ulcerative change of the inner surface, preventing regeneration or migration of mucosal layer from the surrounding area.

PLGA tubular scaffolds, with transverse and longitudinal porosity of controlled size (10 mm length, 1 mm wall thickness, 2 mm luminal diameter, and 100 μm pore size), have been implanted subcutaneously into a rat model. After 5 weeks, the silicon tube, placed inside the scaffolds to maintain luminal patency, was removed and the lumen of the construct was injected with intestinal organoid units.[93] Results demonstrated the development of a neomucosa with the expression of growth factors (i.e., VEGF and b-FGF) and their receptors, suggesting that the preimplantation of the scaffold would make a more favorable environment for intestinal organoid unit proliferation and tissue regeneration. Eight different microporous biodegradable polymeric tubular scaffolds, composed of PGA and/or PLLA in different combinations, obtained using different fabrication techniques (10 mm length, 0.5–1 mm wall thickness, 10–250 μm porosity, 3–5.5 mm outer diameter, and 3–3.5 mm internal diameter) were seeded with intestinal stem cell clusters and implanted into the omentum of syngeneic rats.[94] After 4 weeks, mucosal regeneration was demonstrated in almost all the evaluated scaffolds, suggesting that intestinal organoids can be engrafted onto biodegradable polyester scaffolds. However, variability was observed depending on the chosen polymeric material, processing technique and microstructure. PGA nonwoven mesh constructs, treated with PLLA, allowed the best villous and crypt development, morphology and regenerated surface area, while electrospun microfiber PGA had poor overall engraftment with little or absent crypt or villous formation. The study suggested that optimizing biopolymer composition, fiber size, scaffold porosity, and fabrication techniques could ameliorate construct structural integrity and mechanical stability, minimizing scar formation, decreasing inflammatory response, improving cellular adhesion, and promoting tissue formation and vascularization. PCL scaffolds, obtained by solvent casting and particulate leaching, loaded with b-FGF collagen or PLGA microspheres, were seeded with intestinal smooth muscle cells, wrapped around a silicon tube (5 mm diameter and 10 mm length) and implanted into the rat omentum.[95] The constructs were neovascularized within 1 month, especially the b-FGF-loaded PLGA samples. However, the smooth muscle cells demonstrated a phenotypic switch to their noncontractile forms and the neuronal layers did not regenerate.

Even if promising, most of the results till now reported have been obtained in rats, but humans would require a much greater absorptive area; the tissue-engineered intestinal constructs lack proper motility, due to the difficulty to generate neural tissue, with consequent intestinal obstruction due to aperistalsis, and the optimal cell source has still to be identified.

BILE DUCTS

In vitro scaffold assessment

Most of the *in vitro* studies on bile ducts are aimed to the formation of duct-like structures in cell cultures during liver regeneration. Preferentially, investigations have been done culturing cells (especially hepatocytes) on collagen-conditioned tissue culture plates and very few evaluated the possible use of synthetic scaffolds. PGA fibers (5 mm length and 10 μm in diameter), dip coated with a PCL solution and conditioned with *Matrigel* solution, supported the growth of hBECs and allowed the formation of phenotypically stable epithelial cell aggregates, even after 6 months. The results suggested that this culture model could be used as a long-term strategy for growing, expanding, and exploiting hBECs to obtain artificial bile ducts.[96] Different *in vitro* liver cell cultures have been tested to obtain the formation of duct-like structures. Tissue-engineered cell sheets, obtained by coculturing rat small hepatocytes with nonparenchymal cells on silicon wafers (10 cm diameter), rolled into a 3D cylinder, allowed the formation of bile-like ducts after 2 weeks from implantation in the rat omentum.[97] Immunohistological staining revealed that the cells were similar to differentiated biliary epithelial cells, suggesting that immature hepatocytes may be able to form biliary epithelium. Rat hepatocytes cultured on different nanopillar polystyrene sheets [1.0 mm thickness, 0.18, 0.5, 1.0, 2.0, and 5.0 μm pillar diameters with pillar pitches (pillar center-to-center distance) that were twice the pillar diameter], precoated with collagen solution, were able to form cell spheroids characterized by the presence of bile canaliculi associated to well-developed microvilli.[98] This was observed especially when using a pillar diameter of 2.0 μm, suggesting that it is possible to control the formation of functional bile canaliculi by optimizing the morphological properties of the substrate surface. Finally, peptide (RAD16-I) nanofiber-based hydrogel, seeded with HepG2 (a liver cell line), allowed to obtain 3D cell spheroids with specialized bile canalicular structures, which were larger than those obtained with standard cultures (20–35 μm length) and resembled *in vivo* structures.[99] These studies suggested the feasibility to *in vitro* generate an artificial biliary tree using 3D culturing approach, and its superiority over conventional 2D methods.

In vivo scaffold assessment

For bile duct reconstruction, the ideal biomaterial requires a proper degradation rate, appropriate mechanical strength to adapt to autogenous regeneration rate (resistance to the bile leakage and preventing short- and long-time stricture formation), ability to function as a temporary substitute, and a capacity to induce regeneration.[100] Moreover, an artificial bile duct is thought to properly function if two complications are avoided during the first few months after the transplantation: jaundice, resulting from obstruction of the reconstructed bile duct, and biliary peritonitis, due to bile leakage from the duct.

Different grafts, made of biological (i.e., collagen) or synthetic materials, have been evaluated in *in vivo* preclinical studies. A collagen sponge tube, obtained from a collagen solution (atelocollagen types I and III) and reinforced with a polypropylene mesh framework, was evaluated as prostheses to replace biliary defects in a canine model.[101] A biliary stent was necessary for nonreinforced grafts, as collagen

alone had not enough mechanical strength. However, long-term stenting induced inflammation and inhibited biliary epithelial regeneration. Reinforced grafts maintained the patency, provided satisfactory bile drainage for 12 weeks and allowed the regeneration of bile ducts, whose structure and morphology were similar to the native tissue, presenting neoepithelial layer, collagen bundles and small blood vessels, without the need for long-term biliary stenting. However, the presence of the polypropylene mesh resulted in reduced bile duct flexibility and the increased likelihood of long-term complications.[101] A collagen membrane (2.0 cm × 1.0 cm × 0.1 cm), activated by collagen-binding bFGF (10 μg/cm^2), used as patch to repair a spindle-shaped defect of the extrahepatic bile duct in a pig model, was completely replaced by autologous tissue and allowed biliary regeneration in a short-time observation.[100] The presence of b-FGF accelerated the bile duct regeneration with an intact neo-bile duct wall and normal liver function, no signs of stenosis were detected even for long-time observation. 3D collagen tubes (4 mm diameter, 1 mm wall thickness, and 200 nm pore size), coated with 2% agarose hydrogel (to avoid bile leakage through the pores) and used for bile duct replacement in pigs, developed a similar structure (i.e., presence of columnar epithelium, connective, and glandular tissue) and function (no signs of bile leak and/or obstruction) of native bile ducts after 4 weeks.[102] The graft is promising for future applications; however, long-term viability of the prosthesis must be evaluated.

An expanded polytetrafluoroethylene (e-PTFE) graft has been evaluated as a patch or as substitute in the management of common bile duct injuries. At short-term follow-up, the graft was associated with low patency rates, development of segmental strictures, and partial or total graft detachment with a consequent foreign body free in the biliary duct lumen.[103–105] A biosynthetic absorbable tubular graft, composed of PGA and trimethylene carbonate (3 mm internal diameter), interposed between the transected ends of the common bile ducts, was able to reconstitute the biliary anatomy without an intestinal bypass. The graft favored ingrowth of native tissues to reconstitute the bilioenteric anatomy, the majority of the bile duct being lined with columnar epithelial cells overlying collagenous connective tissue. However, complications, such as early anastomotic dehiscences, cholangitis, and stent migration, were observed in less than half of the implanted animals (5 dogs of 11) survived for the predetermined periods.[106] Miyazawa et al.[107] obtained an artificial bile duct organoid unit (BDOU) by seeding autologous bone marrow cells on the internal lumen of a bioabsorbable polymer tube, made up of a copolymer of PCL and PLA (50:50) and reinforced with PGA fibers (5 mm diameter, 1 mm in thickness, 95% porosity and absorbed by the body in 6–8 weeks). BDOU, implanted as a bypass graft into the extrahepatic pig bile duct (3 cm length), resulted in bile duct regeneration, morphologically and functionally resembling the native ducts, 6 months after transplantation. No signs of bile leakage or stenosis were observed. However, the same results have been obtained when implanting the unseeded synthetic graft, providing evidence that preseeding did not contribute to epithelial and smooth muscle regeneration. Moreover, the tissue regeneration seemed not to be started from the seeded cells, suggesting that undifferentiated cells in the peripheral circulation might migrate into the graft site to differentiate and grow into a mature bile duct. To confirm this idea, the same group investigated whether juvenile cells, such as bone marrow cells, differentiate into a regenerated bile duct. After 7 weeks post-implantation, cells positive for desmin, a distinct marker of regenerating smooth muscle, were revealed in the subepithelium of the neo-bile duct.[108] The results showed that the tubular artificial bile duct could carry bile, without leakage, to the duodenum in the peritoneal cavity, maintaining the shape in the short term after implantation, and allowing the regeneration of the bile duct epithelium and smooth muscle and, by extension, the regeneration of the entire bile duct tissue. It has also been demonstrated that when the artificial bile duct is degraded and absorbed, a new functional extrahepatic bile duct, similar to the native one, developed in the graft site.[109] The same results were obtained also when the graft was wrapped with the duodenal wall to prevent reflux of bowel fluid into the bile ducts, even if this approach could not provide a perfect substitute for the bile duct sphincter.[110] The same unseeded grafts were implanted in pigs as a bioabsorbable polymeric patch (20 mm × 10 mm spindle shape) to evaluate the possible use for an innovative treatment for biliary stenosis.[111] Results showed that the patch maintained patency, led to duct dilatation, and acted as a scaffold supporting the regeneration of a functional neo-bile duct similar to the native tissue, characterized by cubic columnar epithelium with accessory glands. It also allowed the bile to drain normally, without leaving traces of foreign matter in the body (the patch degraded quickly) and without causing strictures within 4 months after implantation. This study suggested the therapeutic potential of this type of bioengineered patch for the repair and regeneration of narrowed/injured segments of the duct. To establish whether this prosthesis could repair a complete defect of the extrahepatic bile ducts, a 2-cm-long portion of bile ducts has been replaced with a bioabsorbable polymeric tube (4 cm length, 5 mm bore diameter, and 0.5 mm thickness). A silicon tube was inserted as a temporary stent, to prevent early compressive deformation by surrounding organs and for easy evacuation of the degraded polymer. Histological examination at 4 months revealed the presence of neoepithelium with columnar cells, identical to that of native duct, demonstrating that the prosthesis can regenerate an entire bile duct without causing bile leakage, stenosis, or presence of remnants of foreign bodies.[112] The polymeric tube appears to be suitable for bile duct regeneration because it decomposes rapidly, without activating foreign body reactions, has no risk of zoonotic infection and can be easily manipulated. The same group developed also a bioabsorbable biliary stent, which allowed not only dilation of the stenosed bile duct, but induced "a process of favorable bile duct regeneration."[113]

FINAL CONSIDERATIONS

Important findings and a significant improvement in patient management are expected from tissue engineering and a

number of technical procedures have been already recorded in this direction. However, the long-term outcome in many cases is still a critical issue to be addressed. As reported in this review, different methodologies and materials were and are currently used, their actual effectiveness being affected by several limitations in the translation from *in vitro* studies and *in vivo* animal model to preclinical investigations, and the collected observations mainly showed that an effective scaffold is still to come. Published results should be necessarily considered provisional, due to the large variability in terms of materials, fabrication techniques and experimental protocols adopted. At the same time, this is one of the relevant findings that can be deduced, as the organs here considered are not "simple" conduits, as the transport function may suggest, but extremely complex structures whose histology and cell behavior clearly demonstrate. In this regard valuable results can be collected, allowing to discriminate and select the most promising scaffolds. However, this approach needs a confirmation because a direct scale-up to produce the whole organ could not assure the expected positive outcome. Obviously, these studies are necessary to gather preliminary information to direct the subsequent research step, but a critical revision is desirable. Many approaches and animal models are currently under investigation, thus implying large variations and multiple combinations that could not aid in the definition of a proper experimental protocol for clinical studies. Regarding the latter point, only synthetic scaffolds for trachea replacement have moved from "bench-to-bedside," being tested in early clinical experiences. This can suggest that the clinical experimentation is strictly related to the nature of the organ considered. It might be speculated that trachea, from an elementary viewpoint, is a rigid conduit for air passage mainly constituted by cartilaginous tissue with no peristaltic movements. Therefore, the functional aspect implies a remarkable complexity that needs to be fully addressed before to move toward a reasonable translation from the animal model to humans. The reported studies allow to draw this kind of consideration because, for instance, the recovery of an esopagheal defect is affected by several limitations that should be in depth investigated to plan a strategy for the replacement of long segments.

In conclusion, synthetic biomaterials contribute to define promising routes for the development of novel tubular tissue-engineered substitutes. Different intermediate goals have been achieved; however, they should be critically evaluated to improve their outcome and safe translation to humans with the aim to start well-established clinical trials.

ACKNOWLEDGEMENTS

This work was supported by European Project FP7-NMP-2011-SMALL-5: BIOtrachea, Biomaterials for Tracheal Replacement in Age-related Cancer via a Humanly Engineered Airway, (No.280584-2).

REFERENCES

1. Grikscheit TC, Ochoa ER, Srinivasan A, Gaissert H, Vacanti JP. Tissue-engineered esophagus: Experimental substitution by onlay patch or interposition. J Thorac Cardiovasc Surg 2003;126: 537–544.
2. Atala A, Bauer SB, Soker S, Yoo JJ, Retik AB. Tissue-engineered autologous bladders for patients needing cystoplasty. Lancet 2006;367:1241–1246.
3. Pham C, Greenwood J, Cleland H, Woodruff P, Maddern G. Bioengineered skin substitutes for the management of burns: A systematic review. Burns 2007;33:946–957.
4. Macchiarini P, Jungebluth P, Go T, Asnaghi MA, Rees LE, Cogan TA, Dodson A, Martorell J, Bellini S, Parnigotto PP, Dickinson SC, Hollander AP, Mantero S, Conconi MT, Birchall MA. Clinical transplantation of a tissue-engineered airway. Lancet 2008;372: 2023–2030.
5. Baiguera S, D'Innocenzo B, Macchiarini P. Current status of regenerative replacement of the airway. Expert Rev Resp Med 2011;5:487–494.
6. Baiguera S, Del Gaudio C, Jaus MO, Polizzi L, Gonfiotti A, Comin CE, Bianco A, Ribatti D, Taylor DA, Macchiarini P. Long-term changes to in vitro preserved bioengineered human trachea and their implications for decellularized tissues. Biomaterials 2012;33: 3662–3672.
7. Gustafsson Y, Haag J, Jungebluth P, Lundin V, Lim ML, Baiguera S, Ajalloueian F, Del Gaudio C, Bianco A, Moll G, Sjöqvist S, Lemon G, Teixeira AI, Macchiarini P. Viability and proliferation of rat MSCs on adhesion protein-modified PET and PU scaffolds. Biomaterials 2012;33:8094–8103.
8. Grillo H. Tracheal replacement: A critical review. Ann Thorac Surg 2002;73:1995–2004.
9. Liu L, Wu W, Tuo X, Geng W, Zhao J, Wei J, Yan X, Yang W, Li L, Chen F. Novel strategy to engineer trachea cartilage graft with marrow mesenchymal stem cell macroaggregate and hydrolyzable scaffold. Artif Organs 2010;34:426–433.
10. Tani G, Usui N, Kamiyama M, Oue T, Fukuzawa M. In vitro construction of scaffold-free cylindrical cartilage using cell sheet-based tissue engineering. Pediatr Surg Int 2010;26:179–185.
11. Moroni L, Curti M, Welti M, Korom S, Weder W, de Wijn JR, van Blitterswijk CA. Anatomical 3D fiber-deposited scaffolds for tissue engineering: Designing a neotrachea. Tissue Eng 2007;13: 2483–2493.
12. Mäkitie AA, Korpela J, Elomaa L, Reivonen M, Kokkari A, Malin M, Korhonen H, Wang X, Salo J, Sihvo E, Salmi M, Partanen J, Paloheimo KS, Tuomi J, Närhi T, Seppälä J. Novel additive manufactured scaffolds for tissue engineered trachea research. Acta Otolaryngol 2013;133:412–417.
13. Hinderer S, Schesny M, Bayrak A, Ibold B, Hampel M, Walles T, Stock UA, Seifert M, Schenke-Layland K. Engineering of fibrillar decorin matrices for a tissue-engineered trachea. Biomaterials 2012;33:5259–5266.
14. Shi H, Wang W, Lu D, Li H, Chen L, Lu Y, Zeng Y. Cellular biocompatibility and biomechanical properties of N-carboxyethylchitosan/nanohydroxyapatite composites for tissue-engineered trachea. Artif Cells Blood Substit Immobil Biotechnol 2012;40: 120–124.
15. Ott LM, Weatherly RA, Detamore MS. Overview of tracheal tissue engineering: Clinical need drives the laboratory approach. Ann Biomed Eng 2011;39:2091–2113.
16. Ruszymah BH, Chua K, Latif MA, Hussein FN, Saim AB. Formation of in vivo tissue engineered human hyaline cartilage in the shape of a trachea with internal support. Int J Pediatr Otorhinolaryngol 2005;69:1489–1495.
17. Luo X, Zhou G, Liu W, Zhang WG, Cen L, Cui L, Cao Y. In vitro precultivation alleviates post-implantation inflammation and enhances development of tissue-engineered tubular cartilage. Biomed Mater 2009;4:025006.
18. Kojima K, Bonassar LJ, Roy AK, Vacanti CA, Cortiella J. Autologous tissue-engineered trachea with sheep nasal chondrocytes. J Thorac Cardiovasc Surg 2002;123:1177–1184.
19. Kojima K, Bonassar LJ, Roy AK, Mizuno H, Cortiella J, Vacanti CA. A composite tissue-engineered trachea using sheep nasal chondrocyte and epithelial cells. FASEB J 2003;17:823–828.
20. Komura M, Komura H, Kanamori Y, Tanaka Y, Ohatani Y, Ishimaru T, Sugiyama M, Hoshi K, Iwanaka T. Study of mechanical properties of engineered cartilage in an in vivo culture for

design of a biodegradable scaffold. Int J Artif Organs 2010;33: 775–781.
21. Yamashita M, Kanemaru S, Hirano S, Magrufov A, Tamaki H, Tamura Y, Kishimoto M, Omori K, Nakamura T, Ito J. Tracheal regeneration after partial resection: A tissue engineering approach. Laryngoscope 2007;117:497–502.
22. Nakamura T, Sato T, Araki M, Ichihara S, Nakada A, Yoshitani M, Itoi S, Yamashita M, Kanemaru S, Omori K, Hori Y, Endo K, Inada Y, Hayakawa K. In situ tissue engineering for tracheal reconstruction using a luminar remodeling type of artificial trachea. J Thorac Cardiovasc Surg 2009;138:811–819.
23. Kobayashi K, Suzuki T, Nomoto Y, Tada Y, Miyake M, Hazama A, Wada I, Nakamura T, Omori K. A tissue-engineered trachea derived from a framed collagen scaffold, gingival fibroblasts and adipose-derived stem cells. Biomaterials 2010;31:4855–4863.
24. Grimmer JF, Gunnlaugsson CB, Alsberg E, Murphy HS, Kong HJ, Mooney DJ, Weatherly RA. Tracheal reconstruction using tissue-engineered cartilage. Arch Otolaryngol Head Neck Surg 2004;130:1191–1196.
25. Kojima K, Ignotz RA, Kushibiki T, Tinsley KW, Tabata Y, Vacanti CA. Tissue-engineered trachea from sheep marrow stromal cells with transforming growth factor β2 released from biodegradable microspheres in a nude rat recipient. J Thorac Cardiovasc Surg 2004;128:147–153.
26. Yanagi M, Kishida A, Shimotakahara T, Matsumoto H, Nishijima H, Akashi M, Aikou T. Experimental study of bioactive polyurethane sponge as an artificial trachea. ASAIO J 1994;40:M412–M418.
27. Tada Y, Takezawa T, Tani A, Nakamura T, Omori K. Collagen vitrigel scaffold for regenerative medicine of the trachea: Experimental study and quantitative evaluation. Acta Otolaryngol 2012; 132:447–452.
28. Tani A, Tada Y, Takezawa T, Imaizumi M, Nomoto Y, Nakamura T, Omori K. Regeneration of tracheal epithelium using a collagen vitrigel-sponge scaffold containing basic fibroblast growth factor. Ann Otol Rhinol Laryngol 2012;121:261–268.
29. Tatekawa Y, Kawazoe N, Chen G, Shirasaki Y, Komuro H, Kaneko M. Tracheal defect repair using a PLGA-collagen hybrid scaffold reinforced by a copolymer stent with bFGF-impregnated gelatin hydrogel. Pediatr Surg Int 2010;26:575–580.
30. Lin CH, Su JM, Hsu SH. Evaluation of type II collagen scaffolds reinforced by poly(epsilon-caprolactone) as tissue-engineered trachea. Tissue Eng Part C Methods 2008;14:69–77.
31. Komura M, Komura H, Kanamori Y, Tanaka Y, Suzuki K, Sugiyama M, Nakahara S, Kawashima H, Hatanaka A, Hoshi K, Ikada Y, Tabata Y, Iwanaka T. An animal model study for tissue-engineered trachea fabricated from a biodegradable scaffold using chondrocytes to augment repair of tracheal stenosis. J Pediatr Surg 2008;43:2141–2146.
32. Yamamoto Y, Okamoto T, Goto M, Yokomise H, Yamamoto M, Tabata Y. Experimental study of bone morphogenetic proteins-2 slow release from an artificial trachea made of biodegradable materials: Evaluation of stenting time. ASAIO J 2003;49:533–536.
33. Sato T, Araki M, Nakajima N, Omori K, Nakamura T. Biodegradable polymer coating promotes the epithelization of tissue-engineered airway prostheses. J Thorac Cardiovasc Surg 2010; 139:26–31.
34. Acocella F, Brizzola S. Tracheal tissue regeneration. In: Bosworth LA, Downes S, editors. Electrospinning for Tissue Regeneration. Oxford: Woodhead Publishing Limited; 2011. pp 242–279.
35. Omori K, Nakamura T, Kanemaru S, Asato R, Yamashita M, Tanaka S, Magrufov A, Ito J, Shimizu Y. Regenerative medicine of the trachea: The first human case. Ann Otol Rhinol Laryngol 2005;114:429–433.
36. Vacanti CA, Paige KT, Kim WS, Sakata J, Upton J, Vacanti JP. Experimental tracheal replacement using tissue-engineered cartilage. J Pediatr Surg 1994;29:201–204.
37. Kanzaki M, Yamato M, Hatakeyama H, Kohno C, Yang J, Umemoto T, Kikuchi A, Okano T, Onuki T. Tissue engineered epithelial cell sheets for the creation of a bioartificial trachea. Tissue Eng 2006;12:1275–1283.
38. Lin CH, Hsu SH, Su JM, Chen CW. Surface modification of poly(ε-caprolactone) porous scaffolds using gelatin hydrogel as the tracheal replacement. J Tissue Eng Regen Med 2010;5:156–162.
39. Tsukada H, Gangadharan S, Garland R, Herth F, DeCamp M, Ernst A. Tracheal replacement with a bioabsorbable scaffold in sheep. Ann Thorac Surg 2010;90:1793–1797.
40. Naito H, Tojo T, Kimura M, Dohi Y, Zimmermann WH, Eschenhagen T, Taniguchi S. Engineering bioartificial tracheal tissue using hybrid fibroblast-mesenchymal stem cell cultures in collagen hydrogels. Interact Cardiovasc Thorac Surg 2011;12: 156–161.
41. Sekine T, Nakamura T, Ueda H, Matsumoto K, Yamamoto Y, Takimoto Y, Kiyotani T, Shimizu Y. Replacement of the tracheobronchial bifurcation by a newly developed Y-shaped artificial trachea. ASAIO J 1999;45:131–134.
42. Nakamura T, Teramachi M, Sekine T, Kawanami R, Fukuda S, Yoshitani M, Toba T, Ueda H, Hori Y, Inoue M, Shigeno K, Taka TN, Liu Y, Tamura N, Shimizu Y. Artificial trachea and long term follow-up in carinal reconstruction in dogs. Int J Artif Organs 2000;23:718–724.
43. Omori K, Tada Y, Suzuki T, Nomoto Y, Matsuzuka T, Kobayashi K, Nakamura T, Kanemaru S, Yamashita M, Asato R. Clinical application of in situ tissue engineering using a scaffolding technique for reconstruction of the larynx and trachea. Ann Otol Rhinol Laryngol 2008;117:673–678.
44. Jungebluth P, Alici E, Baiguera S, Le Blanc K, Blomberg P, Bozóky B, Crowley C, Einarsson O, Grinnemo KH, Gudbjartsson T, Le Guyader S, Henriksson G, Hermanson O, Juto JE, Leidner B, Lilja T, Liska J, Luedde T, Lundin V, Moll G, Nilsson B, Roderburg C, Strömblad S, Sutlu T, Teixeira AI, Watz E, Seifalian A, Macchiarini P. Tracheobronchial transplantation with a stem-cell-seeded bioartificial nanocomposite: A proof-of-concept study. Lancet 2011;378:1997–2004.
45. Saxena AK, Ainoedhofer H, Höllwarth ME. Esophagus tissue engineering: In vitro generation of esophageal epithelial cell sheets and viability on scaffold. J Pediatr Surg 2009;44:896–901.
46. Saxena AK, Ainoedhofer H, Höllwarth ME. Culture of ovine esophageal epithelial cells and in vitro esophagus tissue engineering. Tissue Eng Part C Methods 2010;16:109–114.
47. Beckstead BL, Pan S, Bhrany AD, Bratt-Leal AM, Ratner BD, Giachelli CM. Esophageal epithelial cell interaction with synthetic and natural scaffolds for tissue engineering. Biomaterials 2005; 26:6217–6228.
48. Zhu Y, Chan-Park MB, Sin Chian K. The growth improvement of porcine esophageal smooth muscle cells on collagen-grafted poly(DL-lactide-co-glycolide) membrane. J Biomed Mater Res B Appl Biomater 2005;75:193–199.
49. Zhu Y, Chian KS, Chan-Park MB, Mhaisalkar PS, Ratner BD. Protein bonding on biodegradable poly(L-lactide-co-caprolactone) membrane for esophageal tissue engineering. Biomaterials 2006; 27:68–78.
50. Zhu Y, Ong WF. Epithelium regeneration on collagen (IV) grafted polycaprolactone for esophageal tissue engineering. Mater Sci Eng C 2009;29:1046–1050.
51. Zhu Y, Leong MF, Ong WF, Chan-Park MB, Chian KS. Esophageal epithelium regeneration on fibronectin grafted poly(L-lactide-co-caprolactone) (PLLC) nanofiber scaffold. Biomaterials 2007;28:861–868.
52. Leong MF, Chian KS, Mhaisalkar PS, Ong WF, Ratner BD. Effect of electrospun poly(D,L-lactide) fibrous scaffold with nanoporous surface on attachment of porcine esophageal epithelial cells and protein adsorption. J Biomed Mater Res A 2009;89:1040–1048.
53. Zhu Y, Ong WF, Chan W, Li Y, Liu Y. Construct of asymmetrical scaffold and primary cells for tissue engineered esophagus. Mater Sci Eng C 2010;30:400–406.
54. Takimoto Y, Nakamura T, Teramachi M, Kiyotani T, Shimizu Y. Replacement of long segments of the esophagus with a collagen-silicone composite tube. ASAIO J 1995;41:M605–M608.
55. Aikawa M, Miyazawa M, Okamoto K, Okada K, Akimoto N, Sato H, Koyama I, Yamaguchi S, Ikada Y. A bioabsorbable polymer patch for the treatment of esophageal defect in a porcine model. J Gastroenterol 2013;48:822–829.
56. Saxena AK, Faraj KA, Damen WF. Comparison of collagen scaffold tubes for possible esophagus organ tissue engineering

applications: In-situ omental implantation study in an ovine model. Eur Surg 2010;42:309–313.
57. Saxena AK, Baumgart H, Komann C, Ainoedhofer H, Soltysiak P, Kofler K, Höllwarth ME. Esophagus tissue engineering: In situ generation of rudimentary tubular vascularized esophageal conduit using the ovine model. J Pediatr Surg 2010;45:859–864.
58. Nakase Y, Nakamura T, Kin S, Nakashima S, Yoshikawa T, Kuriu Y, Sakakura C, Yamagishi H, Hamuro J, Ikada Y, Otsuji E, Hagiwara A. Intrathoracic esophageal replacement by in situ tissue-engineered esophagus. J Thorac Cardiovasc Surg 2008; 136:850–859.
59. Lynen Jansen P, Klinge U, Anurov M, Titkova S, Mertens PR, Jansen M. Surgical mesh as a scaffold for tissue regeneration in the esophagus. Eur Surg Res 2004;36:104–111.
60. Basu J, Mihalko KL, Payne R, Rivera E, Knight T, Genheimer CW, Guthrie KI, Sangha N, Jayo MJ, Jain D, Bertram TA, Ludlow JW. Extension of bladder-based organ regeneration platform for tissue engineering of esophagus. Med Hypotheses 2012;78:231–234.
61. Esposito A, Mezzogiorno A, Sannino A, De Rosa A, Menditti D, Esposito V, Ambrosio L. Hyaluronic acid based materials for intestine tissue engineering: A morphological and biochemical study of cell–material interaction. J Mater Sci Mater Med 2006; 17:1365–1372.
62. Pfluger CA, Burkey DD, Wang L, Sun B, Ziemer KS, Carrier RL. Biocompatibility of plasma enhanced chemical vapor deposited poly(2-hydroxyethyl methacrylate) films for biomimetic replication of the intestinal basement membrane. Biomacromolecules 2010;11:1579–1584.
63. Zakhem E, Raghavan S, Gilmont RR, Bitar KN. Chitosan-based scaffolds for the support of smooth muscle constructs in intestinal tissue engineering. Biomaterials 2012;33:4810–4817.
64. Viney ME, Bullock AJ, Day MJ, MacNeil S. Co-culture of intestinal epithelial and stromal cells in 3D collagen-based environments. Regen Med 2009;4:397–406.
65. Gupta A, Vara DS, Punshon G, Sales KM, Winslet MC, Seifalian AM. In vitro small intestinal epithelial cell growth on a nanocomposite polycaprolactone scaffold. Biotechnol Appl Biochem 2009; 54:221–229.
66. Sung JH, Yu J, Luo D, Shuler ML, March JC. Microscale 3-D hydrogel scaffold for biomimetic gastrointestinal (GI) tract model. Lab Chip 2011;11:389–392.
67. Deng X, Zhang G, Shen C, Yin J, Meng Q. Hollow fiber culture accelerates differentiation of Caco-2 cells. Appl Microbiol Biotechnol 2013;###97:6943–6955.
68. Hori Y, Nakamura T, Kimura D, Kaino K, Kurokawa Y, Satomi S, Shimizu Y. Experimental study on tissue engineering of the small intestine by mesenchymal stem cell seeding. J Surg Res 2002;102:156–160.
69. Nakase Y, Hagiwara A, Nakamura T, Kin S, Nakashima S, Yoshikawa T, Fukuda K, Kuriu Y, Miyagawa K, Sakakura C, Otsuji E, Shimizu Y, Ikada Y, Yamagishi H. Tissue engineering of small intestinal tissue using collagen sponge scaffolds seeded with smooth muscle cells. Tissue Eng 2006;12:403–412.
70. Vacanti JP, Morse MA, Saltzman WM, Domb AJ, Perez-Atayde A, Langer R. Selective cell transplantation using bioabsorbable artificial polymers as matrices. J Pediatr Surg 1988;23:3–9.
71. Organ GM, Mooney DJ, Hansen LK, Schloo B, Vacanti JP. Transplantation of enterocytes utilizing polymer–cell constructs to produce a neointestine. Transplant Proc 1992;24:3009–3011.
72. Organ GM, Mooney DJ, Hansen LK, Schloo B, Vacanti JP. Enterocyte transplantation using cell–polymer devices to create intestinal epithelial-lined tubes. Transplant Proc 1993;25:998–1001.
73. Choi RS, Vacanti JP. Preliminary studies of tissue-engineered intestine using isolated epithelial organoid units on tubular synthetic biodegradable scaffolds. Transplant Proc 1997;29:848–851.
74. Choi RS, Riegler M, Pothoulakis C, Kim BS, Mooney D, Vacanti M, Vacanti JP. Studies of brush border enzymes, basement membrane components, and electrophysiology of tissue-engineered neointestine. J Pediatr Surg 1998;33:991–996.
75. Kaihara S, Kim SS, Benvenuto M, Choi R, Kim BS, Mooney D, Tanaka K, Vacanti JP. Successful anastomosis between tissue-engineered intestine and native small bowel. Transplantation 1999;67:241–245.
76. Kaihara S, Kim SS, Benvenuto MS, Choi R, Kim BS, Mooney D, Tanaka K, Vacanti JP. Anastomosis between tissue-engineered intestine and native small bowel. Transplant Proc 1999;31:661–662.
77. Kaihara S, Kim SS, Benvenuto MS, Kim BS, Mooney D, Tanaka K, Vacanti JP. End-to-end anastomosis between tissue-engineered intestine and native small bowel. Tissue Eng 1999;5: 339–346.
78. Kim SS, Kaihara S, Benvenuto MS, Choi RS, Kim BS, Mooney DJ, Taylor GA, Vacanti JP. Regenerative signals for tissue-engineered small intestine. Transplant Proc 1999;31:657–660.
79. Kim SS, Kaihara S, Benvenuto MS, Choi RS, Kim BS, Mooney DJ, Taylor GA, Vacanti JP. Regenerative signals for intestinal epithelial organoid units transplanted on biodegradable polymer scaffolds for tissue engineering of small intestine. Transplantation 1999;67:227–233.
80. Kim SS, Kaihara S, Benvenuto MS, Choi RS, Kim BS, Mooney DJ, Vacanti JP. Effects of anastomosis of tissue-engineered neointestine to native small bowel. J Surg Res 1999;87:6–13.
81. Tavakkolizadeh A, Berger UV, Stephen AE, Kim BS, Mooney D, Hediger MA, Ashley SW, Vacanti JP, Whang EE. Tissue-engineered neomucosa: Morphology, enterocyte dynamics, and SGLT1 expression topography. Transplantation 2003;75:181–185.
82. Grikscheit TC, Siddique A, Ochoa ER, Srinivasan A, Alsberg E, Hodin RA, Vacanti JP. Tissue-engineered small intestine improves recovery after massive small bowel resection. Ann Surg 2004;240:748–754.
83. Perez A, Grikscheit TC, Blumberg RS, Ashley SW, Vacanti JP, Whang EE. Tissue-engineered small intestine: Ontogeny of the immune system. Transplantation 2002;74:619–623.
84. Ramsanahie A, Duxbury MS, Grikscheit TC, Perez A, Rhoads DB, Gardner-Thorpe J, Ogilvie J, Ashley SW, Vacanti JP, Whang EE. Effect of GLP-2 on mucosal morphology and SGLT1 expression in tissue-engineered neointestine. Am J Physiol Gastrointest Liver Physiol 2003;285:G1345–G1352.
85. Duxbury MS, Grikscheit TC, Gardner-Thorpe J, Rocha FG, Ito H, Perez A, Ashley SW, Vacanti JP, Whang EE. Lymphangiogenesis in tissue-engineered small intestine. Transplantation 2004;77: 1162–1166.
86. Gardner-Thorpe J, Grikscheit TC, Ito H, Perez A, Ashley SW, Vacanti JP, Whang EE. Angiogenesis in tissue-engineered small intestine. Tissue Eng 2003;9:1255–1261.
87. Matthews JA, Sala FG, Speer AL, Warburton D, Grikscheit TC. VEGF optimizes the formation of tissue-engineered small intestine. Regen Med 2011;6:559–567.
88. Sala FG, Matthews JA, Speer AL, Torashima Y, Barthel ER, Grikscheit TC. A multicellular approach forms a significant amount of tissue-engineered small intestine in the mouse. Tissue Eng Part A 2011;17:1841–1850.
89. Sala FG, Kunisaki SM, Ochoa ER, Vacanti J, Grikscheit TC. Tissue-engineered small intestine and stomach form from autologous tissue in a preclinical large animal model. J Surg Res 2009; 156:205–212.
90. Grikscheit T, Ochoa ER, Ramsanahie A, Alsberg E, Mooney D, Whang EE, Vacanti JP. Tissue-engineered large intestine resembles native colon with appropriate in vitro physiology and architecture. Ann Surg 2003;238:35–41.
91. Barthel ER, Speer AL, Levin DE, Sala FG, Hou X, Torashima Y, Wigfall CM, Grikscheit TC. Tissue engineering of the intestine in a murine model. J Vis Exp 2012:e4279.
92. Kaihara S, Kim SS, Kim BS, Mooney D, Tanaka K, Vacanti JP. Long-term follow-up of tissue-engineered intestine after anastomosis to native small bowel. Transplantation 2000;69:1927–1932.
93. Lloyd DA, Ansari TI, Gundabolu P, Shurey S, Maquet V, Sibbons PD, Boccaccini AR, Gabe SM. A pilot study investigating a novel subcutaneously implanted pre-cellularised scaffold for tissue engineering of intestinal mucosa. Eur Cell Mater 2006;11:27–33.
94. Chen DC, Avansino JR, Agopian VG, Hoagland VD, Woolman JD, Pan S, Ratner BD, Stelzner M. Comparison of polyester scaffolds for bioengineered intestinal mucosa. Cells Tissues Organs 2006;184:154–165.

95. Lee M, Wu BM, Stelzner M, Reichardt HM, Dunn JC. Intestinal smooth muscle cell maintenance by basic fibroblast growth factor. Tissue Eng Part A 2008;14:1395–1402.
96. Barralet JE, Wallace LL, Strain AJ. Tissue engineering of human biliary epithelial cells on polyglycolic acid/polycaprolactone scaffolds maintains long-term phenotypic stability. Tissue Eng 2003; 9:1037–1045.
97. Ogawa K, Ochoa ER, Borenstein J, Tanaka K, Vacanti JP. The generation of functionally differentiated, three-dimensional hepatic tissue from two-dimensional sheets of progenitor small hepatocytes and nonparenchymal cells. Transplantation 2004;77:1783–1789.
98. Takahashi R, Sonoda H, Tabata Y, Hisada A. Formation of hepatocyte spheroids with structural polarity and functional bile canaliculi using nanopillar sheets. Tissue Eng Part A 2010;16: 1983–1995.
99. Malinen MM, Palokangas H, Yliperttula M, Urtti A. Peptide nanofiber hydrogel induces formation of bile canaliculi structures in three-dimensional hepatic cell culture. Tissue Eng Part A 2012;18:2418–2425.
100. Li Q, Tao L, Chen B, Ren H, Hou X, Zhou S, Zhou J, Sun X, Dai J, Ding Y. Extrahepatic bile duct regeneration in pigs using collagen scaffolds loaded with human collagen-binding bFGF. Biomaterials 2012;33:4298–4308.
101. Nakashima S, Nakamura T, Miyagawa K, Yoshikawa T, Kin S, Kuriu Y, Nakase Y, Sakakura C, Otsuji E, Hagiwara A, Yamagishi H. In situ tissue engineering of the bile duct using polypropylene mesh-collagen tubes. Int J Artif Organs 2007;30:75–85.
102. Pérez Alonso AJ, Del Olmo Rivas C, Romero IM, Cañizares Garcia FJ, Poyatos PT. Tissue-engineering repair of extrahepatic bile ducts. J Surg Res 2013;179:18–21.
103. Ren W, Shi D. Experimental study on repair of bile duct defects with expanded polytetrafluoroethylene. Zhongguo Xiu Fu Chong Jian Wai Ke Za Zhi 2001;15:305–307.
104. Christensen M, Laursen HB, Rokkjaer M, Jensen PF, Yasuda Y, Mortensen FV. Reconstruction of the common bile duct by a vascular prosthetic graft: An experimental study in pigs. J HepatobiliaryPancreat Surg 2005;12:231–234.
105. Schanaider A, Pannain VL, Müller LC, Maya MC. Expanded polytetrafluoroethylene in canine bile duct injury: A critical analysis. Acta Cir Bras 2011;26:247–252.
106. Nau P, Liu J, Ellison EC, Hazey JW, Henn M, Muscarella P, Narula VK, Melvin WS. Novel reconstruction of the extrahepatic biliary tree with a biosynthetic absorbable graft. HPB (Oxford) 2011;13:573–578.
107. Miyazawa M, Torii T, Toshimitsu Y, Okada K, Koyama I, Ikada Y. A tissue-engineered artificial bile duct grown to resemble the native bile duct. Am J Transplant 2005;5:1541–1547.
108. Miyazawa M, Aikawa M, Okada K, Toshimitsu Y, Okamoto K, Koyama I, Ikada Y. Regeneration of extrahepatic bile ducts by tissue engineering with a bioabsorbable polymer. J Artif Organs 2012;15:26–31.
109. Aikawa M, Miyazawa M, Okada K, Toshimitsu Y, Torii T, Otani Y, Koyama I, Ikada Y. Regeneration of extrahepatic bile duct—Possibility to clinical application by recognition of the regenerative process. J Smooth Muscle Res 2007;43:211–218.
110. Aikawa M, Miyazawa M, Okada K, Toshimitsu Y, Okamoto K, Akimoto N, Koyama I, Ikada Y. Development of a novel reflux-free bilioenteric anastomosis procedure by using a bioabsorbable polymer tube. J Hepatobiliary Pancreat Sci 2010;17:284–290.
111. Aikawa M, Miyazawa M, Okamoto K, Toshimitsu Y, Torii T, Okada K, Akimoto N, Ohtani Y, Koyama I, Yoshito I. A novel treatment for bile duct injury with a tissue-engineered bioabsorbable polymer patch. Surgery 2010;147:575–580.
112. Aikawa M, Miyazawa M, Okamoto K, Toshimitsu Y, Okada K, Akimoto N, Ueno Y, Koyama I, Ikada Y. An extrahepatic bile duct grafting using a bioabsorbable polymer tube. J Gastrointest Surg 2012;16:529–534.
113. Miyazawa M, Aikawa M, Okada K, Torii T, Otani Y, Koyama I. Development of bioabsorbable biliary tract stents for treatment of benign biliary stenosis. Jpn J Gastroenterol Surg 2007;40: 1548.

Airway Transplantation

Philipp Jungebluth, Paolo Macchiarini*

KEYWORDS

• Trachea replacement • Tissue engineering • Allogenic transplantation
• Immunosuppressive medication • Rejection

KEY POINTS

- Replacing long segments or the entire trachea in humans.
- Allotransplantation.
- Surgical challenges.
- Organ rejection.
- Tissue engineering.

A variety of benign or malignant disorders affecting the trachea can theoretically be treated by simple resection and subsequent end-to-end anastomosis of the remaining trachea.[1] This primary reconstruction is, so far, the only curative treatment in patients with tracheal diseases but, unfortunately, it is feasible only when the affected tracheal length does not exceed 6 cm in adults and about 30% of the entire length in children. Besides this technical restriction, local anatomy, previous treatments, and type of pathologic condition can further restrict the already few therapeutic options.

Longer segments cannot be treated surgically because it is impossible to perform safely a direct reconstruction of the airway that, under these circumstances, would ultimately fail because of the excessive tension at the anastomotic site. Benign diseases have been approached with various endoluminal solutions.[1,2] Because most of primary tracheal malignancies are diagnosed in an advanced local stage, only palliative options remain available, such as stenting, tumor debulking or radiotherapy.[1,3] Consequently, tracheal transplantation could be a valid alternative for many patients (Table 1). To this end, different replacement strategies have been investigated in experimental settings and some of them translated to the clinic. However, so far, none of them has turned into a routine clinical procedure. The requirements of an ideal tracheal substitute are multifaceted but crucial for a successful clinical application (Table 2).

TYPES OF TRANSPLANTATIONS

In 1963, Fonkalsrud and Sumida,[4] and, in 1971, Fonkalsrud and colleagues,[5] reported two initial clinical cases of tracheal replacement using the patients' own esophagus in congenital agenesis and long-segment stenosis. Initially, the patients recovered remarkably but then died within the first 6 weeks postoperatively. Both neotrachea required permanent stenting and did not provide normal

The authors declare no competing financial interests.
This work was supported by European Project FP7-NMP- 2011-SMALL-5, BIOtrachea; Bio- materials for Tracheal Replacement in Age-related Cancer via a Humanly Engineered Airway (No. 280584e2); ALF medicine (Stockholm County Council), Transplantation of Bioengineered Trachea in Humans (No. LS1101e0042); The Swedish Heart-Lung Foundation, Trachea Tissue Engineering; Doctor Dorka Stiftung (Hannover, Germany), bioengineering of tracheal tissue; and a megagrant of the Russian Ministry of Education and Science (agreement No. 11.G34.31.0065).
Division of Ear, Nose, and Throat (CLINTEC), Advanced Center for Translational Regenerative Medicine (ACTREM), Karolinska Institutet, Alfred Nobel Allé 8, Huddinge/Stockholm 14186, Sweden
* Corresponding author.
E-mail address: paolo.macchiarini@ki.se

Thorac Surg Clin 24 (2014) 97–106
http://dx.doi.org/10.1016/j.thorsurg.2013.09.005
1547-4127/14/$ – see front matter

Table 1
Indications for potential tracheal transplantation and eligibility criteria

Indications	Benign Diseases	Malignant Diseases
—	• Trauma • Benign stenosis • Relapsing polychondritis • Osteochondroplastica • Amyloidosis • Tuberculosis	• Unresectable tumors • Postlaryngectomy recurrences or diseases
	Eligibility Criteria	
	• Extended (>60% total length) benign & malignant diseases • Already maximally pretreated • Age between 10 and 75 y • No absolute surgical contraindications • No regional and/or micrometastasis (bone-marrow biopsy proven) • Normal psychological or psychiatric habitus • Independent review board, ethics and national transplant clearance • Written informed consent	

function. No similar transplants have been made since. Instead, a variety of approaches have been attempted clinically that use either allotransplantation or tissue engineering (TE) approaches.

TRACHEAL ALLOTRANSPLANTATION

Fresh Cadaveric Trachea

In 1979, Rose and colleagues[6] described the first case of allogenic tracheal replacement using a fresh cadaveric tracheal graft in a 21-year-old male patient with extensive benign tracheal stenosis. In a two-stage procedure, the graft was initially implanted into the sternocleidomastoid muscle region to provide indirect vascularization and subsequently transferred to the orthotopic site. The patient was discharged 9 weeks after the transplantation without immunosuppressive medication and no signs for organ rejection or health status impairment. At that time, it was assumed that the tracheal immunogenicity was not relevant and graft failure was only provoked by graft ischemia and infection.[6] In contrast, Levashov and colleagues[7] transplanted on a donated trachea but with different findings. They used the omentopexy to obtain indirect blood supply of the cadaveric trachea and reported signs of organ rejection at day 10 postoperatively. The investigators affirmed the promising overall outcome 4 months after the transplantation but emphasized the essential need of adequate donor-recipient selection and modern immunosuppressive medication. Similar

Table 2
Requirements of ideal tracheal substitute

Scaffold for Tissue Replacement	Characteristics
General properties	• Nonimmunogenic • Nontoxic • Nontumorigenic • Allows for cell adhesion, migration, proliferation, and differentiation
Tracheal-specific properties	• Airtight and liquid-tight seals • Mechanical properties to react on both lateral and • Longitudinal forces • Support airway patency and respiratory function
Required mechanical properties based on native trachea	± 75° (right/left axial rotation at 0° maximum flexion) ± 75° (right/left axial rotation at 0° flexion) Flexion/extension 70°/60° and 40% of strain limit (flexion-extension bending) 40%:20% for tension/compression (axial/tension/compression) Lateral (right/left) bending: 48° and expected strain limit of 40%

findings were obtained by Delaere and colleagues[8] in a small animal model confirming the necessity of immunosuppressive medication for tracheal transplantation. In another in-depth evaluation of the antigenic profile of the human trachea, Shaari and colleagues[9] discovered the underlying mechanism of the immune competence of human trachea.

Despite the obvious significance of immunogenicity, most research was focused on graft revascularization. Klepetko and colleagues[10] demonstrated that the structural and functional properties of an allogenic graft could be maintained with heterotopic transplantation into the omentum. In a large animal study, Macchiarini and colleagues[11] described a harvesting technique to revascularize the entire trachea that, to be successful, required heavy immunosuppression to control rejection and perfect venous drainage. This experience has been applied by Duque and colleagues,[12] in Columbia, who have reported a series of 20 clinical laryngeal and tracheal transplants. An extension of this technique, a composite laryngotracheal (7 cm) graft transplant, was recently used in a 51-year-old woman already on immunosuppression.[13] Postoperatively, the patient continues to rely on a tracheotomy but has had the return of an oral and nasal airway, vocalization, smell, and taste.

The pros of this method are excellent vascularity and maintenance of functional integrity. The cons include life-long heavy immunosuppression and donor dependence.

In Situ Processed Fresh Cadaveric Trachea

Like Rose and colleagues,[6] Delaere and colleagues[14] investigated the interesting approach of using fresh cadaveric allografts. The harvested trachea was initially transplanted into the subcutaneous tissue of the recipient's forearm to induce neovascularization of the graft. Meanwhile, immunosuppressive medication was initiated and continued for the next 229 days. Within the observation period, the posterior wall of the heterotopic implanted graft became necrotic, and was removed and replaced by buccal mucosa of the recipient. After 4 months, the allograft was placed into the orthotopic position and a 4.5 cm defect of the patient's trachea replaced. At the time of orthotopic transplantation, the graft showed cartilage rings composed of viable cartilage tissue and epithelial lining consisting of squamous epithelium and respiratory epithelium.

The pro of this method is the need for immunosuppression is only early, not life-long. The cons are long-lasting and multiple procedures. So far, only short-segment replacement could be resected using standard techniques.

Cryopreserved, Irradiated, or Chemically Preserved Trachea

To avoid immunosuppressive medication, various attempts to reduce graft immunogenicity, such as cryopreservation,[15] irradiation, or detergent enzymatic treatment were investigated. Unfortunately, it was soon evident that the mechanical and structural macroscopic properties and cell adhesion and behavior would be damaged.[15–18] The long processing time was also a concern, especially for patients with malignancies. Regarding chemically fixated tracheae, Jacobs and colleagues[19] reported on 131 patients (100 adults and 31 children) who were treated with such processed grafts.[20] The technique was only applied in patients with benign tracheal disorders, except for one who had adenoid cystic carcinoma, with satisfactory results. However, because it requires an intact posterior tracheal wall, this technique is unfeasible for extended circumferential malignancies. The common denominator of these reconstructive methods is the need of permanent stenting. The pro of these methods is that there is no need for immunosuppressive medication. The cons are that they are donor dependent, have an extended processing time, are partly posterior wall dependent, involve stenting, and are nonvital.

Fresh or Cryopreserved Cadaveric Aorta

Some groups investigated the use of aortic grafts to replace the affected part of the windpipe. Carbognani and colleagues[21] introduced the technique of using a cryopreserved aortic allograft. Their study showed the technical feasibility of the method but also the imperative necessity of always placing a permanent stent into the graft to provide normal function and limit fibroblasts colonization. Wurtz and colleagues[22] reported satisfying clinical results without immunosuppressive medication by using either fresh or cryopreserved aortic homografts.[23] Nevertheless, the lack of cartilage-ring development and, therefore, related loss of structural integrity requires permanent stenting and other mechanical support.[22,24] The pro for these methods is that there is no need for immunosuppressive medication. The cons are donor dependence and permanent intraluminal stenting.

TE

Hermes Grillo,[1] a pioneer of airway surgery, stated that TE could become the most promising therapeutic concept for patients with

inoperable tracheal lesions. Experimental studies demonstrated the potential of TE for nearly every solid or tubular organ and each type of tissue. Initial clinical applications for a variety of these, such as heart valves, urine bladder, tubular structures, suggest the technologic feasibility and potential.[25–28] The concept of TE is based on four components: (1) scaffold or matrix, (2) cells, (3) bioreactor, and (4) various bioactive molecules.

The Scaffold

The scaffold is the basic component that provides the structural integrity of the graft. Characteristics must meet both general and organ requirements, including trachea-specific criteria. General requirements are that it is nonimmunogenic, nontoxic, and nontumorigenic, as well as allows for cell adhesion, migration, proliferation, and differentiation. Trachea-specific characteristics include airtight and liquid-tight seals at the start; mechanical properties that will react on both lateral and longitudinal forces, and support airway patency; and adequate respiratory function.

The biologic scaffold

Various biologic scaffolds have been investigated for their potential use but the ideal scaffold source depends on the target tissue. For the trachea in particular, three natural tissues have been tested in detail: the trachea,[29–31] porcine jejunum,[32] and the aorta.[33] The primary goal of TE is to provide a nonimmunogenic scaffold that can be transplanted without any subsequent need of immunosuppressive medication. Because the major histocompatibility complexes I and II are key for adverse immune reaction, it is imperative to remove them from the donor tissue. Decellularization, using various methods such as detergent and enzymatic solutions (ionic, nonionic, resolvent, chelating, alkaline, acidic, zwitterionic) and/or physical methods (perfusion, agitation, static), has demonstrated its efficiency in doing so. During the removal of the genomic DNA, the nanofiber architecture of the extracellular matrix (ECM) remained intact and the bioengineered ECM consisted of several proteins (laminin, elastin, collagen) of significant importance for cell homing, differentiation, migration, and proliferation. Each decellularization strategy has a different impact on the in vivo degradation process of the ECM, which essentially influences tissue remodeling stimulation, angiogenesis (neoformation of vessels), and cell homing.

To date, initial cases of clinical transplantation using biologic scaffolds processed by detergent enzymatic method have been reported with promising early outcome for both a decellularized trachea[27,34] and a porcine jejunum.[32,35] Macchiarini and colleagues performed a series that included nine patients suffering from various disorders and treated with a decellularized and reseeded trachea. Notably, they recognized unpredicted mechanical impairments within 12 months in about 30% of the patients (Macchiarini, personal communication, 2013). The pros of this method are that there is no need for immunosuppressive medication and preservation of the ECM. The cons are donor dependency, processing time, and biomechanical degeneration.

The artificial scaffold

Even though the initial clinical experience with biologic scaffolds seems promising, drawbacks do still exist, even though the biologic scaffolds do yet require a human donation. The decellularization protocol lasts approximately 2 to 3 weeks, which might not be practical for patients with malignant diseases that require an early treatment. In addition, the mechanical properties are a disadvantage, particularly for longer segments that require recurrent stenting because of the clinically observed instable biomechanics. Therefore, other alternatives are more desired.

As discussed previously, the assumption that the trachea is only a tubular structure to transport air from the larynx to the lungs is obsolete; other functions and characteristics have been elucidated. This complexity explains why synthetic grafts failed in serving as tracheal grafts.

> *Only a living substitute, therefore vascularized, can pretend to fulfill the anatomic mechanical and anti-infectious functions of the trachea.*
>
> —*Macchiarini*[36]

Artificial material that is not vascularized and is nonvital incorporates a low level of integrity, indicates a trend for migration and contamination, and is usually rather stiff and nonflexible. The absence of vascularization and immunocompetence must be solved to overcome all drawbacks of synthetic materials and their associated complications.[1]

Why artificial?

Synthetic scaffolds have unlimited availability, can be customized and manufactured to meet the patients needs, are inexpensive and fast to process, and can be sterilized without altering cell biology. Various biodegradable and nondegradable materials have been evaluated, including Marlex mesh (Chevron Phillips Chemical Company LP, TX, USA), polyethylene oxide/polypropylene oxide copolymer (Pluronic F-127, Invitrogen, Ltd,

Paisley, UK), polyester urethane, polyethylene glycol–based hydrogel, polyhydroxy acids, poly-ε-caprolactone, polypropylene mesh, poly (lactic–co-glycolic acid) polymer, gelatin sponge, and alginate gel.[1] To date only few clinical applications have been reported using synthetic based scaffolds.[37–39]

Various matters must be considered to turn synthetic materials into viable tissue. Aside from using cells to reseed the scaffold, pharmaceutical interventions are crucial to support the regeneration of the implanted graft. Moreover, the blood supply can be provided by indirect vascularization via surgical techniques, such as with the omentum major, latissimus dorsi flap, musculofascial flap, or other pedicles. The further development of these strategies will help to improve the outcome of synthetic-based trachea because of the enhanced integrity of the graft and ameliorated in situ regeneration of the transplant.

The pros of this method are that it is not donor dependent, there is no need for immunosuppressive medication, it is anatomically tailored, processing is fast and low-cost, and the nature of its mechanical properties. The cons are that the material is nonvital and there is a risk for contamination.

Composite scaffolds

Biologic and synthetic materials can also be combined into one scaffold to optimize the mechanical and bioactive properties of the graft. The coating of artificial scaffolds with various natural ligands and ECM-proteins may enhance cell adherence and proliferation while mechanical forces maintain. Research has been performed on collagen-coated poly-propylene scaffolds. In addition, various gels incorporating the cells for the internal and external surface were investigated.[40] The outcome of all these surface modification studies did not result in entirely convincing data; therefore, clinical transfer has not been realized.[41,42] In contrast, defects of the trachea smaller than 50 mm, have been successfully treated with the technology of composites using a Marlex mesh tube covered by collagen sponge.[43] Therefore, combinations of biologic and synthetic components may provide novel alternatives to TE in the future. The pros of this method are that it is not donor dependent, there is no need for immunosuppressive medication, it can be customized, and processing is fast, and cost-effective. The cons are that it is stent-dependent, nonvital, and there is a risk for contamination.

Scaffold-free

A recently developed technology of scaffold-free cell sheets is so far only applicable for very small defects but not for circumferential defects or longer gap reconstructions due to the lack of structural integrity.

The pros are that this method is not donor dependent and there is no need for immunosuppressive medication. The cons are that it is not feasible for long gap and circumferential reconstruction.

Cells

The cell type and source can differ and is highly dependent on the target tissue (Fig. 1). Considerations include stem versus differentiated cells, and allogenic versus autologous cells.

Aside from in vitro seeded cells, bone marrow-derived cells and resident stem or progenitor cells may contribute to tissue regeneration.[44] Go and colleagues,[45] and Jungebluth and colleagues,[38] demonstrated the necessity of seeding cells before tracheal transplantation to avoid graft collapse and bacterial contamination. Seguin and colleagues[44] provided similar evidence for the involvement of bone marrow–derived mesenchymal stem cells to tracheal regeneration. In addition, resident stem and progenitor cells, responsible for tissue regeneration and repair, have been detected in so-called stem cell niches along the airways, so far mainly in animals but similarities may exist in humans.[46,47]

Stem cells

Pluripotent stem cells The use of pluripotent cells, including embryonic stem cells (ESCs) and induced pluripotent stem cells (iPSCs) is widely debated. In particular, ESCs are controversial because of significant ethical concerns. When Takahashi and Yamanaka[48] first described the technology of reprogramming mature cells into pluripotent stem cells, it was presumed that this cell type would soon be transferred to the clinic and be an ideal autologous alternative to ESCs. However, in experimental studies it has been elucidated that both iPSCs (depending on the reprogramming method) and ESCs seem to be prone to immune recognition and consequent rejection. In addition, the reprogramming for IPSCs is insufficient, which makes clinical use currently unrealistic. The pros of pluripotent cells are that they are not donor dependent (iPSCs) and there is no need for immunosuppressive medication (method dependent). The cons are ethical concerns, donor dependency (ESCs), and the need for immunosuppressive medication.

Multipotent stem cells Multipotent or adult stem cells, such as mesenchymal (MSCs), hematopoietic stem cells (HSCs), or amniotic fluid stem cells,

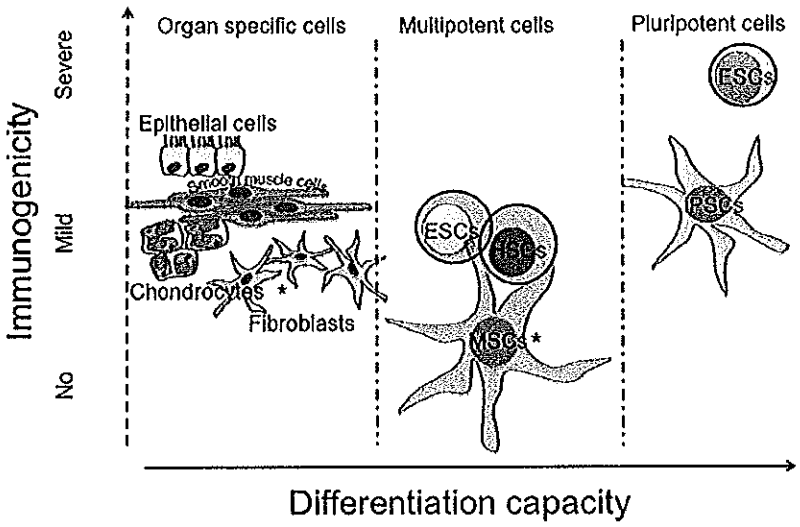

Fig. 1. Immunogenicity of various cell types potentially usable in TE. EPCs, endothelial progenitor cells; ESCs, embryonic stem cells; HSCs, hematopoietic stem cells; iPSCs, induced pluripotent stem cells; MSC, mesenchymal stromal cells. Already clinically applied (*asterisks*).

can differentiate into various cell types. These stem cells are usually obtained from the recipient (eg, bone marrow, peripheral blood, fat tissue) with essentially no ethical concerns and, therefore, can be applied without the use of immunosuppression. These so-called adult stem cells have already been used in many tracheal-related and nonrelated clinical settings.[27,49–51] Mononuclear cells (MNCs) have become clinically interesting (NCT01110252) because they include stem and progenitor cells, can be isolated from the bone marrow or the peripheral blood, and be actively mobilized to increase the yield of isolated cells.[37]

The pros of this method are there is no need for immunosuppressive medication, it is not donor dependent (depending on the cell type), multipotent differentiation, good availability, immunomodulatory capacity, and nearly no ethical issues. The con is that it is donor dependent.

Terminally differentiated cells

Epithelial, smooth muscle, and endothelial cells, and chondrocytes, have been clinically applied[14,27,32,35] for different tracheal replacement strategies. All these cells have low ethical implications, which make the clinical transfer simple.

The pros for this method are no need for immunosuppressive medication (depending on cell source), it is not donor dependent (if autologous), and isolation is simple. The cons are that it is donor dependent (if allogenic), immunosuppression (for allogenic) is needed, it is terminally differentiated, and the cell numbers are low.

Autologous versus allogenic cells

The advantage of using autologous cells is that it eliminates the patient's need for lifelong immunesuppressants. Regarding adult stem and progenitor cells, the available number and application field are high because of their self-renewal and differentiation capacity. In contrast, terminally differentiated cells have a limited source due to autologous cell or tissue donations making them inappropriate for some specific clinical scenarios. Allogenic cells have an unlimited availability but, aside from MSCs, require lifelong immunosuppressive medication.

The pros of allogenic cells are the unlimited cells numbers and the capacity for differentiation depending on the cell type. The cons are the need for immunosuppressive medication (except for MSCs). The pros of autologous cells are that they are not donor dependent and no immunosuppressive medication is needed. The cons are limited cell numbers and that they are inappropriate for malignant diseases (see Fig. 1).

Bioreactor

To provide the ideal conditions for TE of the airways, the natural environment should be ideally mimicked or used as a bioreactor. The external conditions influence all cellular parameters such as adhesion, engraftment, proliferation, differentiation, migration, and apoptosis. Asnaghi and colleagues[52] introduced a double-chamber rotating bioreactor for trachea engineering in a clinical setting with controlled and monitored conditions.

A more developed version of this bioreactor has been used for the clinical transplantation of natural decellularized scaffolds[27,34] and synthetic-based grafts.[37,38] Despite these initial promising clinical applications, there is the possibility of using the organism of the organ recipient as a biologic bioreactor with an single-[53,54] or multistage in vivo engineering strategy.[14]

In vitro pros are controlled and monitored conditions and customized devices. The cons are risk of contamination, lack of native characteristics, the need for additional substrates (eg, hormones, growth factors), cost, and labor demands.

In vivo pros are an ideal environment and it is cost-effective. The con is that there is no control of cell behavior (proliferation, migration, differentiation).

Pharmaceutical Intervention

Bioactive and signaling molecules, hormones, and other factors may be used to overcome the difficulties associated to engineered tissue transplantation, especially contamination and, even more significant, necrosis. Vascularization or, more precisely, neovascularization plays the most crucial role in this context and usually results in ischemia of the transplanted tissue. Direct and indirect vascularization can be achieved via surgical techniques as previously described.[11] However, additional strategies are necessary to provide sufficient angiogenesis within the transplanted construct. Therefore, other vascular growth promoting factors are required, such as vascular endothelial growth factor, fibroblast growth factor, and so forth. Aside from the bioactive factors that drive the neovascularization, further components such as endothelial cells are necessary to form the novel vessels. To this end, strategies that can mobilize progenitor and stem cells from their niches are of interest (Fig. 2), including granulocyte colony-stimulating factor (G-CSF), which was administrated in some early patients who underwent tracheal transplantation.[37] G-CSF can mobilize endothelial progenitor cells (EPCs) to support neoangiogenesis and MSCs can positively influence wound healing. MSCs, specifically CXCR-4–positive MSCs, can be attracted to the transplantation site and promote the regeneration of the implanted graft via their immunomodulatory capacity. The cell homing is initiated and driven by various blood activation products, chemokines, and/or growths factors and can be mediated through the SDF-1/CXCR4 pathway. Usually, an ischemic environment dominates the surgical wound due to initially poorly developed

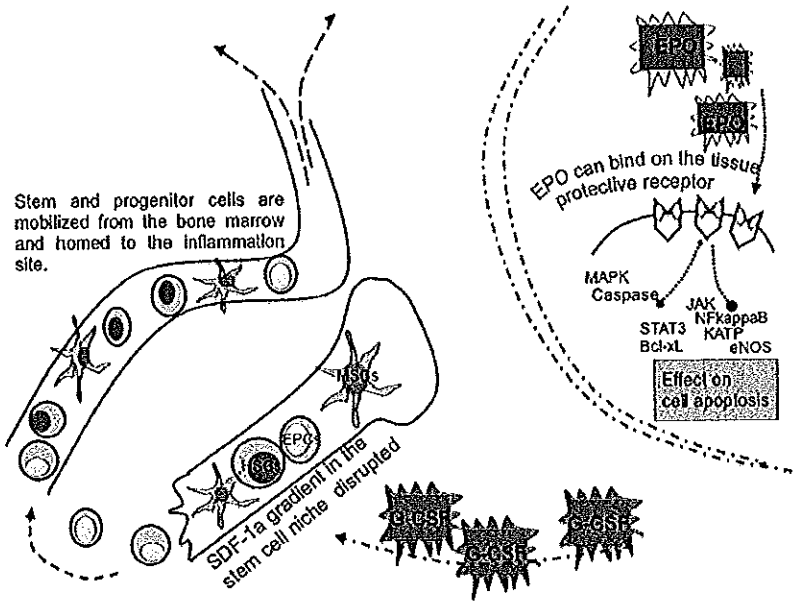

Fig. 2. Pharmaceutical intervention and bioactive molecules. EPCs, endothelial progenitor cells; EPO, erythropoietin; G-CSF, granulocyte colony-stimulating factor; HSCs, hematopoietic stem cells. Genes involved in apoptosis: Bcl-xL, B-cell lymphoma-extra large; eNOS, endothelial nitric oxide synthase; JAK, Janus kinase; KATP, ATP-sensitive K(+); MAPK, mitogen-activated protein kinases; MSC, mesenchymal stromal cells; NFkappaB, nuclear factor kappa-light-chain-enhancer of activated B cells; STAT3, signal transducer and activator of transcription 3.

neovascularization, which provokes increased cell death. Antiapoptotic strategies, therefore, may have beneficial impact on transplanted tissues. Erythropoietin (EPO) can certainly represent such a tool via its tissue protective function that has been described previously.[55,56] Aside from regulating the erythropoiesis, EPO influences the expression of several antiapoptotic genes, including Janus tyrosine kinase-2 (JAK-2) STAT5 (signal transducer and activator of transcription 5)-Bcl-2, phosphatidylinositol 3, protein kinase B, mitogen-activated protein kinase, and nuclear factor-κB. Using EPO may provide a protective effect for resident cells (within the wound environment) and to cells that are exposed to ischemic environment on the tracheal graft due to the lack of early vascularization.

Further strategies focus on the modification of the scaffold to improve cell–surface interaction and the material's biocompatibility and, therefore, the cell adhesion, proliferation, and differentiation. The pro of this method is support of the endogenous regenerative capacity. The cons are unknown risks and side-effects.

SUMMARY

Trachea transplantation remains a highly challenging procedure and, so far, no ultimate solution has been discovered. For many decades, physicians and researchers made immense efforts to overcome the hurdles of replacing a simple connection between the larynx and the lungs. It turned out to be much more difficult and, in particular, more complex than previously assumed. Various purely surgical techniques have been evaluated; however, because of technical challenges, they have not proven their clinical feasibility. In addition, conventional allogenic transplantation requires lifelong immunosuppressive medication and is associated with negative side effects. Recently, early clinical achievements in tissue-engineered trachea provide clinical evidence that this method might be the next promising therapeutic alternative in tracheal replacement (Table 3). Progress has been made in investigating underlying mechanisms and pathways of cell–surface interactions, cell migration, and differentiation; however, we are far from fully understanding the complexity of tracheal tissue regeneration. TE is

Table 3
Overview of clinical cases using TE tracheal grafts

	Decellularized Trachea Transplantation (2008–2011)	Outcome
Patients	9 male/female (3:6) (11–72 y)	4:5 (dead/alive)
Indications		
Benign diseases (n = 6)	4	All 4 alive, partly biodegradable stent-dependent
• Severe tracheomalacia or bronchomalacia	1	Alive, no need for stent support
• Long-segment congenital stenosis	1	Patient died of fulminant gastrointestinal bleeding
• Tracheoesophageal fistula		
Malignant diseases (n = 3)	3	All patients died of systemic tumor recurrence
• Primary tracheal carcinoma		
	Synthetic-based Trachea (2011–2013)	**Outcome**
Patients	Eight male/female, 3:5 (2–43 y)	2:6 (dead/alive)
Indications		
Benign diseases (n = 6)		1 (out of 6) patient died of unrelated causes
• Severe tracheomalacia or bronchomalacia	4	To date, all patients are alive (only the POSS/PCU scaffold requires stent treatment because of abnormal granulation tissue and fistula formation)
• Long-segment congenital stenosis	1	
• Congenital agenesis	1	
Malignant diseases (n = 2)	2	1 patient died of severe gastrointestinal bleeding
• Primary tracheal carcinoma		

a step in the right direction but only the future will elucidate the real impact of this technology on tracheal replacement.

REFERENCES

1. Grillo HC. Tracheal replacement: a critical review. Ann Thorac Surg 2002;73:1995–2004.
2. Nakahira M, Nakatani H, Takeuchi S, et al. Safe reconstruction of a large cervico-mediastinal tracheal defect with a pectoralis major myocutaneous flap and free costal cartilage grafts. Auris Nasus Larynx 2006;33:203–6.
3. Macchiarini P. Primary tracheal tumours. Lancet Oncol 2006;7:83–91.
4. Fonkalsrud EW, Sumida S. Tracheal replacement with autologous esophagus for tracheal stricture. Arch Surg 1971;102:139–42.
5. Fonkalsrud EW, Martelle RR, Maloney JV. Surgical treatment of tracheal agenesis. J Thorac Cardiovasc Surg 1963;45:520–5.
6. Rose K, Sesterhenn K, Wustrow F. Tracheal allotransplantation in man. Lancet 1979;1:433.
7. Levashov Yu N, Yablonsky PK, Cherny SM, et al. One-stage allotransplantation of thoracic segment of the trachea in a patient with idiopathic fibrosing mediastinitis and marked tracheal stenosis. Eur J Cardiothorac Surg 1993;7:383–6.
8. Delaere PR, Liu Z, Sciot R, et al. The role of immunosuppression in the long-term survival of tracheal allografts. Arch Otolaryngol Head Neck Surg 1996; 122:1201–8.
9. Shaari CM, Farber D, Brandwein MS, et al. Characterizing the antigenic profile of the human trachea: implications for tracheal transplantation. Head Neck 1998;20:522–7.
10. Klepetko W, Marta GM, Wisser W, et al. Heterotopic tracheal transplantation with omentum wrapping in the abdominal position preserves functional and structural integrity of a human tracheal allograft. J Thorac Cardiovasc Surg 2004;127:862–7.
11. Macchiarini P, Lenot B, De Montpreville V, et al. Heterotopic pig model for direct revascularization and venous drainage of tracheal allografts. Paris-Sud University Lung Transplantation Group. J Thorac Cardiovasc Surg 1994;108:1066–75.
12. Duque E, Duque J, Nieves M, et al. Management of larynx and trachea donors. Transplant Proc 2007; 39:2076–8.
13. Farwell DG, Birchall MA, Macchiarini P, et al. Laryngotracheal transplantation: technical modifications and functional outcomes. Laryngoscope 2013;123(10):2502–8. http://dx.doi.org/10.1002/lary.24053.
14. Delaere P, Vranckx J, Verleden G, et al. Tracheal allotransplantation after withdrawal of immunosuppressive therapy. N Engl J Med 2010;362:138–45.
15. Kunachak S, Kulapaditharom B, Vajaradul Y, et al. Cryopreserved, irradiated tracheal homograft transplantation for laryngotracheal reconstruction in human beings. Otolaryngol Head Neck Surg 2000;122:911–6.
16. Yokomise H, Inui K, Wada H, et al. High-dose irradiation prevents rejection of canine tracheal allografts. J Thorac Cardiovasc Surg 1994;107:1391–7.
17. Liu Y, Nakamura T, Sekine T, et al. New type of tracheal bioartificial organ treated with detergent: maintaining cartilage viability is necessary for successful immunosuppressant free allotransplantation. ASAIO J 2002;48:21–5.
18. Hisamatsu C, Maeda K, Tanaka H, et al. Transplantation of the cryopreserved tracheal allograft in growing rabbits: effect of immunosuppressant. Pediatr Surg Int 2006;22:881–5.
19. Jacobs JP, Quintessenza JA, Andrews T, et al. Tracheal allograft reconstruction: the total North American and worldwide pediatric experiences. Ann Thorac Surg 1999;68:1043-51 [discussion: 1052].
20. Elliott MJ, Haw MP, Jacobs JP, et al. Tracheal reconstruction in children using cadaveric homograft trachea. Eur J Cardiothorac Surg 1996;10: 707–12.
21. Carbognani P, Spaggiari L, Solli P, et al. Experimental tracheal transplantation using a cryopreserved aortic allograft. Eur Surg Res 1999;31: 210–5.
22. Wurtz A, Porte H, Conti M, et al. Tracheal replacement with aortic allografts. N Engl J Med 2006;355: 1938–40.
23. Wurtz A, Porte H, Conti M, et al. Surgical technique and results of tracheal and carinal replacement with aortic allografts for salivary gland-type carcinoma. J Thorac Cardiovasc Surg 2010;140:387–93.e2.
24. Wurtz A, Hysi I, Kipnis E, et al. Tracheal reconstruction with a composite graft: fascial flap-wrapped allogenic aorta with external cartilage-ring support. Interact Cardiovasc Thorac Surg 2013;16:37–43.
25. Olausson M, Patil PB, Kuna VK, et al. Transplantation of an allogeneic vein bioengineered with autologous stem cells: a proof-of-concept study. Lancet 2012;6736:1–8.
26. Atala A, Bauer SB, Soker S, et al. Tissue-engineered autologous bladders for patients needing cystoplasty. Lancet 2006;367:1241–6.
27. Macchiarini P, Jungebluth P, Go T, et al. Clinical transplantation of a tissue-engineered airway. Lancet 2008;372:2023–30.
28. Cebotari S, Lichtenberg A, Tudorache I, et al. Clinical application of tissue engineered human heart valves using autologous progenitor cells. Circulation 2006;114:I132–7.
29. Jungebluth P, Go T, Asnaghi A, et al. Structural and morphologic evaluation of a novel

detergent-enzymatic tissue-engineered tracheal tubular matrix. J Thorac Cardiovasc Surg 2009; 138:586–93 [discussion: 592–3].
30. Conconi MT, DeCoppi P, Di Liddo R, et al. Tracheal matrices, obtained by a detergent-enzymatic method, support in vitro the adhesion of chondrocytes and tracheal epithelial cells. Transpl Int 2005;18:727–34.
31. Zang M, Zhang Q, Chang EI, et al. Decellularized tracheal matrix scaffold for tissue engineering. Plast Reconstr Surg 2012;130:532–40.
32. Walles T, Giere B, Hofmann M, et al. Experimental generation of a tissue-engineered functional and vascularized trachea. J Thorac Cardiovasc Surg 2004;128:900–6.
33. Seguin A, Radu D, Holder-Espinasse M, et al. Tracheal replacement with cryopreserved, decellularized, or glutaraldehyde-treated aortic allografts. Ann Thorac Surg 2009;87:861–7.
34. Elliott MJ, De Coppi P, Speggiorin S, et al. Stem-cell-based, tissue engineered tracheal replacement in a child: a 2-year follow-up study. Lancet 2012;380:994–1000.
35. Macchiarini P, Walles T, Biancosino C, et al. First human transplantation of a bioengineered airway tissue. J Thorac Cardiovasc Surg 2004;128:638–41.
36. Macchiarini P. La transplantation de trachée et trachéo-oesophagienne [Thesis]. Berançon (France): Université Franche-Comte; 1997.
37. Jungebluth P, Alici E, Baiguera S, et al. Tracheobronchial transplantation with a stem-cell-seeded bioartificial nanocomposite: a proof-of-concept study. Lancet 2011;378:1997–2004.
38. Jungebluth P, Haag JC, Lim ML, et al. Verification of cell viability in bioengineered tissues and organs before clinical transplantation. Biomaterials 2013; 34:4057–67.
39. Available at: http://www.nytimes.com/2013/04/30/science/groundbreaking-surgery-for-girl-born-without-windpipe.html?_r=0.
40. Tada Y, Suzuki T, Takezawa T, et al. Regeneration of tracheal epithelium utilizing a novel bipotential collagen scaffold. Ann Otol Rhinol Laryngol 2008; 117:359–65.
41. Yanagi M, Kishida A, Shimotakahara T, et al. Experimental study of bioactive polyurethane sponge as an artificial trachea. ASAIO J 1994;40:M412–8.
42. Grimmer JF, Gunnlaugsson CB, Alsberg E, et al. Tracheal reconstruction using tissue-engineered cartilage. Arch Otolaryngol Head Neck Surg 2004;130:1191–6.
43. Omori K, Tada Y, Suzuki T, et al. Clinical application of in situ tissue engineering using a scaffolding technique for reconstruction of the larynx and trachea. Ann Otol Rhinol Laryngol 2008;117:673–8.
44. Seguin A, Baccari S, Holder-Espinasse M, et al. Tracheal regeneration: evidence of bone marrow mesenchymal stem cell involvement. J Thorac Cardiovasc Surg 2013;145(5):1297–304.e2. http://dx.doi.org/10.1016/j.jtcvs.2012.09.079.
45. Go T, Jungebluth P, Baiguero S, et al. Both epithelial cells and mesenchymal stem cell-derived chondrocytes contribute to the survival of tissue-engineered airway transplants in pigs. J Thorac Cardiovasc Surg 2010;139:437–43.
46. Kim CF, Jackson EL, Woolfenden AE, et al. Identification of bronchioalveolar stem cells in normal lung and lung cancer. Cell 2005;121:823–35.
47. Reya T, Morrison SJ, Clarke MF, et al. Stem cells, cancer, and cancer stem cells. Nature 2001;414: 105–11.
48. Takahashi K, Yamanaka S. Induction of pluripotent stem cells from mouse embryonic and adult fibroblast cultures by defined factors. Cell 2006;126: 663–76.
49. Gupta PK, Chullikana A, Parakh R, et al. A double blind randomized placebo controlled phase I/II study assessing the safety and efficacy of allogeneic bone marrow derived mesenchymal stem cell in critical limb ischemia. J Transl Med 2013; 11:143.
50. Miettinen JA, Salonen RJ, Ylitalo K, et al. The effect of bone marrow microenvironment on the functional properties of the therapeutic bone marrow-derived cells in patients with acute myocardial infarction. J Transl Med 2012;10:66.
51. Le Blanc K, Frassoni F, Ball L, et al. Mesenchymal stem cells for treatment of steroid-resistant, severe, acute graft-versus-host disease: a phase II study. Lancet 2008;371:1579–86.
52. Asnaghi MA, Jungebluth P, Raimondi MT, et al. A double-chamber rotating bioreactor for the development of tissue-engineered hollow organs: from concept to clinical trial. Biomaterials 2009; 30:5260–9.
53. Bader A, Macchiarini P. Moving towards in situ tracheal regeneration: the bionic tissue engineered transplantation approach. J Cell Mol Med 2010;14: 1877–89.
54. Jungebluth P, Bader A, Baiguera S, et al. The concept of in vivo airway tissue engineering. Biomaterials 2012;33:4319–26.
55. Brines M, Cerami A. Erythropoietin-mediated tissue protection: reducing collateral damage from the primary injury response. J Intern Med 2008;264:405–32.
56. Hoch M, Fischer P, Stapel B, et al. Erythropoietin preserves the endothelial differentiation capacity of cardiac progenitor cells and reduces heart failure during anticancer therapies. Cell Stem Cell 2011;9:131–43.

Appendix 13

Biomaterials 35 (2014) 5307–5315

Contents lists available at ScienceDirect

Biomaterials

journal homepage: www.elsevier.com/locate/biomaterials

Biomechanical and biocompatibility characteristics of electrospun polymeric tracheal scaffolds

Fatemeh Ajalloueian [a,1], Mei Ling Lim [a,1], Greg Lemon [a], Johannes C. Haag [a], Ylva Gustafsson [a], Sebastian Sjöqvist [a], Antonio Beltrán-Rodríguez [a], Costantino Del Gaudio [b], Silvia Baiguera [a], Alessandra Bianco [b], Philipp Jungebluth [a], Paolo Macchiarini [a,*]

[a] Advanced Center for Translational Regenerative Medicine (ACTREM), Department of Clinical Science, Intervention and Technology (CLINTEC), Karolinska Institutet, Stockholm, Sweden
[b] University of Rome "Tor Vergata", Department of Industrial Engineering, Intrauniversitary Consortium for Material Science and Technology (INSTM), Research Unit Tor Vergata, Rome, Italy

ARTICLE INFO

Article history:
Received 13 January 2014
Accepted 7 March 2014
Available online 3 April 2014

Keywords:
Electrospinning
Tracheal scaffold
Biocompatibility
Cell seeding
Static and dynamic cultures
Correlation

ABSTRACT

The development of tracheal scaffolds fabricated based on electrospinning technique by applying different ratios of polyethylene terephthalate (PET) and polyurethane (PU) is introduced here. Prior to clinical implantation, evaluations of biomechanical and morphological properties, as well as biocompatibility and cell adhesion verifications are required and extensively performed on each scaffold type. However, the need for bioreactors and large cell numbers may delay the verification process during the early assessment phase. Hence, we investigated the feasibility of performing biocompatibility verification using static instead of dynamic culture. We performed bioreactor seeding on 3-dimensional (3-D) tracheal scaffolds (PET/PU and PET) and correlated the quantitative and qualitative results with 2-dimensional (2-D) sheets seeded under static conditions. We found that an 8-fold reduction for 2-D static seeding density can essentially provide validation on the qualitative and quantitative evaluations for 3-D scaffolds. *In vitro* studies revealed that there was notably better cell attachment on PET sheets/scaffolds than with the polyblend. However, the *in vivo* outcomes of cell seeded PET/PU and PET scaffolds in an orthotopic transplantation model in rodents were similar. They showed that both the scaffold types satisfied biocompatibility requirements and integrated well with the adjacent tissue without any observation of necrosis within 30 days of implantation.

1. Introduction

Bioengineered tracheae, using decellularized tissue, have recently been successfully transplanted into patients [1–3]. However, biological scaffolds are donor dependent and require long processing time and cost. Besides, the tracheal dimensions would require donor-recipient matching. In order to overcome these drawbacks, customized synthetic scaffolds might be the next potential solution.

In 2011, the first synthetic-based tracheal scaffold, seeded with patient's autologous stem cells was transplanted in a clinical setting [4]. This Y-shaped scaffold was manufactured from the preoperative chest CT and three-dimensional images of the patient trachea using a nanocomposite polymer (POSS-PCU; polyhedral oligomeric silsesquioxane [POSS] covalently bonded to poly-[carbonate-urea] urethane [PCU]) [5]. U shaped rings of POSS-PCU were prepared through casting methodologies and were placed around a Y-shaped glass mandrel. Then, the whole construct was placed in a POSS-PCU solution, followed by a coagulation procedure which resulted in a porous scaffold [4]. However, due to the stiffness of the scaffold, an abnormal granulation tissue formation developed within the post-operative course. Moreover, it led to chronic fistula at the distal anastomotic sites of the left main bronchus, which required endoscopic interventions.

The need to improve the biomechanical properties of the scaffold and our willing to mimic the native tracheal extracellular

* Corresponding author. Advanced Center for Translational Regenerative Medicine, (ACTREM), Division of Ear, Nose, and Throat (CLINTEC), Karolinska Institutet, Alfred Nobels Allé 8, Huddinge, SE-141 86 Stockholm, Sweden. Tel.: +46 760 503 213 (mobile); fax: +46 8 774 7907.
E-mail address: paolo.macchiarini@ki.se (P. Macchiarini).
[1] Contributed equally to this work.

http://dx.doi.org/10.1016/j.biomaterials.2014.03.015
0142-9612/

matrix (ECM), led to fabrication of the next generation of scaffolds to include FDA approved polymers like polyethylene terephthalate (PET) and polyurethane (PU). Electrospinning was applied as the main fabrication technique. This technology is simple, fast and can provide fibrous networks similar to biomimetic characteristics of the native ECM [6,7]. A polyblend of PET/PU (50% weight ratio for each) was the first electrospun tracheal scaffold clinically applied. Although this construct contained all criteria for an optimal scaffold, we noticed local collapse with the scaffold one year post-transplantation. The slump of biomechanical properties seemed to originate from non-optimal balance in the degradation rate of applied PU and the production of new extracellular matrix. So, we proceeded to further develop the electrospun scaffolds by reducing the amount of PU or completely eliminating it from the scaffold structure composition.

Here, we present the evaluations performed on electrospun scaffolds. It includes biomechanical characterization, structural analyses and biological verifications. The latter demanded significant resources due to various cell-seeding studies using bioreactors. Hence, we investigated if a 2-D static cell seeding model could correlate well to 3-D scaffold seeding *via* a bioreactor. This may help to replace the 3-D seeding during a preclinical testing phase whilst providing the relevant information required for a clinical translation.

2. Materials and methods

2.1. Fabrication of electrospun scaffolds

The first clinically applied electrospun tracheal scaffold was produced as a polyblend of polyethylene terephthalate (PET) and polyurethane (PU) with 50% weight ratio of each (Nanofiber Solutions, Ohio, USA) based on the CT images of the patient's trachea. The electrospun body was reinforced with C-shaped rings to withstand the pulling and compressive forces from surrounding tissues.

Tracheal scaffolds of (i) PET/PU (weight composition of 70/30 respectively) and (ii) pure PET were two candidates for next clinical application (Harvard Apparatus Regenerative Technology®, HART, Holliston, MA, USA). The scaffolds were processed according to the manufacturer's procedure: (i) The PET solution was prepared by dissolving 14wt% polyethylene terephthalate (PET) (Indorama Ventures, IL, USA) in 1,1,1,3,3,3-hexafluoroisopropanol (HFIP) (Sigma–Aldrich, MA, USA) at 50 °C using magnetic stirring carried out for 3 h. The polyurethane (PU) pellets (Bionate, DSM Biomedical, Netherlands) were added to the already prepared solution to make a 6wt% PU solution using the same dissolving procedure (50 °C using magnetic stirring carried out for 3 h). Similar dissolution procedure was applied for preparation of the PET solution (20wt%). Electrospinning of both solutions was carried out, with a voltage of 14–16 kV applied to the blunt needle (21 G) tip of the syringe (filled with the solution). The feed rate was 10 mL/h and the needle tip to collector distance was 15 cm. The collector was a mandrel with D shaped cross section, designed based on the CT images of patient's trachea and rotated at a speed of 200 revolutions per minute (rpm). The air relative humidity and temperature were 40% and 23 °C respectively. The electrospinning was continued until the desired thickness (1/2 of total thickness) was reached. Cartilage rings produced out of PET using injection-molding technique were placed (based on a predefined intervals) and fixed over the electrospun layer. Electrospinning was continued to reach the final thickness. The fabricated scaffold was kept in a vacuum oven for 12 h at 60 °C to ensure no residual solvent remains. The scaffolds were then treated using radio frequency oxygen gas plasma for 1 min. For sterilization, they were exposed to 25 kGy (330,000 mJ/cm^2) of gamma irradiation.

2.2. Scaffold characterization

The morphology of electrospun nanofibers was studied with the help of scanning electron microscopy (SEM). The average fiber diameter of the electrospun scaffolds was measured by applying ImageJ 1.46R (NH, Maryland, USA) to the SEM micrographs.

Tensile properties of the synthetic scaffolds of PET50/PU50, PET70/PU30 and PET were determined using a universal testing machine (UTM; Lloyds LRX, USA) fitted with a calibrated load cell of 1 kN. Test specimens (full 3-D scaffolds) were tested at a crosshead speed of 1 mm/s at ambient conditions. Scaffolds were glued (from flat part at the back) to clamps fixed at the UTM grips. Dimensions were measured using calibrated Mitutoyo CS callipers and were entered to the instrument software. Force and displacement were recorded during testing. Strain was calculated as displacement divided by the original gauge length. Maximum force and corresponding strain are reported. 5 scaffolds were used for each of the three scaffold types.

The porosity was calculated using the formula of

$$\text{Porosity}(\%) = \left(1 - \frac{\rho}{\rho^0}\right) * 100$$

where ρ is the bulk density and ρ^0 is the apparent density, which is 1.41 g/cm^3 and 1.19 g/cm^3 for the applied PET and PU respectively. The bulk density was calculated using a piece of electrospun mat with known mass and dimension by using this formula:

$$\rho\left(\frac{g}{cm^3}\right) = \frac{\text{Mass(g)}}{\text{Thickness(cm)} \times \text{area(cm}^2\text{)}}$$

2.3. In vitro and in vivo experimental studies

Male Sprague Dawley rats ($n = 13$) were used for both the *in vitro* and the *in vivo* orthotopic transplantation studies. The "Principles of laboratory animal care" formulated by the National Society for Medical Research and the "Guide for the care and use of laboratory animals" prepared by the Institute of Laboratory Animal Resources, National Research Council, and published by the National Academy Press, revised 1996, have been applied to all the animals. Ethical permissions were provided by the local authorities (the Stockholm South Ethical Committee; Sweden; registration number S74-12).

2.4. Mesenchymal stromal cell isolation

Cells were isolated from male Sprague Dawley rats ($n = 5$). Mesenchymal stromal cells (MSCs) were isolated and processed as previously described [8]. Briefly, femur and tibia were cleared from surrounding tissue and phosphate buffered saline (PBS, Invitrogen, Sweden) was flushed out the bone marrow. The obtained cells were centrifuged and the pellet was resuspended in DMEM supplemented whit 10% Fetal Bovine Serum (FBS, Invitrogen, Sweden) and 1% antibiotic-antimycotic (Invitrogen, Sweden). Cells were seeded in a culture flask (BD, CA, USA) and were incubated at 37 °C in 5% CO_2. After 24 h of incubation, the medium was discarded to remove all non-adherent cells. Cells from passages 3 to 7 were used in this study.

2.5. Dynamic cultures

The number of rat MSCs required for seeding the tracheal scaffolds was calculated using a mathematical model that predicts, for a given number of cells seeded initially, the final percentage area of the interior and exterior surfaces that are covered by cells at the end of the incubation. The model was developed by considering the dynamic processes of cell attachment and detachment occurring at the surface of an artificial scaffold or decellularized organ incubated within the *in-breath*™ bioreactor (Harvard Bioscience Inc., Holliston, MA, USA). Cell proliferation on the scaffold, and cell reattachment from the bioreactor bath onto the scaffold, are assumed to be negligible.

The model predicts that the number of cells, N_s, required for seeding either the interior or exterior surface to achieve a cell coverage, C (%), is given by

$$N_s = \frac{0.01C\pi D_s L}{\beta A_a}$$

Where β is a parameter expressing the ratio of the rate of cell attachment to the rate of cell detachment from cells seeded onto the scaffold surface, and A_a is the average surface area of an attached cell. The scaffold is assumed to be an annular cylinder with diameter (interior or exterior) D_s and length L.

The parameter value $\beta = 0.41$ was obtained by fitting the equation to experimental data of the cell coverage achieved using bioreactor seeding of electrospun adult tracheal scaffolds, made from PET/PU(50/50 percentage composition by weight), with rat MSCs. The parameter value $A_a = 281\ \mu m^2$ was determined by image analysis of rat MSCs attached to thin layers of electrospun PET/PU fibers [8]. The tracheal scaffolds used in the experiments had interior diameter $D_i = 10$ mm, exterior diameter $D_o = 12$ mm, and length $L = 94$ mm.

Substituting the given parameter values into the equation gives the number of cells required to seed the interior and exterior surfaces of the tracheal scaffold to a confluence of 70% as $N_i = 18 \times 10^6$ and $N_o = 22 \times 10^6$ respectively i.e. equivalent to seeding density of approximately $B_d = 6.1 \times 10^5$ cells per square centimeter.

The scaffold was fixed on organ holder (Fig. 1A) and placed inside the specific bioreactor designed for seeding. It was washed two times with phosphate buffered saline (PBS, Invitrogen, Sweden) and two times (each time for 30 min) with stem cell media containing Dulbecco's Modified Eagle Medium (DMEM, Invitrogen, Sweden) supplemented with 10% Fetal Bovine Serum (FBS, Invitrogen, Sweden) and 1% antibiotic-antimycotic (Invitrogen, Sweden). The scaffolds were then seeded with rat MSCs and incubated for 48 h.

2.6. Static cultures

Sheets were cut from 3-D scaffolds (flat external part) using 6 mm biopsy punches, placed in 96 well plates and seeded with different cell densities in the

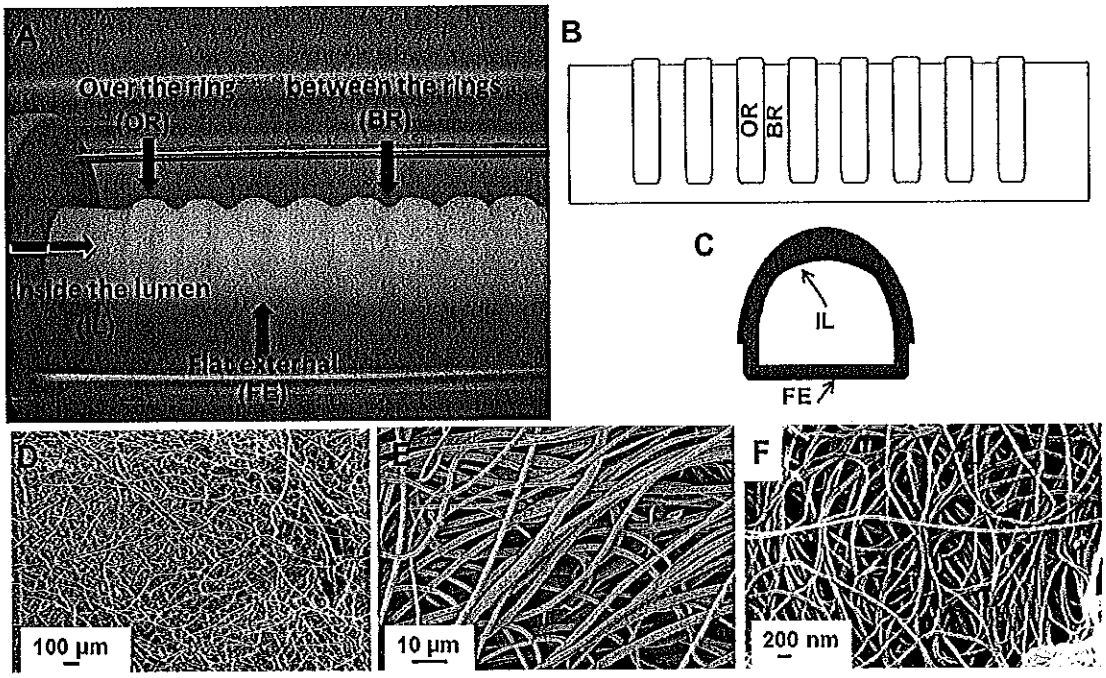

Fig. 1. Macroscopic and microscopic appearance of an electrospun tracheal scaffold. The scaffold is fixed on organ holder and different parts are shown on the image (A); schematic depiction of scaffold from front (B) and side (C) view; SEM images of a tracheal scaffold made from PET under two different magnifications of 100× (D) and 3000× (E) respectively; and SEM image of a rat native trachea (F).

range of 6250 to 100,000 (6250; 12,500; 25,000; 50,000 and 100,000) per well (96 well plates with surface area of 0.32 cm^2).

2.7. Phalloidin and DAPI staining on seeded synthetic scaffolds

Samples from the static and bioreactor cell seeding were fixed in 4% formaldehyde (Histolab, Sweden) for 10 min. They were washed and stained for 30 min with Phalloidin (Molecular Probes, Sweden) diluted in PBS/0.1% Triton X-100 (2 U/ml) (Sigma–Aldrich, Sweden), followed by counterstaining with 4′,6′-diamidino-2-phenylindole (DAPI, Sigma–Aldrich, Sweden). Stained cells were visualized with a fluorescent microscope (Olympus BX-60, Japan). Cell adhesion was quantified by manual counting of nuclear stained cells with ImageJ 1.46R (NH, Maryland, USA) (5 samples; 3 areas on each) and the average was reported.

2.8. Colorimetric cell activity assay

A 3-(4,5-dimethylthiazol-2-yl)-2,5-diphenyl-tetrazolium-bromid (MTT)-assay (Roche, Sweden) was used to evaluate the cell metabolic activity. All samples were analyzed in triplicates. After 48 h of cell seeding, culture medium was removed and 100 μl of fresh medium and 10 μl MTT solutions were added to each well in a 96 well plate. Cells were incubated in the dark at 37 °C (5% CO_2) for 4 h. Next, 10% sodium dodecyl sulfate (SDS) in 0.01 M HCl (100 μl) was added to each well and the plates were further incubated overnight at 37 °C (5% CO_2). The solution was then transferred to another 96-well plate and the optical density of the formazan solution was measured for absorbency at 570 nm with a spectrophotometer (SpectraMax 250, Molecular Devices, CA, USA). Non-seeded scaffold was used as negative control.

2.9. Quantification of cell coverage

A colorimetric approach [9] was used to quantify the percentage cell coverage of the seeded samples. Briefly, a single color digital image, showing a uniformly illuminated top view of all the samples including the unseeded controls, was obtained and imported into MATLAB®. The regions of the image corresponding to each of the samples were extracted using mouse and cursor input. For the samples in each group the color change was calculated using the equation

$$\Delta C = \frac{Y_c - Y_s}{Y_c - Y_m} \times 100\%$$

where Y_s is the average of the grayscale values of the pixels in the sample, Y_c is the average of the grayscale values of the pixels in the control sample, and Y_m is the average of the grayscale values of pixels from regions where there was maximum purple staining.

The cell coverage was then calculated using the formula

$$\theta = \exp\left(\alpha\left(\left(\frac{\Delta C}{100\%}\right)^{\beta} - 1\right)\right) \times 100\%$$

Where $\alpha = 4.25$ and $\beta = 0.58$.

2.10. Quantitative analysis

2.10.1. Dynamic culture of 3-D scaffolds

After 48 h of cell seeding on 3-D scaffolds (PET/PU and PET), we aimed to evaluate DAPI/Phalloidin staining, MTT absorbency, cell coverage based on formazan crystals and SEM imaging. However, for the 3-D scaffolds (bioreactor seeding), we observed that the quantitative data for either of the variables ("number of adhered cells", "absorbency" or "cell coverage") depends on the position under study. For this reason, we performed counting in four different positions for DAPI stained nuclei; which is representative for "number of adhered cells". Three positions are located on the outer surface (Fig. 1A–C) and are referred as: the part over the rings (OR), the part between the rings (BR) and the flat external part at the back of the trachea (FE). The forth position is inside the lumen (IL). For the two other variables i.e. MTT absorbency and cell coverage, we quantify the variables based on being from external parts (OR, BR and FE) or internal part.

For quantification of each of the variables, nine samples were taken from inside the lumen and nine samples from external parts (three from each of the BR, OR and FE), so that the weighted average with weights 3:1:1:1 respectively was reported.

2.10.2. Correlating static and dynamic culture

In order to evaluate the correlation between static and dynamic cultures, a graph was plotted for each variable (i.e. number of adhered cells, absorbency and cell coverage) versus the different cell densities in static seeding on PET70/PU30 and PET sheets. We further compared the quantitative outcomes of bioreactor seeding on 3-D scaffolds with the data from static seeding on 2-D sheets. The weighted average for each variable was used as "Y" input to the formula of the curve (line) of best fit to corresponding data of static cell seeding and the equivalent "X" was interpolated. The average of the three interpolated data was the optimum cell density for performing static cell seeding.

2.11. Scanning electron microscopy

To evaluate cell adhesion on 2-D sheets and 3-D scaffolds, small pieces from 2-D seeded sheets and different positions on the 3-D seeded scaffolds were fixed with 2.5% glutaraldehyde (Merck, Germany) in 0.1 M cacodylate buffer (Prolabo, France) for 2 h at room temperature, rinsed in cacodylate buffer, and dehydrated through

ethanol gradient. Samples were dried overnight, gold sputtered and used for analysis by SEM (JSM6490, JEOL, Japan).

2.12. In vivo evaluation of a seeded-tracheal scaffold in a rat model

To evaluate the electrospun tracheal scaffolds in a rat model, PET70/PU30 ($n = 4$) and PET ($n = 4$) scaffolds, with dimensions of 4 mm (external diameter) and 2.2 mm (internal diameter) were seeded with rat MSCs for 48 h prior to implantations.

Eight Sprague Dawley rats (200–300 g) were anesthetized intramuscularly with 100 mg/kg ketamine (Intervet, Boxmeer, Netherlands) and 10 mg/kg xylazine (Intervet) *via* bolus injection and placed into supine position. The entire procedure was performed under spontaneous breathing. The trachea was exposed *via* an anterior cervical midline incision and the division of the sternohyoid muscles. Traction sutures were placed to retract the trachea superiorly and fix it to the position. Thereafter, 4 rings (10 ± 1 mm) of the trachea were resected and the seeded scaffolds were placed in an orthotopic position. The proximal and the distal anastomosis was done using a running 7–0 polyproyplene (Prolene; Ethicon, Inc, Somerville, NJ) suture for the posterior wall and 6–0 absorbable polygalactin (Vicryl, Ethicon) interrupted sutures for the anterior trachea [9]. Then, hemostasis, tissue and skin closure were performed and animals kept on a heating pad to recover. At the study endpoint of 30 days, or whenever health impairment was observed (based on pain assessment scale and general health scale) animals were euthanized. Implanted tracheae were harvested and evaluated for DAPI/Phalloidin staining and MTT assay. Cryosections of explanted tracheae graft was evaluated by immunohistochemistry for the following: von Willebrand Factor (abcam, ab6994; UK), laminin (1:1600, ab6994, Abcam, UK) and pan-keratin (1: 400, 4545, Cell Signaling, USA). Slides were counterstained with DAPI to indicate cell nucleus.

2.13. Animal health assessment

We applied a pain assessment scale [10] which analyzed changes in the faces of the animals, including orbital tightening, nose/cheek flattening, ear changes and whisker changes, to describe potential post-operative pain. Each of the four categories was judged either as absent, moderate or obvious (scoring 0, 1 or 2 points respectively). The Karolinska Institutet health assessment checklist includes six categories; general condition, porphyrin staining, movements and posture, piloerection, respiration and skin. Each category is scored between 0 (normal condition) to 0.4 (severe condition). A total score of over 0.3 indicates the need for termination of the experiment.

2.14. Statistical analysis

Graphpad Prism 5 (Graphpad software, CA, USA) was used to do statistical analyses. Significance levels are shown as "*" for $p < 0.05$, "**" for $p < 0.01$, "***" for $p < 0.001$ and "****" for $p < 0.0001$. All data were compared using an unpaired *t*-test or two-way analysis.

3. Results

We compared biomechanical, morphological and biological properties of three types of electrospun tracheal scaffolds: PET50/PU50 which was applied as the first clinically transplanted electrospun scaffold, PET70/PU30 and PET which have been compared to select the best for next clinical transplantations. As the scaffold is produced from electrospinning, we found similar morphological structure and surface characteristics at all four different positions on each scaffold. However, these different positions (OR, BR, FE and IL) were taken into account for cell studies, since deposition of fibers with similar properties on different parts of the collector resulted in different geometrical surfaces for cell attachment.

3.1. Scaffold characterization

For each of the three types (PET50/PU50, PET70/PU30 and PET), 5 scaffolds were used for characterization (6 samples per scaffold; 3 externally and 3 internally). We observed that all scaffolds represented fibrous microstructure (The external surface of PET scaffold is shown as example in Fig. 1D, E), similar to native tracheal ECM (Fig. 1F), with random orientation. The average fiber diameters were 1.92 ± 0.78 μm (PET50/PU50), 1.78 ± 0.76 μm (PET70/PU30) and 1.88 ± 0.65 μm (PET).

Tensile mechanical properties (maximum force and elongation at break) of electrospun tracheal scaffolds are shown in Table 1. We found that PET50/PU50 demonstrated highest extensibility (138 ± 17%) and lowest tensile strength (114 ± 15 N), which could be due to the 50% weight ratio of elastomeric component (PU). However, PET showed least extensibility (45 ± 17%), but most tensile strength. As expected, PET70/PU30 stands in between PET and PET50/PU50 for both strength and strain.

Table 1
Tensile mechanical properties of electrospun tracheal scaffolds.

Scaffold type	Max force (N)	Max strain (%)	Porosity (%)	Average fiber diameter (μm)
PET50/PU50	114 ± 15	138 ± 17	93.2 ± 1.34	1.97 ± 0.78
PET70/PU30	125.5 ± 11	87 ± 24	90.6 ± 0.83	1.78 ± 0.76
PET	137 ± 8	45 ± 11	84.7 ± 1.14	1.88 ± 0.65

PET50/PU50: polyethylene terephthalate 50%/polyurethane 50%. PET70/PU30: polyethylene terephthalate 70%/polyurethane 30%. Max force (N): maximum force (Newton).

3.2. Bioreactor culture of 3-D tracheal scaffolds

3.2.1. PET50/PU50

To evaluate the biocompatibility of tracheal PET50/PU50 scaffolds, we utilized a bioreactor for dynamic culture. DAPI/Phalloidin images of cells attached to the scaffold internal and external surfaces (Fig. 1S A) showed that the cells were viable and stretched out on both surfaces. We also compared the metabolic activity of attached cells by using MTT assay. We observed (Fig. 1S B) similar absorbencies for both internal and external surfaces without any significant difference.

3.2.2. PET70/PU30 and PET

In order to evaluate the biocompatibility of tracheal PET70/PU30 and PET 3-D scaffolds, a bioreactor was used for dynamic culture. Cell attachment studies were evaluated by DAPI staining after 48 h in a bioreactor for both PET/PU and PET scaffolds at different positions (Figs. 2A and 3A). We counted the stained nuclei and found (Fig. 4A) low number of adhered cells over the rings (OR) compared to the whole scaffold ($p < 0.01$). This trend was observed in both PET/PU (Fig. 4A) and PET (Fig. 4A) scaffolds but there was a significantly higher cell numbers that attached to PET than PET/PU in all four positions ($p < 0.05$). To demonstrate if attached cells were metabolically active, we performed MTT assay and measured the absorbency for internal and external surfaces. In both PET/PU ($p < 0.05$) and PET ($p < 0.05$) scaffolds, the internal surfaces contained cells that were significantly higher in metabolic activity compared to external surfaces (Fig. 4B). We also found that there were higher readouts for PET compared to PET/PU ($p < 0.05$ externally and $p < 0.01$ internally). We further calculated the average of cell coverage on the external and internal surface of PET/PU and PET scaffolds using a mathematical model [9]. We estimated that PET/PU has average cell coverage of 48.5% (external: 39.4% and internal: 57.6%) whilst 60.1% (external: 49.4% and internal: 70.8%) of the PET scaffold surface was covered with MSCs (Fig. 4C). These results suggest that the both scaffold types were functional for cell attachment.

3.3. Static culture on 2-D sheets at different densities: PET70/PU30 and PET

Although the bioreactor seeding studies are vital for comprehensive studies on the tracheal scaffolds, we hypothesized that static seeding on 2-D sheets can provide a simplified method, as there will be a reduction in cells and material cost for the early phase of 3-D scaffold evaluations. We initially conducted static seeding either on PET/PU or PET sheets at the different cell densities by identifying cells with nuclear staining (DAPI) and measuring absorbance with an MTT assay. We noticed that both PET/PU and

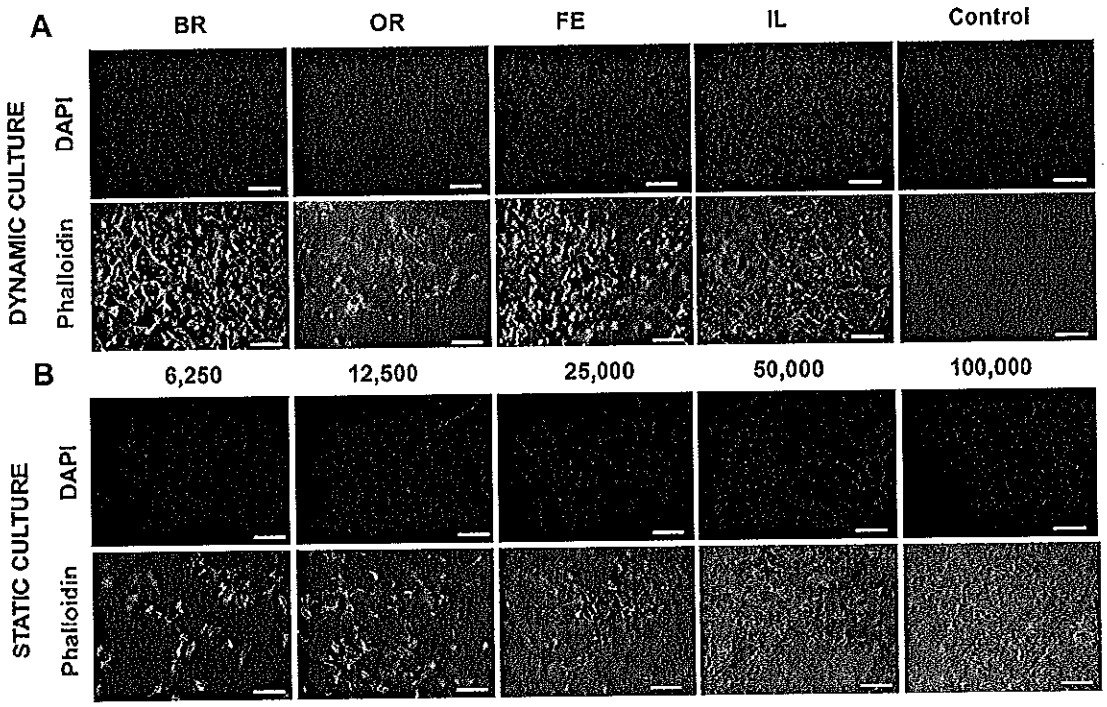

Fig. 2. Fluorescent images of seeded synthetic scaffolds made from PET70/PU30. Dynamic culture of 3-D scaffolds in bioreactor using 40M cells (A) and static culture of 2-D sheets using 6250; 12,500; 25,000; 50,000 or 100,000 cells (B). Cells are stained with Phalloidin (green) and DAPI (blue) after 48 h culture. Magnification 10×, scale bar representing 100 μm. (For interpretation of the references to colour in this figure legend, the reader is referred to the web version of this article.)

PET sheets displayed an increasing trend with higher cell densities (Fig. 4D, E), but PET contained higher cell attachment and metabolic activity in all data points ($p < 0.05$). When mathematical model was applied on the images (Fig. 2SA, B) of formazan crystals, a similar progressive trend for cell coverage on PET/PU (26.6%–82.5%) and PET (39.9%–92.5%) sheets was found (Fig. 4F). This suggests that static seeding on 2-D sheets can be used as a robust and sensitive cell density "ruler" for further quantitative evaluations.

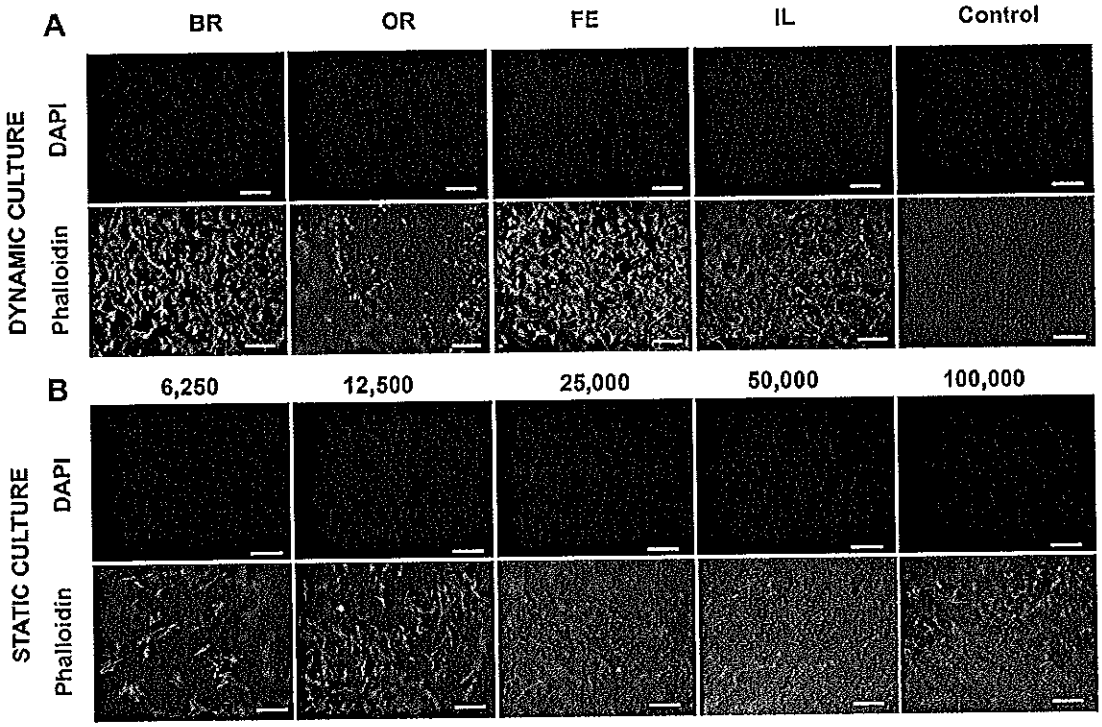

Fig. 3. Fluorescent images of seeded synthetic scaffolds made from PET. Dynamic culture of 3-D scaffolds in bioreactor using 40M cells (A) and static culture of 2-D sheets using 6250; 12,500; 25,000; 50,000 or 100,000 cells (B). Cells are stained with Phalloidin (green) and DAPI (blue) after 48 h culture. Magnification 10×, scale bar representing 100 μm. (For interpretation of the references to colour in this figure legend, the reader is referred to the web version of this article.)

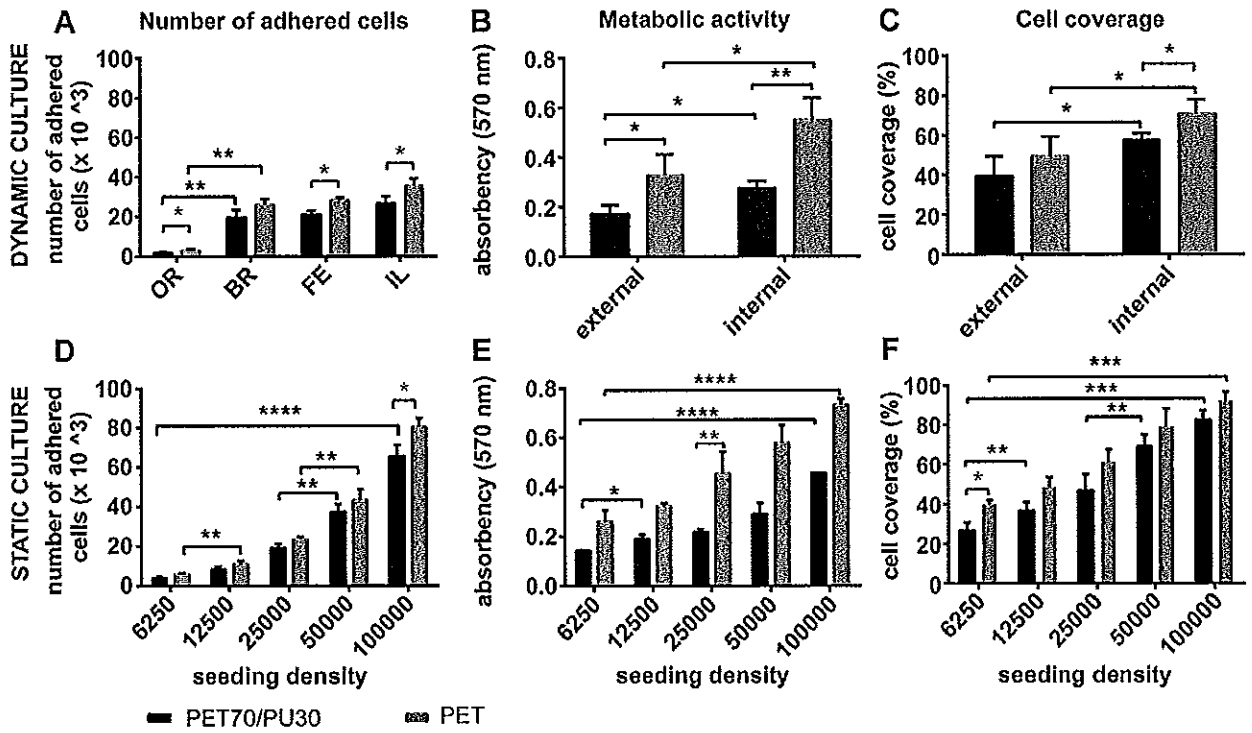

Fig. 4. Quantitative analysis of adherence, metabolic activity and coverage of rat MSCs seeded on PET70/PU30 and PET scaffolds under static and dynamic culture. The graph bars are representing the variables of "number of adhered cells"(A and D); "absorbency at 570 nm" (B and E) and "cell coverage percentage" (C and F) versus the position on the scaffold for 3-D scaffolds seeded in bioreactor under dynamic culture (A, B, C) or different progressive densities in seeding on 2-D sheets under static culture (D, E, F).

3.4. Correlating bioreactor to static culture: PET70/PU30 and PET

In order to understand if 3-D scaffolds seeded in bioreactor can correlate to 2-D sheets from static seeding, a database was created from the outcomes of static seeding. We fitted the relationships between each variable and the density used for static seeding and found; *(i)* a linear relationship was seen between the number of adhered cells and seeding densities in both types of 2-D sheets. However, for *(ii)* absorbency and *(iii)* cell coverage, a power law curve was the best fit to the data.

In order to correlate 3-D bioreactor culture to static culture, we used the average values from 3-D bioreactor evaluations i.e. DAPI, MTT and cell coverage and interpolated the equivalent seeding density in a static 2-D environment. In 3-D PET/PU, the number of adhered cells presented as $Y = 16.3$ to the line of best fit of static seeding and the corresponding seeding density was interpolated ($X_1 = 24{,}116$) from the formula ($Y = 0.6763*X$; Fig. 5A). A similar procedure was performed for the averages of absorbency ($Y = 0.23$) and cell coverage ($Y = 48.48$) for 3-D PET/PU scaffolds, using the formula for the curve of best fit for each of the variables. The results were $X_2 = 23{,}515$ (Fig. 5B) and $X_3 = 22{,}484$ (Fig. 5C) respectively. From the three interpolated outcomes i.e. X_1, X_2 and X_3, we found that the readouts from the different assays i.e. counting the number of nuclear stains (DAPI), measurement of metabolic activity of cells (absorbance) and mathematical modeling of cell coverage were not significantly different to each other. Hence, we determined that the optimal cell density 23,371 ± 825 for 2-D static culture on PET/PU sheets could correlate to the 3-D bioreactor cell culture.

Similar procedures were conducted for PET (Fig. 5D–F). For the three variables of "number of adhered cells", "absorbency" and "cell coverage", the interpolated data was seeding densities of $X_1 = 26{,}842$, (Fig. 5D); $X_2 = 25{,}493$ (Fig. 5E); $X_3 = 26{,}940$ (Fig. 5F) respectively and the average was 26,425 ± 808. This suggests that PET sheets would require 26,425 cells/0.32 cm^2 for static seeding.

3.5. Qualitative evaluations of 2-D sheets and 3-D scaffolds

We further performed qualitative analyses of PET70/PU30 (Fig. 2A, B, 6) and PET (Fig. 3A, B, 6) by DAPI/Phalloidin and SEM imaging. We confirmed that when we utilized 25,000 cells for static seeding on both PET/PU and PET sheets, they closely resembled 3-D scaffolds.

3.6. In vivo evaluation in a small animal model

To evaluate the *in vivo* properties of electrospun PET/PU and PET scaffolds, they were seeded with rat MSCs and were implanted in an orthotopic position (Fig. 7A) in a small animal model. The evaluation of the scaffolds prior and post-implantation using DAPI/Phalloidin staining and MTT assay revealed sufficient cell adhesion i.e. >60% surface coverage and metabolically active cells (*data not shown*). Throughout the entire study period of 30 days, none of the animals, that received either the MSCs seeded PET/PU or the PET scaffold, displayed any symptoms of health impairment. The harvested scaffolds were all patent at the endpoint of the study (30 days), well integrated into the adjacent tissue without any signs for increased inflammatory responses or necrosis (Fig. 7B–D) but with evidence for initial vascularization within the scaffolds wall (Fig. 7E-H) and epithelialization of the internal surface (Fig. 7I) with even iliated cells (Fig. 7J). All animals gained weight within the study period (from 249 ± 30 g to 447 ± 24 g).

4. Discussion

In the field of tissue engineering, a combination of biomaterial-based, target organ-shaped scaffolds with autologous cells is currently the best option for regeneration of many tissues/organs like bladder, trachea and blood vessels [1,4,11–13]. Among the different biopolymers, PET and PU were selected for scaffold

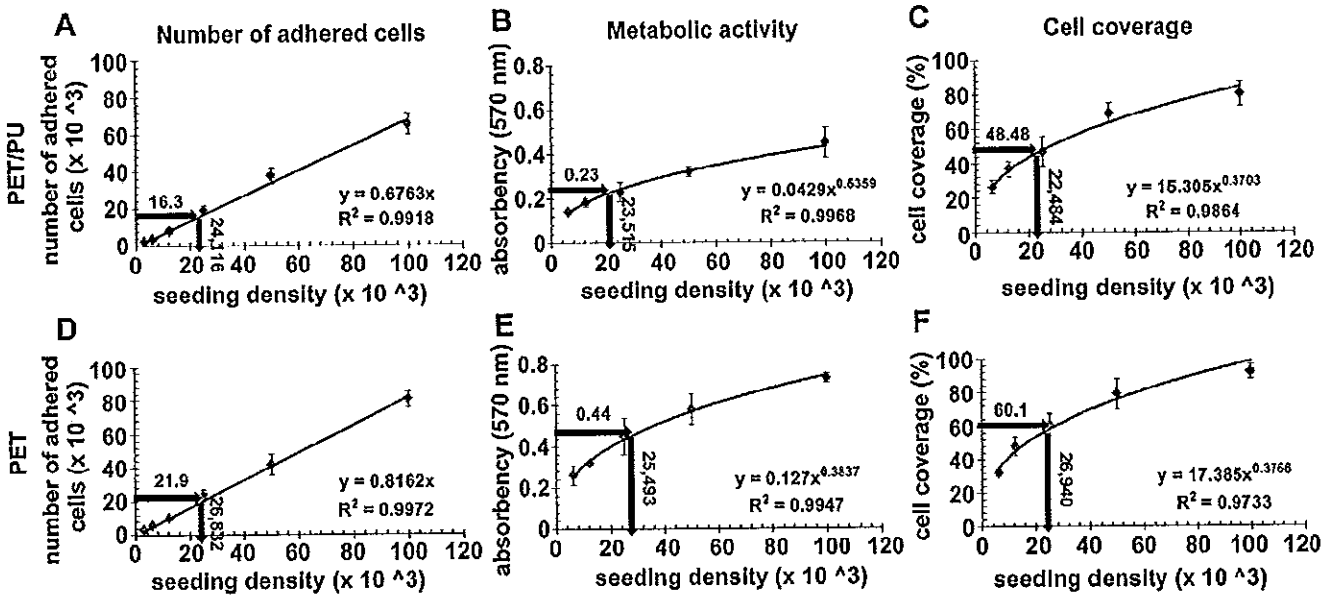

Fig. 5. Finding the correlation between static and dynamic culture. The graphs are showing the best curves fitting each of the variables of "number of adhered cells" (A and D), "absorbency at 570 nm" (B and E) and "cell coverage percentage" (C and F) as a function of "seeding density" for PET70/PU30 (A, B, C) and PET (D, E, F) sheets. For each graph, the "in" arrow enters the average of the related variable from bioreactor seeding to the formula of the curve (line) and a corresponding "seeding density" is interpolated as shown by "out" arrow.

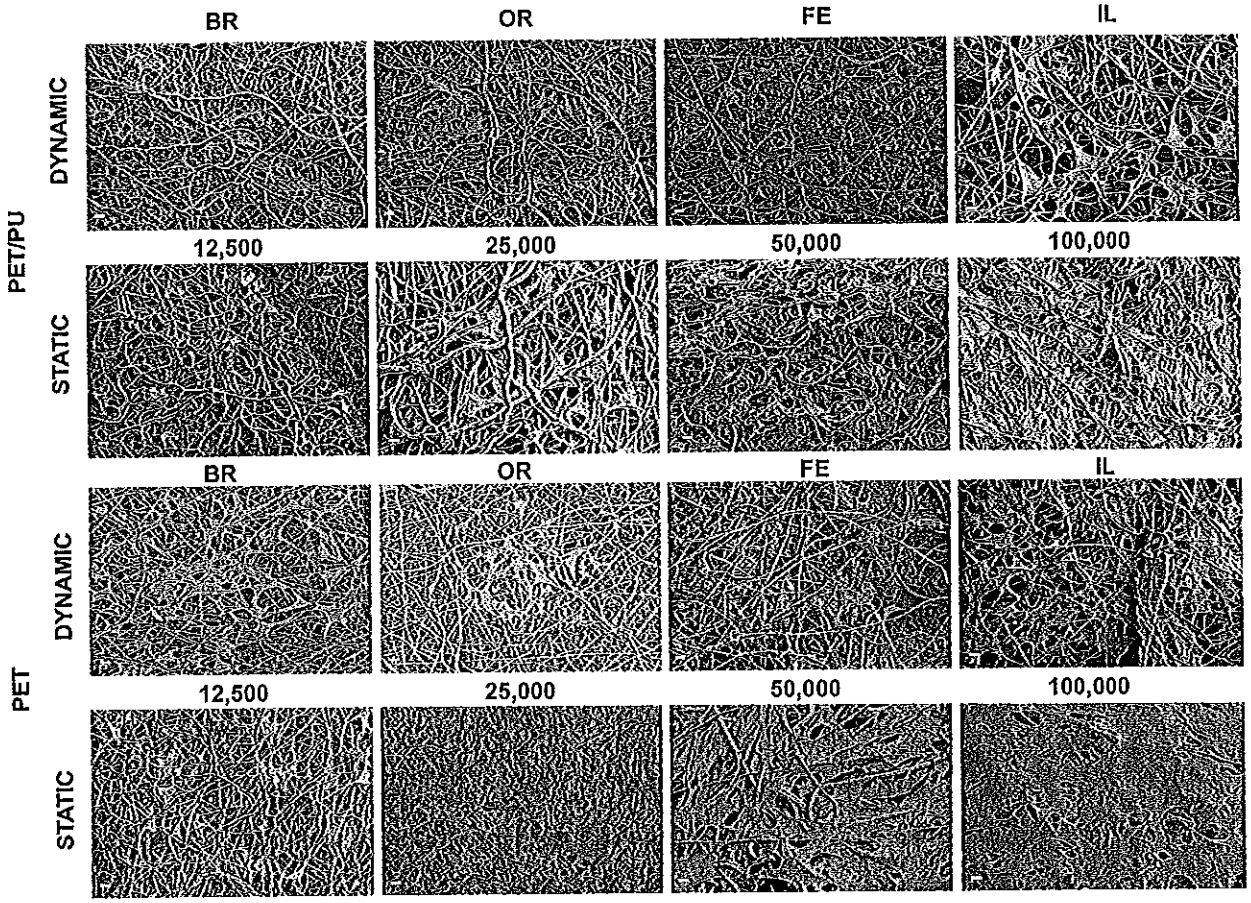

Fig. 6. SEM images of rat MSCs adhered to PET70/PU30 and PET scaffolds. Different parts of 3-D PET/PU and PET scaffolds seeded in bioreactor and 2-D sheets seeded statically under different cell densities are shown; scale bars represent 20 μm.

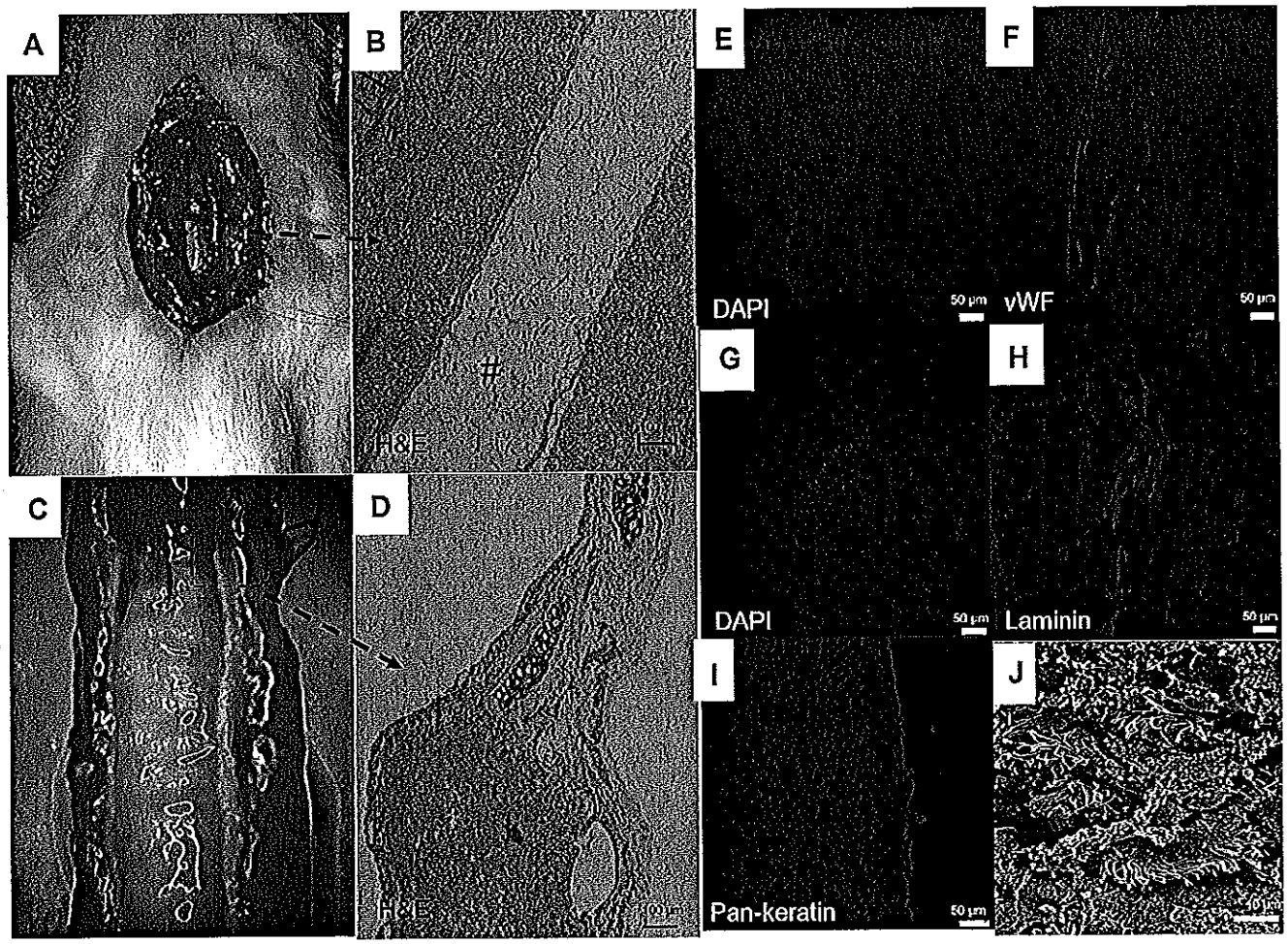

Fig. 7. In vivo evaluation of the electrospun tracheal scaffolds. Macroscopic view of an implanted PET scaffold in orthotopic position (A); Sagittal section of a harvested tracheal graft (PET) (macroscopic view: C; microscopic view: B, D, Hematoxylin & Eosin (H&E) staining, * graft's wall, # luminal side of the graft); Immunohistochemistry staining of the harvested graft: DAPI (E) von Willebrand Factor (F); DAPI (G), Laminin (H); Merge DAPI and Pan-keratin (I) scanning electron microscopic section (Magnification ×3000) of the harvested tracheal (PET) graft (J) with initial signs for ciliated cells at the luminal site of the graft 30 days after transplantation.

fabrication due to being approved by FDA, vast tissue engineering applications [12,14,15], slow rate of degradation [12,16] as well as the possibility of engineering biomechanical and structural properties to match the native tissue.

In 2011, electrospun elastomeric PET50/PU50 polyblend was the first version of synthetic electrospun scaffolds applied clinically. The PET50/PU50 scaffold was found to be ideal for replacement of native trachea because of its high porosity, appropriate strength and extensibility which could provide consistent matching with the morphological and mechanical properties of native trachea [4,17]. Not only the electrospun part was mimicking the fibrous structure of native tracheal ECM, but also the C-shaped cartilaginous rings reinforced the anterior and lateral sides of the trachea to withstand surrounding forces and maintain the airway open. The polyurethane applied for electrospinning (polycarbonate urethane, PCU, Bionate) was an improved version of the polyurethanes family which has good biomechanical stability that is suited for long-term applications [18,19]. However, we noted that this scaffold showed partial collapse one year post-transplantation which may be due to the degradation of applied PU [20]. Although biodegradability can be considered positive as it mitigates the immune reactions and encourages the native tissue to regenerate and remodel, the imbalances in the rate of scaffold degradation and new tissue production can be risky for patients. Hence, it is important to consider the regeneration capacity of tissue or organ types to maintain a substantial mechanical stability for the scaffold.

We further modified the development of tracheal scaffold by reducing the PU composition in electrospinning solution to decrease the degradation rate. Hence, two types of tracheal scaffolds (PET70/PU30 and PET) were further characterized in this study and we found that both the scaffold types contained morphological and biomechanical requirements which were comparable to native trachea [4,17]. It is worth considering that the synthetic scaffolds had similar internal dimensions (transversal and sagittal diameter) compared to native tracheae applied in our previous studies [4,17]. However, the wall thickness of synthetic scaffolds was 50% thinner to the native, which should be taken into account for the comparison of mechanical properties.

To perform the next verification procedure, i.e. biological evaluations, the biomechanically validated 3-D constructs were seeded inside specially designed bioreactors [21]. However, each bioreactor run is costly in terms of time and resources due to the extensive setup, pre-wash (PBS washing) and pre-coating (media wash) steps. Moreover, large number of cells (between 40 and 60 million, depending on whether a pediatric or adult case) are

required for each scaffold. Hence, consuming hundreds of millions of stem cells to perform a biocompatibility validation is inevitable. In this regard, it was desirous to avoid the need to run bioreactors for scaffold validation during the early phase of verifications. Herein, we present the possibility of performing static seeding of cells on 2-D sheets (cut out of 3-D scaffolds) and consider it to be representative for dynamic culture of 3-D scaffolds in bioreactor. Upon approving the biocompatibility of the tracheal scaffolds, based on the low cost, simple and fast 2-D static cell seeding, bioreactor seeding can finally be applied in the clinical verification of the scaffold. Outcomes from cell studies on PET70/PU30 and PET scaffolds have demonstrated that static cell seeding with density of around 25,000 per well (75,000 cells/cm^2) is most representative for the optimum bioreactor seeding (cell density of 610,000 cells/cm^2). Therefore, it can be concluded that in order to have similar cell coverage on a 3-D tracheal scaffold compared to a 2-D sheet, an 8-fold reduction in seeding density can reliably be used to predict biocompatibility of the scaffolds. The correlation technique introduced here may also be applicable for other tubular scaffolds such as vascular grafts and esophagus.

From our extensive validation of the scaffolds, we found that PET is biologically superior to the polyblend construct, due to higher number of viable cells and more cell coverage. Likewise, our *in vivo* animal model approved the materials' biocompatibility and the orthotopic functional properties of both the PET/PU and PET-based tracheal scaffolds. We believe the rat model is more appropriate as the mobility closely resembles humans. The findings from our 30 day study period in a rat model is also equivalent to approximately 900 days of human life which can therefore provide clinically relevant intermediate and long-term information [22].

5. Conclusion

We present here the biochemical and biocompatibility characteristics of different compositions of electrospun tracheal scaffold i.e. PET70/PU30 and PET (100%). We found that both these scaffolds were mechanically strong, had uniform fibrous structure and supported cell viability and attachment. *In vitro* experiments, represented superior properties of PET compared to the PET/PU polyblend, whilst there was no significant difference between their *in vivo* implantation outcomes. We further demonstrated the correlation of the static to dynamic cell culture with the approximate equivalent ratio of 1/8 in term of seeding density. In this way, we can perform static seeding on 2-D sheets as a means to investigate the cyto-compatibility of the whole 3-D scaffold. This can aid to further optimize tracheal and similar tubular scaffolds for clinical applications in an economical, reproducible and simple validation method.

Acknowledgments

This work was supported by European Project FP7-NMP- 2011-SMALL-5: BIOtrachea, Biomaterials for Tracheal Replacement in Age-related Cancer via a Humanly Engineered Airway (No.280584 – 2), ALF medicine (Stockholm County Council): Transplantation of bio-engineered trachea in humans (No. LS1101–0042.), Dr Dorka-Stiftung (Hannover, Germany): bioengineering of tracheal tissue and Mega grant of the Russian Ministry of Education and Science (agreement No. 11.G34.31.0065).

Appendix A. Supplementary data

Supplementary data related to this article can be found at http://dx.doi.org/10.1016/j.biomaterials.2014.03.015

References

[1] Macchiarini P, Jungebluth P, Go T, Asnaghi MA, Rees LE, Cogan TA, et al. Clinical transplantation of a tissue-engineered airway. Lancet 2008;372:2023–30.
[2] Gonfiotti A, Jaus MO, Barale D, Baiguera S, Comin C, Lavorini F, et al. The first tissue-engineered airway transplantation: 5-year follow-up results. Lancet 2013;6736:1–7.
[3] Berg M, Ejnell H, Kovacs A, Nayakawde N, Patil P, Joshi M, et al. Replacement of a tracheal stenosis with a tissue-engineered human trachea using autologous stem cells. Tissue Eng Part A 2014;20:389–97.
[4] Jungebluth P, Alici E, Baiguera S, Blanc K, Blomberg P, Bozóky B, et al. Tracheobronchial transplantation with a stem-cell-seeded bioartificial nanocomposite: a proof-of-concept study. Lancet 2011;378:1997–2004.
[5] Ahmed M, Ghanbari H, Cousins BG, Hamilton G, Seifalian AM. Small calibre polyhedral oligomeric silsesquioxane nanocomposite cardiovascular grafts: influence of porosity on the structure, haemocompatibility and mechanical properties. Acta Biomater 2011;7:3857–67.
[6] Li M, Mondrinos MJ, Chen X, Gandhi MR, Ko FK, Lelkes PI. Co-electrospun poly(lactide-co-glycolide), gelatin, and elastin blends for tissue engineering scaffolds. J Biomed Mater Res A 2006;79:963–73.
[7] Barnes CP, Sell S a, Boland ED, Simpson DG, Bowlin GL. Nanofiber technology: designing the next generation of tissue engineering scaffolds. Adv Drug Deliv Rev 2007;59:1413–33.
[8] Gustafsson Y, Haag J, Jungebluth P, Lundin V, Lim ML, Baiguera S, et al. Viability and proliferation of rat MSCs on adhesion protein-modified PET and PU scaffolds. Biomaterials 2012;33:8094–103.
[9] Jungebluth P, Haag JC, Lim ML, Lemon G, Sjöqvist S, Gustafsson Y, et al. Verification of cell viability in bioengineered tissues and organs before clinical transplantation. Biomaterials 2013;34:4057–67.
[10] Sotocinal SG, Sorge RE, Zaloum A, Tuttle AH, Martin LJ, Wieskopf JS, et al. The rat grimace scale: a partially automated method for quantifying pain in the laboratory rat via facial expressions. Mol Pain 2011;7:55.
[11] Atala A. Tissue engineering of human bladder. Br Med Bull 2011;97:81–104.
[12] Detta N, Errico C, Dinucci D, Puppi D, Clarke DA, Reilly GC, et al. Novel electrospun polyurethane/gelatin composite meshes for vascular grafts. J Mater Sci Mater Med 2010;21:1761–9.
[13] Baudis S, Ligon SC, Seidler K, Weigel G, Grasl C, Bergmeister H, et al. Hard-block degradable thermoplastic urethane-elastomers for electrospun vascular prostheses. J Polym Sci A Polym Chem 2012;50:1272–80.
[14] Nieponice A, Soletti L, Guan J, Hong Y, Gharaibeh B, Maul TM, et al. In vivo assessment of a tissue-engineered vascular graft combining a biodegradable elastomeric scaffold and muscle-derived stem cells in a rat model. Tissue Eng Part A 2010;16:1215–23.
[15] Moreno MJ, Ajji A, Mohebbi-Kalhori D, Rukhlova M, Hadjizadeh A, Bureau MN. Development of a compliant and cytocompatible micro-fibrous polyethylene terephthalate vascular scaffold. J Biomed Mater Res B Appl Biomater 2011;97:201–14.
[16] Chaouch W, Dieval F, Chakfe N, Durand B. Properties modification of PET vascular prostheses. J Phys Org Chem 2009;22:550–8.
[17] Baiguera S, Jungebluth P, Burns A, Mavilia C, Haag J, De Coppi P, et al. Tissue engineered human tracheas for in vivo implantation. Biomaterials 2010;31:8931–8.
[18] Chandy T, Van Hee J, Nettekoven W, Johnson J. Long-term in vitro stability assessment of polycarbonate urethane micro catheters: resistance to oxidation and stress cracking. J Biomed Mater Res B Appl Biomater 2009;89:314–24.
[19] Szelest-Lewandowska A, Masiulanis B, Szymonowicz M, Pielka S, Paluch D. Modified polycarbonate urethane: synthesis, properties and biological investigation in vitro. J Biomed Mater Res A 2007;82:509–20.
[20] Cipriani E, Bracco P, Kurtz SM, Costa L, Zanetti M. In vivo degradation of poly(carbonate-urethane) based spine implants. Polym Degrad Stab 2013;98:1225–35.
[21] Asnaghi MA, Jungebluth P, Raimondi MT, Dickinson SC, Rees LEN, Go T, et al. A double-chamber rotating bioreactor for the development of tissue-engineered hollow organs: from concept to clinical trial. Biomaterials 2009;30:5260–9.
[22] Andreollo NA, Santos EF, Araújo MR, Lopes LR. Rat's age versus human's age: what is the relationship? Arq Bras Cir Dig 2012;25:49–51.

Biomaterials 35 (2014) 5307–5315

Contents lists available at ScienceDirect

Biomaterials

journal homepage: www.elsevier.com/locate/biomaterials

Biomechanical and biocompatibility characteristics of electrospun polymeric tracheal scaffolds

Fatemeh Ajalloueian [a,1], Mei Ling Lim [a,1], Greg Lemon [a], Johannes C. Haag [a], Ylva Gustafsson [a], Sebastian Sjöqvist [a], Antonio Beltrán-Rodríguez [a], Costantino Del Gaudio [b], Silvia Baiguera [a], Alessandra Bianco [b], Philipp Jungebluth [a], Paolo Macchiarini [a,*]

[a] Advanced Center for Translational Regenerative Medicine (ACTREM), Department of Clinical Science, Intervention and Technology (CLINTEC), Karolinska Institutet, Stockholm, Sweden
[b] University of Rome "Tor Vergata", Department of Industrial Engineering, Intrauniversitary Consortium for Material Science and Technology (INSTM), Research Unit Tor Vergata, Rome, Italy

ARTICLE INFO

Article history:
Received 13 January 2014
Accepted 7 March 2014
Available online 3 April 2014

Keywords:
Electrospinning
Tracheal scaffold
Biocompatibility
Cell seeding
Static and dynamic cultures
Correlation

ABSTRACT

The development of tracheal scaffolds fabricated based on electrospinning technique by applying different ratios of polyethylene terephthalate (PET) and polyurethane (PU) is introduced here. Prior to clinical implantation, evaluations of biomechanical and morphological properties, as well as biocompatibility and cell adhesion verifications are required and extensively performed on each scaffold type. However, the need for bioreactors and large cell numbers may delay the verification process during the early assessment phase. Hence, we investigated the feasibility of performing biocompatibility verification using static instead of dynamic culture. We performed bioreactor seeding on 3-dimensional (3-D) tracheal scaffolds (PET/PU and PET) and correlated the quantitative and qualitative results with 2-dimensional (2-D) sheets seeded under static conditions. We found that an 8-fold reduction for 2-D static seeding density can essentially provide validation on the qualitative and quantitative evaluations for 3-D scaffolds. *In vitro* studies revealed that there was notably better cell attachment on PET sheets/scaffolds than with the polyblend. However, the *in vivo* outcomes of cell seeded PET/PU and PET scaffolds in an orthotopic transplantation model in rodents were similar. They showed that both the scaffold types satisfied biocompatibility requirements and integrated well with the adjacent tissue without any observation of necrosis within 30 days of implantation.

1. Introduction

Bioengineered tracheae, using decellularized tissue, have recently been successfully transplanted into patients [1–3]. However, biological scaffolds are donor dependent and require long processing time and cost. Besides, the tracheal dimensions would require donor-recipient matching. In order to overcome these drawbacks, customized synthetic scaffolds might be the next potential solution.

In 2011, the first synthetic-based tracheal scaffold, seeded with patient's autologous stem cells was transplanted in a clinical setting [4]. This Y-shaped scaffold was manufactured from the preoperative chest CT and three-dimensional images of the patient trachea using a nanocomposite polymer (POSS-PCU; polyhedral oligomeric silsesquioxane [POSS] covalently bonded to poly-[carbonate-urea] urethane [PCU]) [5]. U shaped rings of POSS-PCU were prepared through casting methodologies and were placed around a Y-shaped glass mandrel. Then, the whole construct was placed in a POSS-PCU solution, followed by a coagulation procedure which resulted in a porous scaffold [4]. However, due to the stiffness of the scaffold, an abnormal granulation tissue formation developed within the post-operative course. Moreover, it led to chronic fistula at the distal anastomotic sites of the left main bronchus, which required endoscopic interventions.

The need to improve the biomechanical properties of the scaffold and our willing to mimic the native tracheal extracellular

* Corresponding author. Advanced Center for Translational Regenerative Medicine, (ACTREM), Division of Ear, Nose, and Throat (CLINTEC), Karolinska Institutet, Alfred Nobels Allé 8, Huddinge, SE-141 86 Stockholm, Sweden. Tel.: +46 760 503 213 (mobile); fax: +46 8 774 7907.
E-mail address: paolo.macchiarini@ki.se (P. Macchiarini).
[1] Contributed equally to this work.

http://dx.doi.org/10.1016/j.biomaterials.2014.03.015
0142-9612/

matrix (ECM), led to fabrication of the next generation of scaffolds to include FDA approved polymers like polyethylene terephthalate (PET) and polyurethane (PU). Electrospinning was applied as the main fabrication technique. This technology is simple, fast and can provide fibrous networks similar to biomimetic characteristics of the native ECM [6,7]. A polyblend of PET/PU (50% weight ratio for each) was the first electrospun tracheal scaffold clinically applied. Although this construct contained all criteria for an optimal scaffold, we noticed local collapse with the scaffold one year post-transplantation. The slump of biomechanical properties seemed to originate from non-optimal balance in the degradation rate of applied PU and the production of new extracellular matrix. So, we proceeded to further develop the electrospun scaffolds by reducing the amount of PU or completely eliminating it from the scaffold structure composition.

Here, we present the evaluations performed on electrospun scaffolds. It includes biomechanical characterization, structural analyses and biological verifications. The latter demanded significant resources due to various cell-seeding studies using bioreactors. Hence, we investigated if a 2-D static cell seeding model could correlate well to 3-D scaffold seeding *via* a bioreactor. This may help to replace the 3-D seeding during a preclinical testing phase whilst providing the relevant information required for a clinical translation.

2. Materials and methods

2.1. Fabrication of electrospun scaffolds

The first clinically applied electrospun tracheal scaffold was produced as a polyblend of polyethylene terephthalate (PET) and polyurethane (PU) with 50% weight ratio of each (Nanofiber Solutions, Ohio, USA) based on the CT images of the patient's trachea. The electrospun body was reinforced with C-shaped rings to withstand the pulling and compressive forces from surrounding tissues.

Tracheal scaffolds of (i) PET/PU (weight composition of 70/30 respectively) and (ii) pure PET were two candidates for next clinical application (Harvard Apparatus Regenerative Technology®, HART, Holliston, MA, USA). The scaffolds were processed according to the manufacturer's procedure: (i) The PET solution was prepared by dissolving 14wt% polyethylene terephthalate (PET) (Indorama Ventures, IL, USA) in 1,1,1,3,3,3-hexafluoroisopropanol (HFIP) (Sigma–Aldrich, MA, USA) at 50 °C using magnetic stirring carried out for 3 h. The polyurethane (PU) pellets (Bionate, DSM Biomedical, Netherlands) were added to the already prepared solution to make a 6wt% PU solution using the same dissolving procedure (50 °C using magnetic stirring carried out for 3 h). Similar dissolution procedure was applied for preparation of the PET solution (20wt%). Electrospinning of both solutions was carried out, with a voltage of 14–16 kV applied to the blunt needle (21 G) tip of the syringe (filled with the solution). The feed rate was 10 mL/h and the needle tip to collector distance was 15 cm. The collector was a mandrel with D shaped cross section, designed based on the CT images of patient's trachea and rotated at a speed of 200 revolutions per minute (rpm). The air relative humidity and temperature were 40% and 23 °C respectively. The electrospinning was continued until the desired thickness (1/2 of total thickness) was reached. Cartilage rings produced out of PET using injection-molding technique were placed (based on a predefined intervals) and fixed over the electrospun layer. Electrospinning was continued to reach the final thickness. The fabricated scaffold was kept in a vacuum oven for 12 h at 60 °C to ensure no residual solvent remains. The scaffolds were then treated using radio frequency oxygen gas plasma for 1 min. For sterilization, they were exposed to 25 kGy (330,000 mJ/cm^2) of gamma irradiation.

2.2. Scaffold characterization

The morphology of electrospun nanofibers was studied with the help of scanning electron microscopy (SEM). The average fiber diameter of the electrospun scaffolds was measured by applying ImageJ 1.46R (NH, Maryland, USA) to the SEM micrographs.

Tensile properties of the synthetic scaffolds of PET50/PU50, PET70/PU30 and PET were determined using a universal testing machine (UTM; Lloyds LRX, USA) fitted with a calibrated load cell of 1 kN. Test specimens (full 3-D scaffolds) were tested at a crosshead speed of 1 mm/s at ambient conditions. Scaffolds were glued (from flat part at the back) to clamps fixed at the UTM grips. Dimensions were measured using calibrated Mitutoyo CS callipers and were entered to the instrument software. Force and displacement were recorded during testing. Strain was calculated as displacement divided by the original gauge length. Maximum force and corresponding strain are reported. 5 scaffolds were used for each of the three scaffold types.

The porosity was calculated using the formula of

$$\text{Porosity}(\%) = \left(1 - \frac{\rho}{\rho^0}\right)*100$$

where ρ is the bulk density and ρ^0 is the apparent density, which is 1.41 g/cm^3 and 1.19 g/cm^3 for the applied PET and PU respectively. The bulk density was calculated using a piece of electrospun mat with known mass and dimension by using this formula:

$$\rho\left(\frac{g}{cm^3}\right) = \frac{\text{Mass(g)}}{\text{Thickness(cm)} \times \text{area(cm}^2\text{)}}$$

2.3. In vitro and in vivo experimental studies

Male Sprague Dawley rats ($n = 13$) were used for both the *in vitro* and the *in vivo* orthotopic transplantation studies. The "Principles of laboratory animal care" formulated by the National Society for Medical Research and the "Guide for the care and use of laboratory animals" prepared by the Institute of Laboratory Animal Resources, National Research Council, and published by the National Academy Press, revised 1996, have been applied to all the animals. Ethical permissions were provided by the local authorities (the Stockholm South Ethical Committee; Sweden; registration number S74-12).

2.4. Mesenchymal stromal cell isolation

Cells were isolated from male Sprague Dawley rats ($n = 5$). Mesenchymal stromal cells (MSCs) were isolated and processed as previously described [8]. Briefly, femur and tibia were cleared from surrounding tissue and phosphate buffered saline (PBS, Invitrogen, Sweden) was flushed out the bone marrow. The obtained cells were centrifuged and the pellet was resuspended in DMEM supplemented whit 10% Fetal Bovine Serum (FBS, Invitrogen, Sweden) and 1% antibiotic-antimycotic (Invitrogen, Sweden). Cells were seeded in a culture flask (BD, CA, USA) and were incubated at 37 °C in 5% CO_2. After 24 h of incubation, the medium was discarded to remove all non-adherent cells. Cells from passages 3 to 7 were used in this study.

2.5. Dynamic cultures

The number of rat MSCs required for seeding the tracheal scaffolds was calculated using a mathematical model that predicts, for a given number of cells seeded initially, the final percentage area of the interior and exterior surfaces that are covered by cells at the end of the incubation. The model was developed by considering the dynamic processes of cell attachment and detachment occurring at the surface of an artificial scaffold or decellularized organ incubated within the *in-breath*™ bioreactor (Harvard Bioscience Inc., Holliston, MA, USA). Cell proliferation on the scaffold, and cell reattachment from the bioreactor bath onto the scaffold, are assumed to be negligible.

The model predicts that the number of cells, N_s, required for seeding either the interior or exterior surface to achieve a cell coverage, C (%), is given by

$$N_s = \frac{0.01C\pi D_s L}{\beta A_a}$$

Where β is a parameter expressing the ratio of the rate of cell attachment to the rate of cell detachment from cells seeded onto the scaffold surface, and A_a is the average surface area of an attached cell. The scaffold is assumed to be an annular cylinder with diameter (interior or exterior) D_s and length L.

The parameter value $\beta = 0.41$ was obtained by fitting the equation to experimental data of the cell coverage achieved using bioreactor seeding of electrospun adult tracheal scaffolds, made from PET/PU(50/50 percentage composition by weight), with rat MSCs. The parameter value $A_a = 281\ \mu m^2$ was determined by image analysis of rat MSCs attached to thin layers of electrospun PET/PU fibers [8]. The tracheal scaffolds used in the experiments had interior diameter $D_i = 10$ mm, exterior diameter $D_o = 12$ mm, and length $L = 94$ mm.

Substituting the given parameter values into the equation gives the number of cells required to seed the interior and exterior surfaces of the tracheal scaffold to a confluence of 70% as $N_i = 18 \times 10^6$ and $N_o = 22 \times 10^6$ respectively i.e. equivalent to seeding density of approximately $B_d = 6.1 \times 10^5$ cells per square centimeter.

The scaffold was fixed on organ holder (Fig. 1A) and placed inside the specific bioreactor designed for seeding. It was washed two times with phosphate buffered saline (PBS, Invitrogen, Sweden) and two times (each time for 30 min) with stem cell media containing Dulbecco's Modified Eagle Medium (DMEM, Invitrogen, Sweden) supplemented with 10% Fetal Bovine Serum (FBS, Invitrogen, Sweden) and 1% antibiotic-antimycotic (Invitrogen, Sweden). The scaffolds were then seeded with rat MSCs and incubated for 48 h.

2.6. Static cultures

Sheets were cut from 3-D scaffolds (flat external part) using 6 mm biopsy punches, placed in 96 well plates and seeded with different cell densities in the

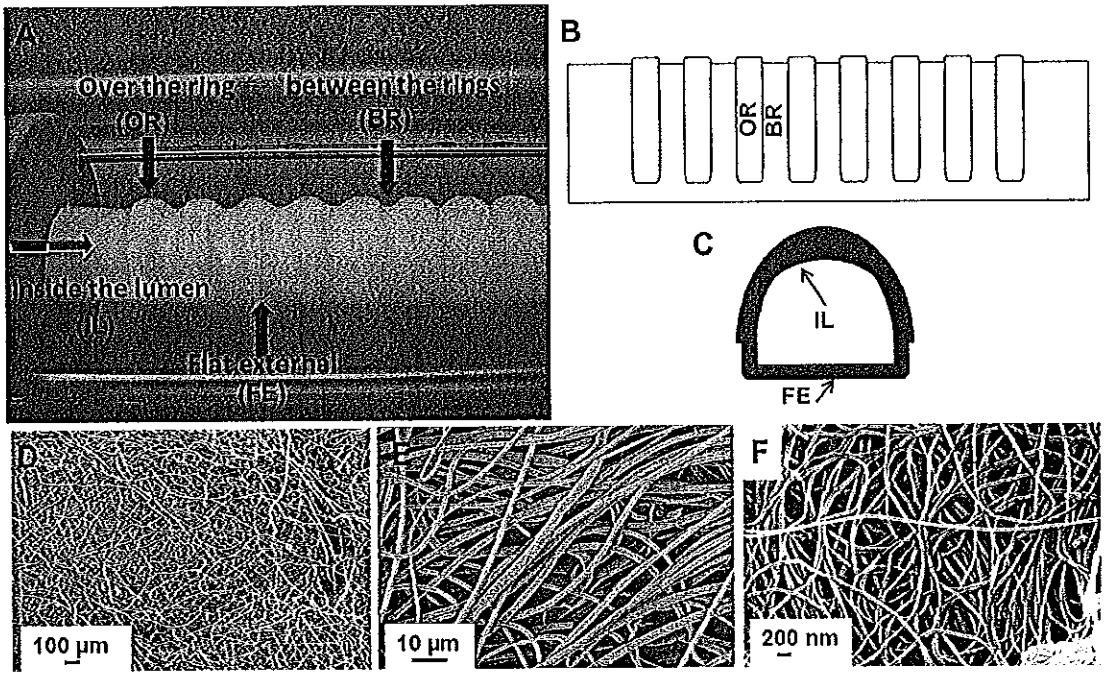

Fig. 1. Macroscopic and microscopic appearance of an electrospun tracheal scaffold. The scaffold is fixed on organ holder and different parts are shown on the image (A); schematic depiction of scaffold from front (B) and side (C) view; SEM images of a tracheal scaffold made from PET under two different magnifications of 100× (D) and 3000× (E) respectively; and SEM image of a rat native trachea (F).

range of 6250 to 100,000 (6250; 12,500; 25,000; 50,000 and 100,000) per well (96 well plates with surface area of 0.32 cm^2).

2.7. Phalloidin and DAPI staining on seeded synthetic scaffolds

Samples from the static and bioreactor cell seeding were fixed in 4% formaldehyde (Histolab, Sweden) for 10 min. They were washed and stained for 30 min with Phalloidin (Molecular Probes, Sweden) diluted in PBS/0.1% Triton X-100 (2 U/ml) (Sigma–Aldrich, Sweden), followed by counterstaining with 4′,6′-diamidino-2-phenylindole (DAPI, Sigma–Aldrich, Sweden). Stained cells were visualized with a fluorescent microscope (Olympus BX-60, Japan). Cell adhesion was quantified by manual counting of nuclear stained cells with ImageJ 1.46R (NH, Maryland, USA) (5 samples; 3 areas on each) and the average was reported.

2.8. Colorimetric cell activity assay

A 3-(4,5-dimethylthiazol-2-yl)-2,5-diphenyl-tetrazolium-bromid (MTT)-assay (Roche, Sweden) was used to evaluate the cell metabolic activity. All samples were analyzed in triplicates. After 48 h of cell seeding, culture medium was removed and 100 μl of fresh medium and 10 μl MTT solutions were added to each well in a 96 well plate. Cells were incubated in the dark at 37 °C (5% CO_2) for 4 h. Next, 10% sodium dodecyl sulfate (SDS) in 0.01 M HCl (100 μl) was added to each well and the plates were further incubated overnight at 37 °C (5% CO_2). The solution was then transferred to another 96-well plate and the optical density of the formazan solution was measured for absorbency at 570 nm with a spectrophotometer (SpectraMax 250, Molecular Devices, CA, USA). Non-seeded scaffold was used as negative control.

2.9. Quantification of cell coverage

A colorimetric approach [9] was used to quantify the percentage cell coverage of the seeded samples. Briefly, a single color digital image, showing a uniformly illuminated top view of all the samples including the unseeded controls, was obtained and imported into MATLAB®. The regions of the image corresponding to each of the samples were extracted using mouse and cursor input. For the samples in each group the color change was calculated using the equation

$$\Delta C = \frac{Y_c - Y_s}{Y_c - Y_m} \times 100\%$$

where Y_s is the average of the grayscale values of the pixels in the sample, Y_c is the average of the grayscale values of the pixels in the control sample, and Y_m is the average of the grayscale values of pixels from regions where there was maximum purple staining.

The cell coverage was then calculated using the formula

$$\theta = \exp\left(\alpha\left(\left(\frac{\Delta C}{100\%}\right)^{\beta} - 1\right)\right) \times 100\%$$

Where $\alpha = 4.25$ and $\beta = 0.58$.

2.10. Quantitative analysis

2.10.1. Dynamic culture of 3-D scaffolds

After 48 h of cell seeding on 3-D scaffolds (PET/PU and PET), we aimed to evaluate DAPI/Phalloidin staining, MTT absorbency, cell coverage based on formazan crystals and SEM imaging. However, for the 3-D scaffolds (bioreactor seeding), we observed that the quantitative data for either of the variables ("number of adhered cells", "absorbency" or "cell coverage") depends on the position under study. For this reason, we performed counting in four different positions for DAPI stained nuclei; which is representative for "number of adhered cells". Three positions are located on the outer surface (Fig. 1A–C) and are referred as: the part over the rings (OR), the part between the rings (BR) and the flat external part at the back of the trachea (FE). The forth position is inside the lumen (IL). For the two other variables i.e. MTT absorbency and cell coverage, we quantify the variables based on being from external parts (OR, BR and FE) or internal part.

For quantification of each of the variables, nine samples were taken from inside the lumen and nine samples from external parts (three from each of the BR, OR and FE), so that the weighted average with weights 3:1:1:1 respectively was reported.

2.10.2. Correlating static and dynamic culture

In order to evaluate the correlation between static and dynamic cultures, a graph was plotted for each variable (i.e. number of adhered cells, absorbency and cell coverage) versus the different cell densities in static seeding on PET70/PU30 and PET sheets. We further compared the quantitative outcomes of bioreactor seeding on 3-D scaffolds with the data from static seeding on 2-D sheets. The weighted average for each variable was used as "Y" input to the formula of the curve (line) of best fit to corresponding data of static cell seeding and the equivalent "X" was interpolated. The average of the three interpolated data was the optimum cell density for performing static cell seeding.

2.11. Scanning electron microscopy

To evaluate cell adhesion on 2-D sheets and 3-D scaffolds, small pieces from 2-D seeded sheets and different positions on the 3-D seeded scaffolds were fixed with 2.5% glutaraldehyde (Merck, Germany) in 0.1 M cacodylate buffer (Prolabo, France) for 2 h at room temperature, rinsed in cacodylate buffer, and dehydrated through

ethanol gradient. Samples were dried overnight, gold sputtered and used for analysis by SEM (JSM6490, JEOL, Japan).

2.12. In vivo evaluation of a seeded-tracheal scaffold in a rat model

To evaluate the electrospun tracheal scaffolds in a rat model, PET70/PU30 ($n = 4$) and PET ($n = 4$) scaffolds, with dimensions of 4 mm (external diameter) and 2.2 mm (internal diameter) were seeded with rat MSCs for 48 h prior to implantations.

Eight Sprague Dawley rats (200–300 g) were anesthetized intramuscularly with 100 mg/kg ketamine (Intervet, Boxmeer, Netherlands) and 10 mg/kg xylazine (Intervet) *via* bolus injection and placed into supine position. The entire procedure was performed under spontaneous breathing. The trachea was exposed *via* an anterior cervical midline incision and the division of the sternohyoid muscles. Traction sutures were placed to retract the trachea superiorly and fix it to the position. Thereafter, 4 rings (10 ± 1 mm) of the trachea were resected and the seeded scaffolds were placed in an orthotopic position. The proximal and the distal anastomosis was done using a running 7–0 polyproyplene (Prolene; Ethicon, Inc, Somerville, NJ) suture for the posterior wall and 6–0 absorbable polygalactin (Vicryl, Ethicon) interrupted sutures for the anterior trachea [9]. Then, hemostasis, tissue and skin closure were performed and animals kept on a heating pad to recover. At the study endpoint of 30 days, or whenever health impairment was observed (based on pain assessment scale and general health scale) animals were euthanized. Implanted tracheae were harvested and evaluated for DAPI/Phalloidin staining and MTT assay. Cryosections of explanted tracheae graft was evaluated by immunohistochemistry for the following: von Willebrand Factor (abcam, ab6994; UK), laminin (1:1600, ab6994, Abcam, UK) and pan-keratin (1: 400, 4545, Cell Signaling, USA). Slides were counterstained with DAPI to indicate cell nucleus.

2.13. Animal health assessment

We applied a pain assessment scale [10] which analyzed changes in the faces of the animals, including orbital tightening, nose/cheek flattening, ear changes and whisker changes, to describe potential post-operative pain. Each of the four categories was judged either as absent, moderate or obvious (scoring 0, 1 or 2 points respectively). The Karolinska Institutet health assessment checklist includes six categories; general condition, porphyrin staining, movements and posture, piloerection, respiration and skin. Each category is scored between 0 (normal condition) to 0.4 (severe condition). A total score of over 0.3 indicates the need for termination of the experiment.

2.14. Statistical analysis

Graphpad Prism 5 (Graphpad software, CA, USA) was used to do statistical analyses. Significance levels are shown as "*" for $p < 0.05$, "**" for $p < 0.01$, "***" for $p < 0.001$ and "****" for $p < 0.0001$. All data were compared using an unpaired *t*-test or two-way analysis.

3. Results

We compared biomechanical, morphological and biological properties of three types of electrospun tracheal scaffolds: PET50/PU50 which was applied as the first clinically transplanted electrospun scaffold, PET70/PU30 and PET which have been compared to select the best for next clinical transplantations. As the scaffold is produced from electrospinning, we found similar morphological structure and surface characteristics at all four different positions on each scaffold. However, these different positions (OR, BR, FE and IL) were taken into account for cell studies, since deposition of fibers with similar properties on different parts of the collector resulted in different geometrical surfaces for cell attachment.

3.1. Scaffold characterization

For each of the three types (PET50/PU50, PET70/PU30 and PET), 5 scaffolds were used for characterization (6 samples per scaffold; 3 externally and 3 internally). We observed that all scaffolds represented fibrous microstructure (The external surface of PET scaffold is shown as example in Fig. 1D, E), similar to native tracheal ECM (Fig. 1F), with random orientation. The average fiber diameters were 1.92 ± 0.78 μm (PET50/PU50), 1.78 ± 0.76 μm (PET70/PU30) and 1.88 ± 0.65 μm (PET).

Tensile mechanical properties (maximum force and elongation at break) of electrospun tracheal scaffolds are shown in Table 1. We found that PET50/PU50 demonstrated highest extensibility (138 ± 17%) and lowest tensile strength (114 ± 15 N), which could be due to the 50% weight ratio of elastomeric component (PU). However, PET showed least extensibility (45 ± 17%), but most tensile strength. As expected, PET70/PU30 stands in between PET and PET50/PU50 for both strength and strain.

Table 1
Tensile mechanical properties of electrospun tracheal scaffolds.

Scaffold type	Max force (N)	Max strain (%)	Porosity (%)	Average fiber diameter (μm)
PET50/PU50	114 ± 15	138 ± 17	93.2 ± 1.34	1.97 ± 0.78
PET70/PU30	125.5 ± 11	87 ± 24	90.6 ± 0.83	1.78 ± 0.76
PET	137 ± 8	45 ± 11	84.7 ± 1.14	1.88 ± 0.65

PET50/PU50: polyethylene terephthalate 50%/polyurethane 50%. PET70/PU30: polyethylene terephthalate 70%/polyurethane 30%. Max force (N): maximum force (Newton).

3.2. Bioreactor culture of 3-D tracheal scaffolds

3.2.1. PET50/PU50

To evaluate the biocompatibility of tracheal PET50/PU50 scaffolds, we utilized a bioreactor for dynamic culture. DAPI/Phalloidin images of cells attached to the scaffold internal and external surfaces (Fig. 1S A) showed that the cells were viable and stretched out on both surfaces. We also compared the metabolic activity of attached cells by using MTT assay. We observed (Fig. 1S B) similar absorbencies for both internal and external surfaces without any significant difference.

3.2.2. PET70/PU30 and PET

In order to evaluate the biocompatibility of tracheal PET70/PU30 and PET 3-D scaffolds, a bioreactor was used for dynamic culture. Cell attachment studies were evaluated by DAPI staining after 48 h in a bioreactor for both PET/PU and PET scaffolds at different positions (Figs. 2A and 3A). We counted the stained nuclei and found (Fig. 4A) low number of adhered cells over the rings (OR) compared to the whole scaffold ($p < 0.01$). This trend was observed in both PET/PU (Fig. 4A) and PET (Fig. 4A) scaffolds but there was a significantly higher cell numbers that attached to PET than PET/PU in all four positions ($p < 0.05$). To demonstrate if attached cells were metabolically active, we performed MTT assay and measured the absorbency for internal and external surfaces. In both PET/PU ($p < 0.05$) and PET ($p < 0.05$) scaffolds, the internal surfaces contained cells that were significantly higher in metabolic activity compared to external surfaces (Fig. 4B). We also found that there were higher readouts for PET compared to PET/PU ($p < 0.05$ externally and $p < 0.01$ internally). We further calculated the average of cell coverage on the external and internal surface of PET/PU and PET scaffolds using a mathematical model [9]. We estimated that PET/PU has average cell coverage of 48.5% (external: 39.4% and internal: 57.6%) whilst 60.1% (external: 49.4% and internal: 70.8%) of the PET scaffold surface was covered with MSCs (Fig. 4C). These results suggest that the both scaffold types were functional for cell attachment.

3.3. Static culture on 2-D sheets at different densities: PET70/PU30 and PET

Although the bioreactor seeding studies are vital for comprehensive studies on the tracheal scaffolds, we hypothesized that static seeding on 2-D sheets can provide a simplified method, as there will be a reduction in cells and material cost for the early phase of 3-D scaffold evaluations. We initially conducted static seeding either on PET/PU or PET sheets at the different cell densities by identifying cells with nuclear staining (DAPI) and measuring absorbance with an MTT assay. We noticed that both PET/PU and

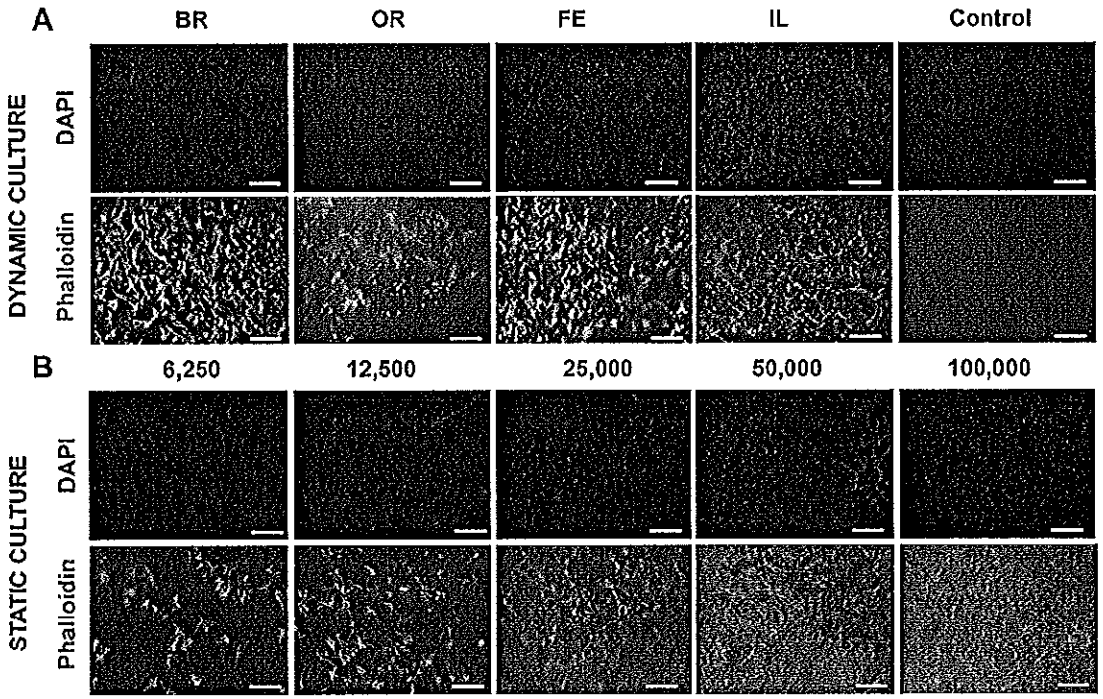

Fig. 2. Fluorescent images of seeded synthetic scaffolds made from PET70/PU30. Dynamic culture of 3-D scaffolds in bioreactor using 40M cells (A) and static culture of 2-D sheets using 6250; 12,500; 25,000; 50,000 or 100,000 cells (B). Cells are stained with Phalloidin (green) and DAPI (blue) after 48 h culture. Magnification 10×, scale bar representing 100 μm. (For interpretation of the references to colour in this figure legend, the reader is referred to the web version of this article.)

PET sheets displayed an increasing trend with higher cell densities (Fig. 4D, E), but PET contained higher cell attachment and metabolic activity in all data points ($p < 0.05$). When mathematical model was applied on the images (Fig. 2SA, B) of formazan crystals, a similar progressive trend for cell coverage on PET/PU (26.6%–82.5%) and PET (39.9%–92.5%) sheets was found (Fig. 4F). This suggests that static seeding on 2-D sheets can be used as a robust and sensitive cell density "ruler" for further quantitative evaluations.

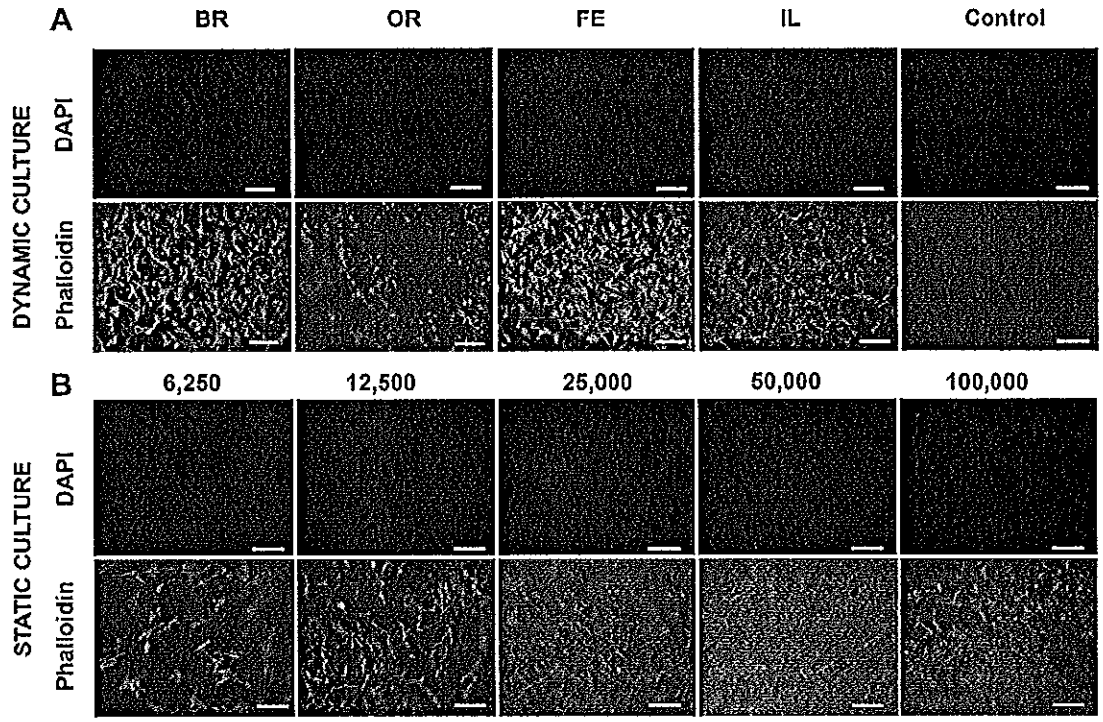

Fig. 3. Fluorescent images of seeded synthetic scaffolds made from PET. Dynamic culture of 3-D scaffolds in bioreactor using 40M cells (A) and static culture of 2-D sheets using 6250; 12,500; 25,000; 50,000 or 100,000 cells (B). Cells are stained with Phalloidin (green) and DAPI (blue) after 48 h culture. Magnification 10×, scale bar representing 100 μm. (For interpretation of the references to colour in this figure legend, the reader is referred to the web version of this article.)

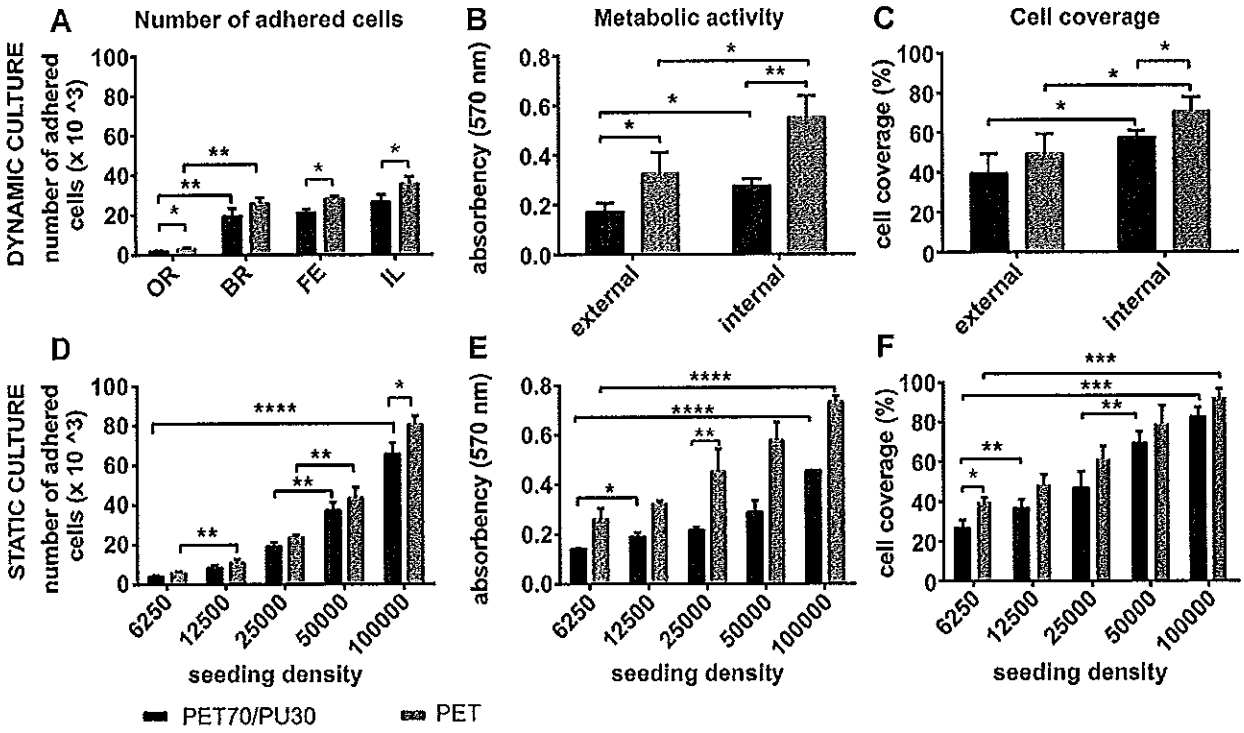

Fig. 4. Quantitative analysis of adherence, metabolic activity and coverage of rat MSCs seeded on PET70/PU30 and PET scaffolds under static and dynamic culture. The graph bars are representing the variables of "number of adhered cells"(A and D); "absorbency at 570 nm" (B and E) and "cell coverage percentage" (C and F) versus the position on the scaffold for 3-D scaffolds seeded in bioreactor under dynamic culture (A, B, C) or different progressive densities in seeding on 2-D sheets under static culture (D, E, F).

3.4. Correlating bioreactor to static culture: PET70/PU30 and PET

In order to understand if 3-D scaffolds seeded in bioreactor can correlate to 2-D sheets from static seeding, a database was created from the outcomes of static seeding. We fitted the relationships between each variable and the density used for static seeding and found; *(i)* a linear relationship was seen between the number of adhered cells and seeding densities in both types of 2-D sheets. However, for *(ii)* absorbency and *(iii)* cell coverage, a power law curve was the best fit to the data.

In order to correlate 3-D bioreactor culture to static culture, we used the average values from 3-D bioreactor evaluations i.e. DAPI, MTT and cell coverage and interpolated the equivalent seeding density in a static 2-D environment. In 3-D PET/PU, the number of adhered cells presented as $Y = 16.3$ to the line of best fit of static seeding and the corresponding seeding density was interpolated ($X_1 = 24{,}116$) from the formula ($Y = 0.6763*X$; Fig. 5A). A similar procedure was performed for the averages of absorbency ($Y = 0.23$) and cell coverage ($Y = 48.48$) for 3-D PET/PU scaffolds, using the formula for the curve of best fit for each of the variables. The results were $X_2 = 23{,}515$ (Fig. 5B) and $X_3 = 22{,}484$ (Fig. 5C) respectively. From the three interpolated outcomes i.e. X_1, X_2 and X_3, we found that the readouts from the different assays i.e. counting the number of nuclear stains (DAPI), measurement of metabolic activity of cells (absorbance) and mathematical modeling of cell coverage were not significantly different to each other. Hence, we determined that the optimal cell density 23,371 ± 825 for 2-D static culture on PET/PU sheets could correlate to the 3-D bioreactor cell culture.

Similar procedures were conducted for PET (Fig. 5D–F). For the three variables of "number of adhered cells", "absorbency" and "cell coverage", the interpolated data was seeding densities of $X_1 = 26{,}842$, (Fig. 5D); $X_2 = 25{,}493$ (Fig. 5E); $X_3 = 26{,}940$ (Fig. 5F) respectively and the average was 26,425 ± 808. This suggests that PET sheets would require 26,425 cells/0.32 cm^2 for static seeding.

3.5. Qualitative evaluations of 2-D sheets and 3-D scaffolds

We further performed qualitative analyses of PET70/PU30 (Fig. 2A, B, 6) and PET (Fig. 3A, B, 6) by DAPI/Phalloidin and SEM imaging. We confirmed that when we utilized 25,000 cells for static seeding on both PET/PU and PET sheets, they closely resembled 3-D scaffolds.

3.6. In vivo evaluation in a small animal model

To evaluate the *in vivo* properties of electrospun PET/PU and PET scaffolds, they were seeded with rat MSCs and were implanted in an orthotopic position (Fig. 7A) in a small animal model. The evaluation of the scaffolds prior and post-implantation using DAPI/Phalloidin staining and MTT assay revealed sufficient cell adhesion i.e. >60% surface coverage and metabolically active cells (*data not shown*). Throughout the entire study period of 30 days, none of the animals, that received either the MSCs seeded PET/PU or the PET scaffold, displayed any symptoms of health impairment. The harvested scaffolds were all patent at the endpoint of the study (30 days), well integrated into the adjacent tissue without any signs for increased inflammatory responses or necrosis (Fig. 7B–D) but with evidence for initial vascularization within the scaffolds wall (Fig. 7E-H) and epithelialization of the internal surface (Fig. 7I) with even iliated cells (Fig. 7J). All animals gained weight within the study period (from 249 ± 30 g to 447 ± 24 g).

4. Discussion

In the field of tissue engineering, a combination of biomaterial-based, target organ-shaped scaffolds with autologous cells is currently the best option for regeneration of many tissues/organs like bladder, trachea and blood vessels [1,4,11–13]. Among the different biopolymers, PET and PU were selected for scaffold

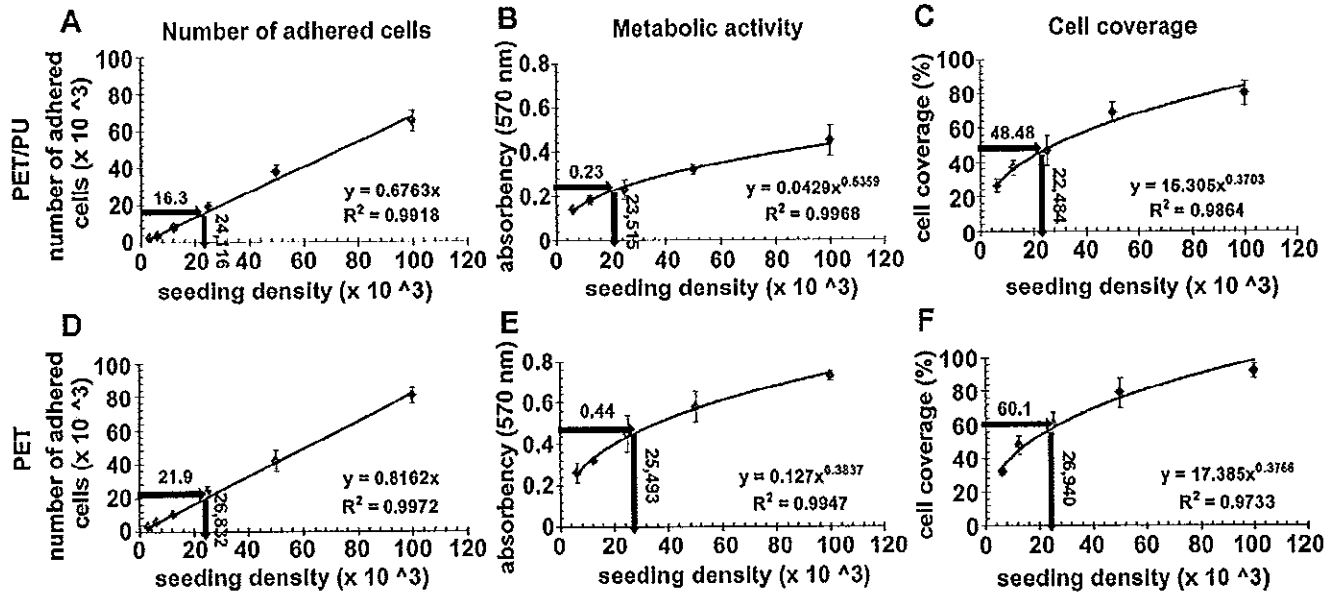

Fig. 5. Finding the correlation between static and dynamic culture. The graphs are showing the best curves fitting each of the variables of "number of adhered cells" (A and D), "absorbency at 570 nm" (B and E) and "cell coverage percentage" (C and F) as a function of "seeding density" for PET70/PU30 (A, B, C) and PET (D, E, F) sheets. For each graph, the "in" arrow enters the average of the related variable from bioreactor seeding to the formula of the curve (line) and a corresponding "seeding density" is interpolated as shown by "out" arrow.

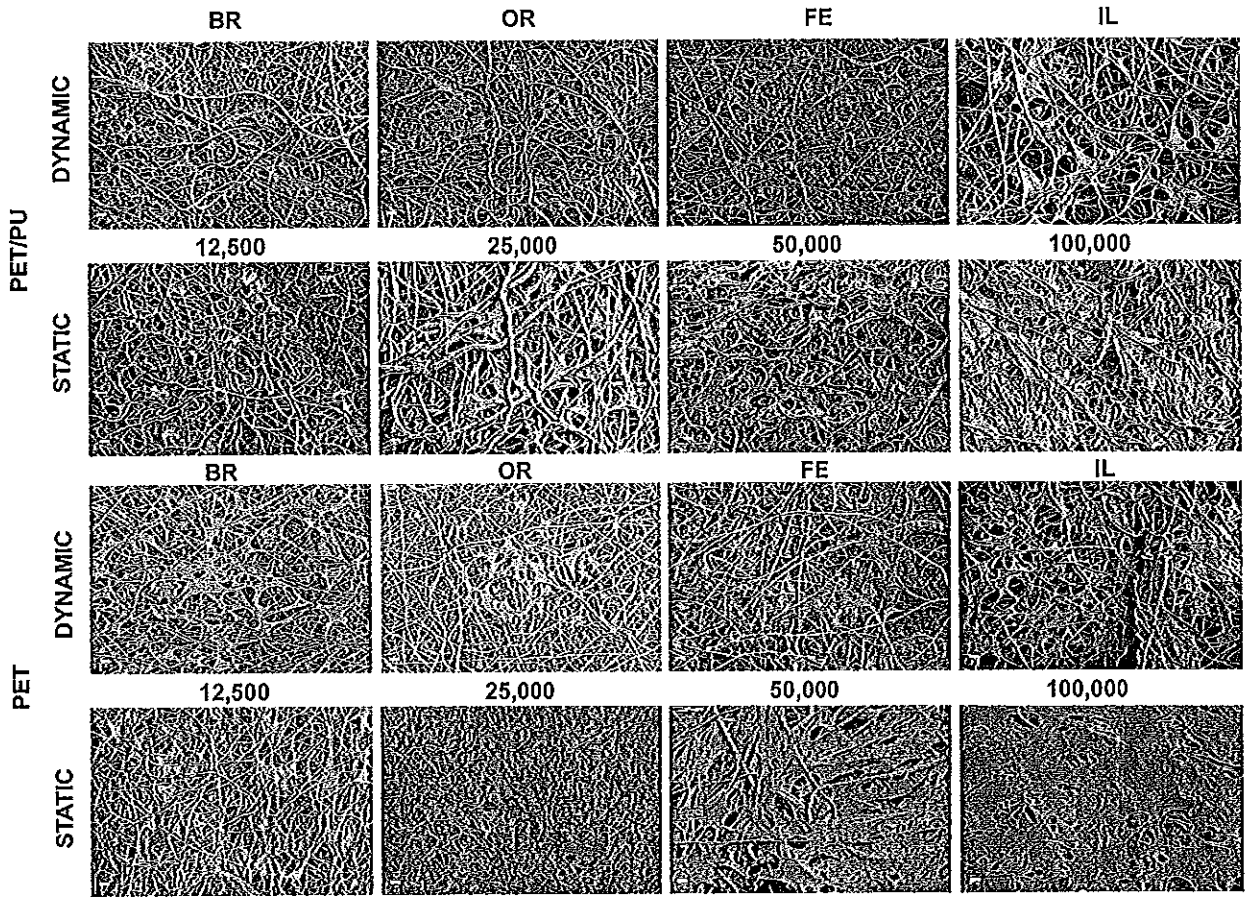

Fig. 6. SEM images of rat MSCs adhered to PET70/PU30 and PET scaffolds. Different parts of 3-D PET/PU and PET scaffolds seeded in bioreactor and 2-D sheets seeded statically under different cell densities are shown; scale bars represent 20 μm.

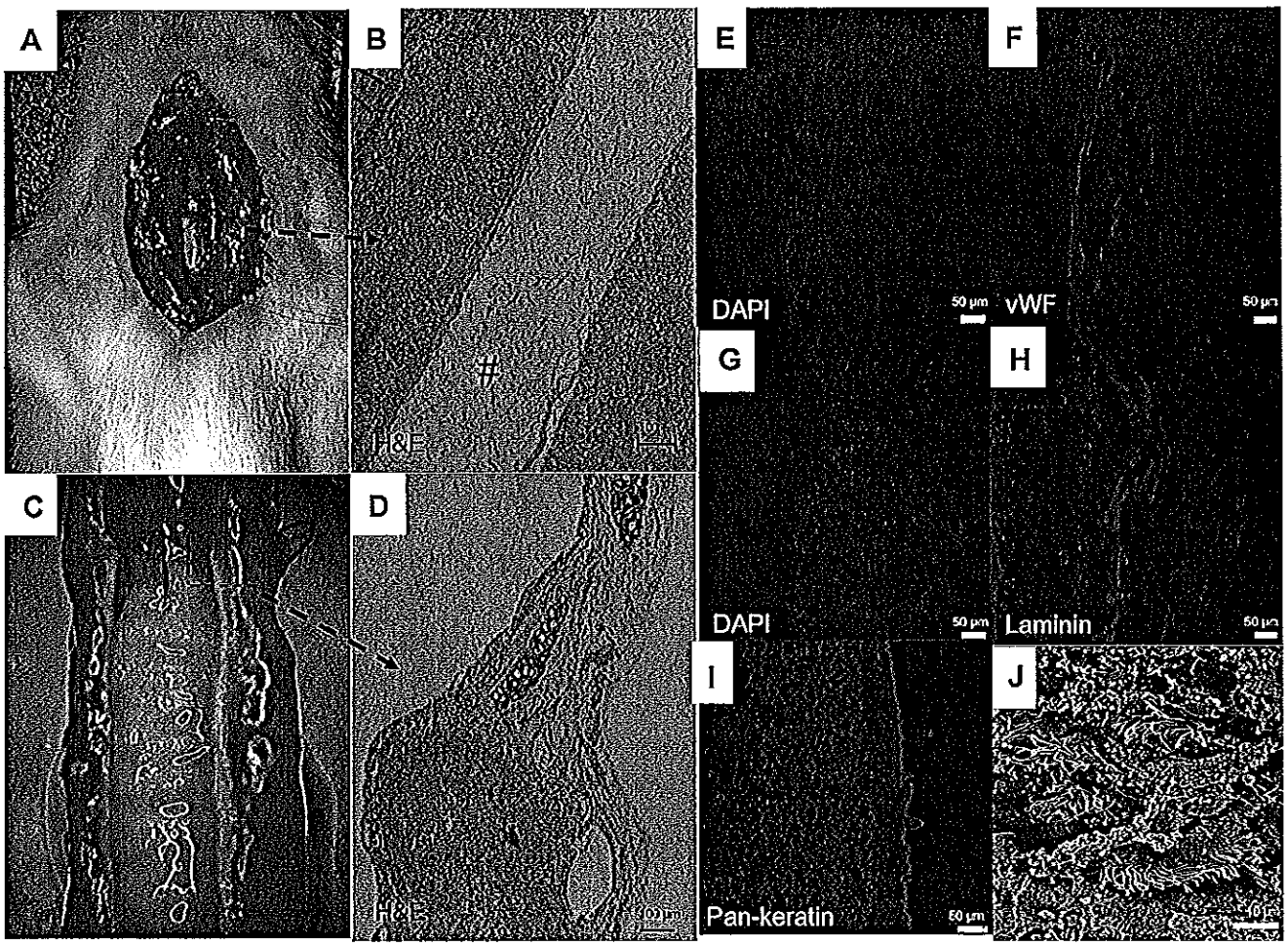

Fig. 7. In vivo evaluation of the electrospun tracheal scaffolds. Macroscopic view of an implanted PET scaffold in orthotopic position (A); Sagittal section of a harvested tracheal graft (PET) (macroscopic view: C; microscopic view: B, D, Hematoxylin & Eosin (H&E) staining, * graft's wall, # luminal side of the graft); Immunohistochemistry staining of the harvested graft: DAPI (E) von Willebrand Factor (F); DAPI (G), Laminin (H); Merge DAPI and Pan-keratin (I) scanning electron microscopic section (Magnification ×3000) of the harvested tracheal (PET) graft (J) with initial signs for ciliated cells at the luminal site of the graft 30 days after transplantation.

fabrication due to being approved by FDA, vast tissue engineering applications [12,14,15], slow rate of degradation [12,16] as well as the possibility of engineering biomechanical and structural properties to match the native tissue.

In 2011, electrospun elastomeric PET50/PU50 polyblend was the first version of synthetic electrospun scaffolds applied clinically. The PET50/PU50 scaffold was found to be ideal for replacement of native trachea because of its high porosity, appropriate strength and extensibility which could provide consistent matching with the morphological and mechanical properties of native trachea [4,17]. Not only the electrospun part was mimicking the fibrous structure of native tracheal ECM, but also the C-shaped cartilaginous rings reinforced the anterior and lateral sides of the trachea to withstand surrounding forces and maintain the airway open. The polyurethane applied for electrospinning (polycarbonate urethane, PCU, Bionate) was an improved version of the polyurethanes family which has good biomechanical stability that is suited for long-term applications [18,19]. However, we noted that this scaffold showed partial collapse one year post-transplantation which may be due to the degradation of applied PU [20]. Although biodegradability can be considered positive as it mitigates the immune reactions and encourages the native tissue to regenerate and remodel, the imbalances in the rate of scaffold degradation and new tissue production can be risky for patients. Hence, it is important to consider the regeneration capacity of tissue or organ types to maintain a substantial mechanical stability for the scaffold.

We further modified the development of tracheal scaffold by reducing the PU composition in electrospinning solution to decrease the degradation rate. Hence, two types of tracheal scaffolds (PET70/PU30 and PET) were further characterized in this study and we found that both the scaffold types contained morphological and biomechanical requirements which were comparable to native trachea [4,17]. It is worth considering that the synthetic scaffolds had similar internal dimensions (transversal and sagittal diameter) compared to native tracheae applied in our previous studies [4,17]. However, the wall thickness of synthetic scaffolds was 50% thinner to the native, which should be taken into account for the comparison of mechanical properties.

To perform the next verification procedure, i.e. biological evaluations, the biomechanically validated 3-D constructs were seeded inside specially designed bioreactors [21]. However, each bioreactor run is costly in terms of time and resources due to the extensive setup, pre-wash (PBS washing) and pre-coating (media wash) steps. Moreover, large number of cells (between 40 and 60 million, depending on whether a pediatric or adult case) are

required for each scaffold. Hence, consuming hundreds of millions of stem cells to perform a biocompatibility validation is inevitable. In this regard, it was desirous to avoid the need to run bioreactors for scaffold validation during the early phase of verifications. Herein, we present the possibility of performing static seeding of cells on 2-D sheets (cut out of 3-D scaffolds) and consider it to be representative for dynamic culture of 3-D scaffolds in bioreactor. Upon approving the biocompatibility of the tracheal scaffolds, based on the low cost, simple and fast 2-D static cell seeding, bioreactor seeding can finally be applied in the clinical verification of the scaffold. Outcomes from cell studies on PET70/PU30 and PET scaffolds have demonstrated that static cell seeding with density of around 25,000 per well (75,000 cells/cm^2) is most representative for the optimum bioreactor seeding (cell density of 610,000 cells/cm^2). Therefore, it can be concluded that in order to have similar cell coverage on a 3-D tracheal scaffold compared to a 2-D sheet, an 8-fold reduction in seeding density can reliably be used to predict biocompatibility of the scaffolds. The correlation technique introduced here may also be applicable for other tubular scaffolds such as vascular grafts and esophagus.

From our extensive validation of the scaffolds, we found that PET is biologically superior to the polyblend construct, due to higher number of viable cells and more cell coverage. Likewise, our *in vivo* animal model approved the materials' biocompatibility and the orthotopic functional properties of both the PET/PU and PET-based tracheal scaffolds. We believe the rat model is more appropriate as the mobility closely resembles humans. The findings from our 30 day study period in a rat model is also equivalent to approximately 900 days of human life which can therefore provide clinically relevant intermediate and long-term information [22].

5. Conclusion

We present here the biochemical and biocompatibility characteristics of different compositions of electrospun tracheal scaffold i.e. PET70/PU30 and PET (100%). We found that both these scaffolds were mechanically strong, had uniform fibrous structure and supported cell viability and attachment. *In vitro* experiments, represented superior properties of PET compared to the PET/PU polyblend, whilst there was no significant difference between their *in vivo* implantation outcomes. We further demonstrated the correlation of the static to dynamic cell culture with the approximate equivalent ratio of 1/8 in term of seeding density. In this way, we can perform static seeding on 2-D sheets as a means to investigate the cyto-compatibility of the whole 3-D scaffold. This can aid to further optimize tracheal and similar tubular scaffolds for clinical applications in an economical, reproducible and simple validation method.

Acknowledgments

This work was supported by European Project FP7-NMP- 2011-SMALL-5: BIOtrachea, Biomaterials for Tracheal Replacement in Age-related Cancer via a Humanly Engineered Airway (No.280584 – 2), ALF medicine (Stockholm County Council): Transplantation of bio-engineered trachea in humans (No. LS1101–0042.), Dr Dorka-Stiftung (Hannover, Germany): bioengineering of tracheal tissue and Mega grant of the Russian Ministry of Education and Science (agreement No. 11.G34.31.0065).

Appendix A. Supplementary data

Supplementary data related to this article can be found at http://dx.doi.org/10.1016/j.biomaterials.2014.03.015

References

[1] Macchiarini P, Jungebluth P, Go T, Asnaghi MA, Rees LE, Cogan TA, et al. Clinical transplantation of a tissue-engineered airway. Lancet 2008;372:2023–30.
[2] Gonfiotti A, Jaus MO, Barale D, Baiguera S, Comin C, Lavorini F, et al. The first tissue-engineered airway transplantation: 5-year follow-up results. Lancet 2013;6736:1–7.
[3] Berg M, Ejnell H, Kovacs A, Nayakawde N, Patil P, Joshi M, et al. Replacement of a tracheal stenosis with a tissue-engineered human trachea using autologous stem cells. Tissue Eng Part A 2014;20:389–97.
[4] Jungebluth P, Alici E, Baiguera S, Blanc K, Blomberg P, Bozóky B, et al. Tracheobronchial transplantation with a stem-cell-seeded bioartificial nanocomposite: a proof-of-concept study. Lancet 2011;378:1997–2004.
[5] Ahmed M, Ghanbari H, Cousins BG, Hamilton G, Seifalian AM. Small calibre polyhedral oligomeric silsesquioxane nanocomposite cardiovascular grafts: influence of porosity on the structure, haemocompatibility and mechanical properties. Acta Biomater 2011;7:3857–67.
[6] Li M, Mondrinos MJ, Chen X, Gandhi MR, Ko FK, Lelkes PI. Co-electrospun poly(lactide-co-glycolide), gelatin, and elastin blends for tissue engineering scaffolds. J Biomed Mater Res A 2006;79:963–73.
[7] Barnes CP, Sell S a, Boland ED, Simpson DG, Bowlin GL. Nanofiber technology: designing the next generation of tissue engineering scaffolds. Adv Drug Deliv Rev 2007;59:1413–33.
[8] Gustafsson Y, Haag J, Jungebluth P, Lundin V, Lim ML, Baiguera S, et al. Viability and proliferation of rat MSCs on adhesion protein-modified PET and PU scaffolds. Biomaterials 2012;33:8094–103.
[9] Jungebluth P, Haag JC, Lim ML, Lemon G, Sjöqvist S, Gustafsson Y, et al. Verification of cell viability in bioengineered tissues and organs before clinical transplantation. Biomaterials 2013;34:4057–67.
[10] Sotocinal SG, Sorge RE, Zaloum A, Tuttle AH, Martin LJ, Wieskopf JS, et al. The rat grimace scale: a partially automated method for quantifying pain in the laboratory rat via facial expressions. Mol Pain 2011;7:55.
[11] Atala A. Tissue engineering of human bladder. Br Med Bull 2011;97:81–104.
[12] Detta N, Errico C, Dinucci D, Puppi D, Clarke DA, Reilly GC, et al. Novel electrospun polyurethane/gelatin composite meshes for vascular grafts. J Mater Sci Mater Med 2010;21:1761–9.
[13] Baudis S, Ligon SC, Seidler K, Weigel G, Grasl C, Bergmeister H, et al. Hard-block degradable thermoplastic urethane-elastomers for electrospun vascular prostheses. J Polym Sci A Polym Chem 2012;50:1272–80.
[14] Nieponice A, Soletti L, Guan J, Hong Y, Gharaibeh B, Maul TM, et al. In vivo assessment of a tissue-engineered vascular graft combining a biodegradable elastomeric scaffold and muscle-derived stem cells in a rat model. Tissue Eng Part A 2010;16:1215–23.
[15] Moreno MJ, Ajji A, Mohebbi-Kalhori D, Rukhlova M, Hadjizadeh A, Bureau MN. Development of a compliant and cytocompatible micro-fibrous polyethylene terephthalate vascular scaffold. J Biomed Mater Res B Appl Biomater 2011;97:201–14.
[16] Chaouch W, Dieval F, Chakfe N, Durand B. Properties modification of PET vascular prostheses. J Phys Org Chem 2009;22:550–8.
[17] Baiguera S, Jungebluth P, Burns A, Mavilia C, Haag J, De Coppi P, et al. Tissue engineered human tracheas for in vivo implantation. Biomaterials 2010;31:8931–8.
[18] Chandy T, Van Hee J, Nettekoven W, Johnson J. Long-term in vitro stability assessment of polycarbonate urethane micro catheters: resistance to oxidation and stress cracking. J Biomed Mater Res B Appl Biomater 2009;89:314–24.
[19] Szelest-Lewandowska A, Masiulanis B, Szymonowicz M, Pielka S, Paluch D. Modified polycarbonate urethane: synthesis, properties and biological investigation in vitro. J Biomed Mater Res A 2007;82:509–20.
[20] Cipriani E, Bracco P, Kurtz SM, Costa L, Zanetti M. In vivo degradation of poly(carbonate-urethane) based spine implants. Polym Degrad Stab 2013;98:1225–35.
[21] Asnaghi MA, Jungebluth P, Raimondi MT, Dickinson SC, Rees LEN, Go T, et al. A double-chamber rotating bioreactor for the development of tissue-engineered hollow organs: from concept to clinical trial. Biomaterials 2009;30:5260–9.
[22] Andreollo NA, Santos EF, Araújo MR, Lopes LR. Rat's age versus human's age: what is the relationship? Arq Bras Cir Dig 2012;25:49–51.

Karolinska Universitetssjukhuset 11002521SV1
Öron-,näs- och halskliniken, Huddinge
Avdelning B82
141 86 STOCKHOLM
tel: 08-585 877 91 fax:08-585 873 25

Appendix 14

* 2011-11-21 08:40 Jan-Erik Juto, Läk H - ÖNH-avd B82 (låst)

INTAGNINGSANT.

Patientansvarig läkare Jan-Erik Juto (läk) /1f3x/

Intagningsorsak

Inkommer för en bronkoskopi och borttagning av förändring i ingången till intermediärbronken efter att ha op radikalt för en lågdifferentierad mucoepidermoid cancer i trakea juni 2011 med insättande av plastgraft. Sammantaget har efter radikalop vistats först på rehabilitering och sedan 2 mån tillbaka hemskriven till privatboende i Reykjavik. Bor tillsammans med familj, fru och barn från Eiritrea i Reykjavik.

Först under op var man tvungen att grafta hö lungartär förutom att man satte in plastgraften i trakea och övre delen av hö huvudbronk men väl ovanför ovanlobsbronken.

Pat har kontrollerats i Reykjavik av professor Tomas Gudbjartsson, thoraxkirurg, som också medverkade vid op i juni.

Pat har utvecklat en granulationsliknande förändring distalt om graften i höjd med ovanlobsbronken den man har biopserat ifrån och enl telefonuppgift från Reykjavik icke malignt utfall vid undersökning. Man önskar nu en rensning av granulationen där material förstås bör sändas till PAD för undersökning och även odling bör tagas från luftrören.

Läkemedelsavstämning Medicinfri sedan 2 mån tillbaka, då fått en kur med ett Trimetoprimpreparat som utsattes efter fullbordad kur 2 v sedan.

Status

Allmäntillstånd	Ser lite medtagen ut. Går obehindrat. Produktivt spute. Uppger att han gått ner cirka 7 kg efter op.
Munhåla och svalg	Retningsfria slemhinnor.
Halsens mjukdelar	Palperas u a. Välläkt sår efter trakeostomat och ingrepp i thorax.
Hjärta	Regelbunden rytm, cirka 110 slag/min.
Blodtryck	90/70 mmHg i vila vä arm.
Lungor	Inga andningsljud på hö sida. Relativt rena andningsljud på vä sida.

Karolinska Universitetssjukhuset 11002521SV1
Öron-,näs- och halskliniken, Huddinge
Avdelning B82
141 86 STOCKHOLM
tel: 08-585 877 91 fax:08-585 873 25

Bedömning

Man som kommer för revision av luftväg efter luftvägskirurgi pga cancer med insättning av en graft i trakea av plast. Inkommer för rengöring, odling och preparat för PAD. Op som planerats i jetventilation och rak bronkoskopi.

---------- slut utskrift ----------

Karolinska Universitetssjukhuset 11002521SV1
Öron-,näs- och halskliniken, Huddinge
Avdelning B82
141 86 STOCKHOLM
tel: 08-585 877 91 fax:08-585 873 25

Appendix 15

2011-11-21 12:09 Jan-Erik Juto, Läk H - ÖNH-avd B82 (låst)

OPERATIONSBERÄTTELSE

Patientansvarig läkare Jan-Erik Juto (läk) /1f3x/

Operatör Jan-Erik Juto (läk) /1f3x/

Operations- åtgärdskod UGC05 Rigid bronkoskopi med biopsi från bronk eller trakea
GCA32 Endoskopisk inläggning av stent i bronk

Operationsförlopp JET-ventilation. Rigid bronkoskopi.

Dr Henriksson tar 7,5 Storz bronkoskop och JET-ventilation. Undertecknad tar över och identifierar granulationer i ovankanten på graften som är insatt för ngr månader sedan. Det finns även granulationer distalt där graften slutar båda på höger och vänster sida, d v s i höger huvudbronk och vid vänster huvudbronk. Börjar först med att se att det finns passage ner i vänster bronk, den är förträngd av granulationerna men ej mer än till kanske 20 %. Jag går först ner och resecerar granulationerna på höger sida i huvudbronken. Det går att reducera dem. Det är någorlunda lättblödande men går att reducera massorna ner, det går inte att kunna se säkert avgång för ovanlobsbronken. Det är relativt lättblödande här. Man kan sedan se ner i mellan- och underlobsbronker. Beslut om att sätta en stent och det är 14 mm diameter och 30 mm lång med referensnummer: 6479, det är covered Boston Scientific, bronkial stent ultraflex. Vidgar och anpassar läget så att jag får en god passage ner i intermediärbronken. Suger rent. Går sedan över på vänster sida. Här finns granulationer enl ovan där graften slutar. Det är även här lättblödande. Man anar en liten glugg kl 1, d v s inåt medialt framåt precis vid kanten på graften. Sätter även här en stent som har samma referensnummer, d v s 6479 och är 14 x 30 mm covered Boston Scientific ultraflex och får här då även en god passage efter stentjustering. Går sedan upp och det granulationer i överkanten på graften och dessa reduceras ner efter Adrenalintork mot mindre blödningar så avstannar dessa, suger rent. Sätter ingen stent här. Gör sedan en biopsi mitt i graften och man ser att här finns en cirkulation ..... sedan ut mot plastgraften, d v s det finns en epitelialisering på ngt sätt på insidan av graften. Efter rengöring så tar vi sedan sköljprover från höger underlob och proverna delas upp och tages till bakteriologisk odling och till TB-odling och till svampodling. Op avslutas med att PAD från höger

Karolinska Universitetssjukhuset 11002521SV1
Öron-,näs- och halskliniken, Huddinge
Avdelning B82
141 86 STOCKHOLM
tel: 08-585 877 91 fax:08-585 873 25

bronkgränsen mot graften, granulationerna som är borttagna skickas liksom granulationen i överkanten av graften som togs bort i separata burkar till fryssnitt. Op avslutas.

---------- slut utskrift ----------

Karolinska Universitetssjukhuset 11002521SV1
Öron-,näs- och halskliniken, Huddinge
Avdelning B82
141 86 STOCKHOLM
tel: 08-585 877 91 fax:08-585 873 25

Appendix 16

* 2011-11-21 18:04 Pernilla Säll, Ssk H - ÖNH-avd B82 (signerad)
Rättelse: 2011-11-21 20:27 Pernilla Säll, Ssk

OMVÅRDNADSSTATUS

Andning Kopplar bort saturationen efter att pt varit upp. Ligger på 92% vilket är lägsta gränsen enligt Dr Juto. Uppmanar och instruerar pt att blåsa i BA-tuben.

Cirkulation Mår bättre. Har slutat shivra. Har dock fortfarande tempstegring, vg se mätvärden

Nutrition Har ätit fisksopp under kvällen. Druckit bra. Får även en näringdryck till kvällen.
Skall fasta på nytt från 24/ 04.00.

Elimination Har kissat postop

Aktivitet Fullt rörlig, sköter ADL självständigt

Smärta

Smärtintensitet enl VAS 0 enh

Sammansatt status Pt skall på CT imorgonbitti kl. 7:30. Har en grön infart vä hand som fungerar.
Planerad op imorgon som nr 2 på operationsprogrammet.

Pt uppger att han ej står på några lm längre. Dr Juto eller Dr Maccarina får uppdatera pt lm-lista under morgondagen.

---------- slut utskrift ----------

Karolinska Universitetssjukhuset 11002521SV1
Öron-,näs- och halskliniken, Huddinge
Avdelning B82
141 86 STOCKHOLM
tel: 08-585 877 91 fax:08-585 873 25

Appendix 17

* 2011-11-22 12:05 Jan-Erik Juto, Läk H - ÖNH-avd B82 (låst)

OPERATIONSBERÄTTELSE

Operatör Jan-Erik Juto (läk) /1f3x/

Operations- åtgärdskod
UGC05 Rigid bronkoskopi med biopsi från bronk eller trakea
GCA10 Avlägsnande av främmande kropp i bronk
GCA32 Endoskopisk inläggning av stent i bronk

Operationsförlopp

Jet-ventilation. Går ner med 7,5:ans Storz bronkoskop med optik kopplad via kamera till display. Jag kommer ner genom graften och ner till stentar och jag ser att hö bronk distalt om stenten som insattes igår är fylld med pus. Det ser bättre ut på vä sida. Suger rent. Det fyller sig nerifrån hela tiden på hö sida. Det går så småningom att minska flödet, så att man får någorlunda rent ner i underloben. Identifierar B6:an och kan dessutom identifiera en bronkavgång kl 1, vinklar utåt hö, sitter 1 cm från graftkantens nedre del och detta bör kunna vara ovanlobsbronken. Jag använder Mitomycin mot granulationsytor sedan stenten har tagits ut, försöker och rensuga, det tömmer sig en del serös vätska även i anastomosen mellan graft och bronk kl 6, 7 hö sida. Suger rent efter att Mitomycin applicerats mot granulationsytor, (efter dom granulationer som togs bort för 1 dygn sedan). Sätter en ny stent utåt, den justeras så att den täcker övre granulationsytorna och lämnar underlob och B6:an. Även vad jag kan förstår den mynning som sannolikt är ovanlobsbronkens mynning, fri, denna sitter visserligen i nätverket, som inte coatad i stenten.
Härefter går jag över på vä sida, skjuter ner den befintliga stenten, sätter en Mytomycin mot granulationsytorna runtom. Ser fistelbildningen som ligger medialt och i kanten på graftet, denna sida kl 2, 3. Avslutar med att dra upp stenten igen så att jag får en fin täckning över applicerade och behandlade ytor. Går sedan upp och sätter Mytomycin på granulationsytor efter gårdagens borttagande av granulationer kl 3 och 6 i övre begränsningen på graftet. Härefter någorlunda fina förhållanden, suger åter rent i hö huvudbronk distalt mot underloben. Operationen avslutas.

---------- slut utskrift ----------

FRÅN

STOCKHOLMS LÄNS LANDSTING
Karolinska Universitetssjukhuset
Karolinska Universitetslaboratoriet
Klin Pat/Cyt lab

Tfn

B: 11002-521-SV1
S: 11002-521-SV1
F: 11002-521-S03
R: 1026-8211193-9
L: T21415-11

SVAR PATOLOGI/CYTOLOGI

Appendix 18

TILL

Karolinska Universitetssjukhuset
Öron-,näs- och halskliniken, Huddinge
Avdelning B82
141 86 STOCKHOLM

Regnr
T21415-11

Provtagningstid: 2011-12-20 10:59
Ankomstid lab: 2011-12-21

Remittent: Jacob Lien
Tfn:

Preparatets natur: slemhinna/granulation från trachea
Frågeställning: granulation? ca?

Anamnes: Pat med trachealgraft med granulationsliknande flärp som nyps bort i trachea
Strålbehandlad: Nej

SVAR

UTLÅTANDE
2012-01-03 T21415/2011
2011-442098

Material från trachea, utgöres av granulationsvävnad med kärlrikt luckert stroma samt riklig förekomst av plasmaceller men även akuta inflammatoriska celler. Inga hållpunkter för malignitet i det undersökta materialet.

Sammanfattningsvis bilden är väl förenlig med granulationsvävnad.
DIAGNOS
Se ovan.
BIOBANKSINFORMATION
Provet får användas för samtliga, enligt biobankslagen, godkända ändamål.

Katalin Dobra 2012-01-03
----------slut----------

Framställd
2012-01-03 16:30

FRÅN

STOCKHOLMS LÄNS LANDSTING

Karolinska Universitetssjukhuset
Karolinska Universitetslaboratoriet
Klin Pat/Cyt lab

Tfn

B: 11001-341-306
S: 11001-341-306
F: 11001-341-306
R: 1026-7588461-7
L: T13678-11

SVAR PATOLOGI/CYTOLOGI

Appendix 19

TILL

Karolinska Universitetssjukhuset
Thoraxkliniken, Solna
N 13/23 Thorax
171 76 Stockholm

Regnr
T13678-11

Provtagningstid:	2011-08-24 08:00	Remittent:	Karl-Henrik Grinnemo
Ankomstid lab:	2011-08-25	SNABBSVAR:	Tfn: 0858582443

Preparatets natur: Syntetisk trachea graft
Frågeställning: Cellinväxt? Extracellulärmatrix struktur?

Anamnes: Pat som op med trachea graft i juni. Detta är ett syntetiskt graft coatat med mesenchymala stamceller. Vi har tagit provbitar före implantation som vi vill få analyserade angående cellinväxt, matrix struktur? Jag hänvisar till telefonkontakt med Överläkare Bela Bozoky. Var snäll och meddela läkaren att proverna har anlänt.
Strålbehandlad: Nej

SVAR

UTLÅTANDE
2011-08-26 T13678/2011
2011-442098

I snitten från de insända fyra små vävnadsbitarna kan ett poröst främmande material av syntetisk graft identifieras. Några detekterbara cellkomponenter eller matrixstruktur ses ej.

DIAGNOS
Se ovan.

BIOBANKSINFORMATION
Patienten vill inte att provet lagras, men svarstalong saknas eller har ännu ej registrerats. Provet lagras tills vidare i avvaktan på att svarstalong inkommer/registreras.

Bela Bozoky 2011-09-02

----------slut----------

Framställd
2011-09-02 11:33

Karolinska Universitetssjukhuset 11002521SV1
Öron-,näs- och halskliniken, Huddinge
Avdelning B82
141 86 STOCKHOLM
tel: 08-585 877 91 fax:08-585 873 25

Appendix 20

* 2011-12-20 11:04 Jacob Lien, Läk H - ÖNH-avd B82 (signerad)

OPERATIONSBERÄTTELSE

Operatör Jacob Lien (läk) /1crx/

Assistent Jan-Erik Juto (läk) /1f3x/

Gert Henriksson

Operations- åtgärdskod
UGC05 Rigid bronkoskopi med biopsi från bronk eller trakea
GCA10 Avlägsnande av främmande kropp i bronk
GCA32 Endoskopisk inläggning av stent i bronk

Operationsförlopp
JET-ventilation. Går ner med 7,5:ans Storz bronkoskop. Optik kopplad via kamera till display. Går ner till graftkanten och man ser en liten granulation kl 3 till 4. Fortsätter ner mot vä bronk, här ser man en stent som har glidit upp en aning. Suger rent och vi kan lossa den lätt och drar ut hela stentet. Dessförinnan har dr Juto nypt bort ngr granulationer i nederkant. Man ser i övergången mellan graft och bronk kl 3-4 fistelbildning. Suger rent här.
Går därefter upp på hö-sidan där vi inte ser ngn nämnvärd granulationsbildning. Kan lösa stentet i underkant, drar ut hela stentet och vi kan därefter identifiera ovanlob och mellanlobsavgång där det troligtvis är lite vridet efter op, så att ovanloben ligger inte helt där förväntat. Suger rent. Lägger därefter på vä-sidan en 14 x 40 Boston täckt 25 mm just nedom carinas överkant, ref.nr 6480.
Därefter går vi över på hö-sidan och lägger ner en stent som mäter 14 x 30, täckt 15 mm Boston. Här lämnar vi då i nederkant så att den täckta delen inte ligger över ovanlobsavgången, ref.nr 6479. Därefter tar dr Juto bort en granulationsbit som hänger kl 3-4 i ovankant av graftet i trakea. Avslutar med att suga rent. Op avslutas.

Postoperativ planering
Om cirka 8 v planeras för op igen med ev extraktion och byte av stentar. Hem om 1-2 dgr.

---------- slut utskrift ----------